UNIVERSITÀ DEGLI STUDI DI TORINO

Department of Clinical and Biological Sciences

PhD Programme in Complex Systems for Life Sciences

XXXIV Cycle

TFEB influence on melanoma proliferation and metabolism

Candidate: **Dott.ssa Camilla Ariano**

Advisor: **Prof. Federico Bussolino**

Tutor: **Dott.ssa Gabriella Doronzo**

INDEX

ACKNOWLEDGEMENTS

I want to thank Dott.ssa Gabriella Doronzo for the support she gave me in these 5 years from Master Degree to PhD, the patience she put at the beginning in teaching me “the art of laboratory” but mostly for her believing in myself.

I am grateful to Prof. Federico Bussolino for the chance he gave me in attending his laboratory and for all the people I met and worked with.

In particular, I want to thank Dott.ssa Stefania Rosano for our constant enriching exchange of views and for what she means to me; Dott.ssa Stefania Giove for her constant presence and always supportive words and actions; Dott.ssa Giulia Mana for her kindness and practical sense in every situation.

To my family, my friends and every person I got in touch and taught me something.

Finally, to Andrea, Birillo and Grethel for supporting me even when I didn’t deserve it and for their eternal and unconditional love to who I used to be.

ABSTRACT

Introduction

It is known that cancer cells are characterized by cellular programs that favour survival, growth and proliferation, leading to tumour formation and progression. In particular, proliferation and metabolism alterations support and sustain malignant growth.

The transcription factor EB (TFEB), member of the MiT family, is traditionally involved in autophagy and lysosomal function as well as in the cellular adaptation to stress conditions. Besides its traditional role, TFEB is implicated in metabolism, immunity, angiogenesis, inflammation, proliferation, and drug resistance. Alterations in MiT family members have been found in different human tumours. In particular, amplification and single nucleotide mutations of MITF are frequent in melanomas.

Modulation of TFEB in renal and pancreas cancer cells both *in vivo* and *in vitro* alters cell proliferation. Moreover, we previously reported that TFEB induces endothelial proliferation modulating genes involved in G1/S phase of cell cycle such as CDK4, E2F and E2F targeted genes.

Metabolism is a promising target for cancer therapy and is identified as a mechanism of resistance to both classical and targeted therapy.

Few data are available in literature about the role of TFEB on cancer metabolism, but it is known that TFEB influences normal cell metabolism.

Results

We investigated the role of Tfeb in the regulation of proliferative features and metabolic aspects of melanoma cells. By loss of function approach, we explored Tfeb effects in different melanoma cell lines characterized by the

most important mutations described in melanoma patients. Specifically, we focused on the murine D4M cell line, carrying the V600E mutation on *Braf* and the *Pten* loss.

Through allograft model in mice, we demonstrated that D4M tumors carrying sh-*Tfeb* are smaller compared to the control ones (70%), due to a reduction of the proliferation rate (50%). Interestingly, sh-*Tfeb* tumors also present a reduced vascular area.

We confirmed our observations *in vitro:* D4M melanoma cells carrying sh-*Tfeb* compared to control cells show a reduction of the proliferative rate (30%), a block in G1-S phase of cell cycle mediated by a strong transcriptional reduction of different key genes involved in G1-S transition. In particular, we reported a strong decrease in the transcription and protein synthesis of Ccnd1 and Cdk4.

While Tfeb can directly regulate *Cdk4* expression, we found out that its effect on *Ccnd1* is mediated through MAPK pathway.

We also evaluated that sh-*Tfeb* D4M melanoma cells *in vivo* and *in vitro* present a general metabolic alteration characterized by the impairment of glycolysis (60%), TCA cycle (49%), oxidative phosphorylation (46%) and cholesterol synthesis (48%). These metabolic effects are connected with a reduction of the cellular ATP amount (30%). Conversely, *Tfeb* silencing causes an increase of fatty acid β-oxidation (200%) and mitochondrial stress and damage (220%).

Conclusions

Our data suggest a pivotal role for TFEB in maintaining D4M active proliferative behaviour and operative metabolic pathways necessary for energy request satisfaction.

INTRODUCTION

Cutaneous melanoma derives from skin melanocytes, pigment-producing cells located in the epidermis, whose primary function is to protect keratinocytes from DNA damage induced by UV (Wellbrock and Arozarena, 2016).

Melanoma is the most frequent form of cancer found in young adults (Raimondi et al, 2020) with a high risk of metastatic spread, although most patients have localized disease at the time of the diagnosis and are treated by surgical excision of the primary tumor (Rastrelli et al, 2014).

The frequency of malignant melanoma has been increasing worldwide: from being a rare cancer one century ago, it is now the fifth most common form of cancer in men and the sixth in women in the United States, where the incidence of malignant melanoma has increased by 270% from 1973 to 2002 (Rastrelli et al, 2014).

Unlike other solid tumors, melanoma mostly affects young and middle-aged people with median age at the time of diagnosis of 57. Moreover, the white population has an approximately 10-fold greater risk of developing cutaneous melanoma than black, Asian or Hispanic populations (Rastrelli et al, 2014).

Four major variants of primary cutaneous melanoma have been classically described: superficial spreading melanoma (SSM), nodular melanoma (NMM), lentigo maligna melanoma (LMM), and acral lentiginous melanoma (ALM) (Ostrowski and Fisher, 2021).

Melanoma has been proved to be a multi-factorial disease arising from interactions between genetic susceptibility and environmental elements. The most important known environmental factor is the exposure to UV rays

that can induce genotoxic effect, whereas host risk factors are the number of melanocytic nevi, familiar history and genetic susceptibility. Particular phenotypic features such as red hair, fair skin, lots of freckles, light eyes, sun sensitivity and an inability to tan, raise the risk of developing melanoma by approximately 50% (Rastrelli et al, 2014).
Moreover, it has been demonstrated that melanoma, as other malignancies, develops through a stepwise process that brings to the accumulation of genetic mutations leading to uncontrolled cell proliferation and the appearance of an invasive cell phenotype. The clear sequence of genetic alterations that drives melanocyte transformation is still incompletely understood but starts to be unveiled through the massive use of NGS for the genetic characterization melanoma lesions (Savoia et al, 2019).
In recent years, targeted therapies and immunotherapy have improved the outcomes of metastatic melanoma, but relapse still occurs. For this reason, challenges remain in investigating the biology of therapeutic resistance (Ostrowski and Fisher, 2021).

The transcription factors of the microphthalmia/transcription factor E (MIT-TFE) family, to which belongs the Transcription Factor EB (TFEB), have a central role in melanocyte and melanoma homeostasis. In particular, TFEB, per se or through its interaction with other MiT/TFE proteins, is able to modulate different transcriptional pathways supporting melanoma development. Increasing evidence indicates a correlation between TFEB expression level and melanoma oncogenesis, chemio-resistance, immune response and patient survival indicating TFEB as a good candidate for melanoma therapy.

1. MiT family and TFEB

1.1 MiT family

MiT family of basic helix-loop-helix leucine-zipper (bHLH-Zip) transcription factors is composed by TFEB (Transcription Factor EB), TFE3 (Transcription Factor E3), TFEC (Transcription Factor EC) and MITF (Microphthalmia-associated Transcription Factor), as classified by Steingrímsson et al in 2004 (Steingrímsson et al, 2004).

MITF was the first component to be discovered in 1993 when was observed that mutation in the microphthalmia (mi) locus caused in mice a particular phenotype characterized by loss of pigmentation, reduced eye size, failure of secondary bone resorption, reduced numbers of mast cells, and early onset of deafness (Hughes et al, 1993; Hodgkinson et al,1993). Then, the human homolog was found (Tachibana et al, 1994).

MITF-TFE proteins are structurally related and conserved through evolution in vertebrates. The specific roles played by the different mammalian MiT members seem to be exerted by a single protein in invertebrate organisms, suggesting that the common ancestor gene underwent multiple rounds of duplication that allowed a functional specialization (Napolitano and Ballabio, 2016).

Their tissue expression and activity are highly regulated by alternative splicing, promoter usage, and post-translational modifications (La Spina et al, 2021).

They share a similar structure owning a high sequence homology: a basic helix-loop-helix leucine zipper (bHLH-Zip) dimerization motif, a transactivation region and DNA-contacting basic domains as homo-/hetero-

dimers. The external portions of these regions are highly variable (Fisher et al, 1991; Hemesath et al, 1994).

In particular, they have an identical basic region required for DNA binding with which they bind to E-box (CANNTG), M-box (TCATGTGA) and CLEAR-box (GTCACGTGAC) elements in the promoter regions of their target genes (Steingrímsson et al, 2004). The specific activity of each MiT-TFE family member is considerably dependent on the expression signature in different tissues (Kuiper et al, 2004).

The specificity of DNA binding by each transcription factor of family is related to the sequences flanking the E-box (Ephrussi box). Overall, they share a high degree of overlap not only in their structure, but also in their activity and regulatory machinery (Bahrami et al, 2020).

The palindromic CACGTG E-box is a motif also recognized by other bHLH-Zip transcription factors, such as MYS, MAX and MAD proteins (Napolitano and Ballabio, 2016).

TFEB, MITF and TFE3 also contain a conserved activation domain that is important for their transcriptional activation (Beckmann and Kadesch, 1990; Sato et al., 1997). The activation domain is missing in TFEC, which is the most divergent member of the family and appears to inhibit transcription, rather than activating it (Zhao et al, 1993).

MiT proteins can bind the DNA both as homodimers and heterodimers with any other family member, but cannot dimerize with other bHLH-Zip transcription factors (Hemeseath et al, 1994; Pogenberg et al, 2012). However, the difference in the functions of MiT homodimers compared to heterodimers is still unknown (Muhle-Goll et al, 1994; Napolitano and Ballabio, 2016).

Even though TFEB was initially identified as the only member of the MITF-TFE family able to regulate the expression of numerous lysosomal and

autophagic genes, it was later discovered that TFE3 is also a master regulator of lysosomal biogenesis and autophagy (Martina et al, 2014b; Martina and Puertollano, 2017).

The mechanism of TFE3 activation in response to nutrient levels, its binding to CLEAR elements and its ability to induce lysosomal biogenesis and autophagy are characteristics shared with TFEB (Martina et al, 2014b). In some cell types, TFEB and TFE3 seem partially redundant in their ability to induce lysosomal biogenesis and both must be present for a maximal response (Martina et al, 2014b, Pastore et al, 2016).

However, as that the expression of TFEB and TFE3 is differentially regulated during development and that they are present in different tissues with different signatures, it is plausible that some of their biological functions should be unique (Martina and Puertollano, 2014a; Raben and Puertollano, 2016).

Given that the mechanism of nutrient regulation by TFEB and TFE3 appears to be conserved across different species, it is plausible to imagine the existence through the evolution of a process dedicated to the metabolic control of the cellular response to stress mediated by the cross-talk between the lysosome and the nucleus (Martina and Puertollano, 2017).

MITF is predominantly expressed in melanocytes and retinal pigment epithelial cells, but is also expressed in a variety of other cell types such as osteoclasts, natural killer cells, macrophages, mast cells, B cells, and cardiac muscle cells (Ploper and De Robertis, 2015). However, it has been seen that it is crucial for melanocyte development and differentiation, and has been termed a lineage-specific oncogene in melanoma (Levy et al, 2006).

MITF is subject to differential splicing and differential promoter usage, giving rise to multiple isoforms that differ in their first exon. Many of these isoforms

show a tissue-restricted expression pattern. For example, MITF-M is an isoform preferentially expressed in melanoblasts and melanocytes (Takeda et al, 2002).
Mutations in the MITF gene can give rise to mice that have a white coat color, are deaf, and present microphthalmia (Steingrímsson et al, 2004).

TFEC is the least studied member of the MiT family. Its expression is restricted to macrophages and its function has not been properly analyzed (Ploper and De Robertis, 2015).

1.2 TFEB gene and protein

TFEB was isolated for the first time thanks to its binding to the major late promoter of adenovirus (Carr et al, 1990).
Human TFEB is located on chromosome 6 (6p21.1) and encodes a 2364-bp mRNA transcript, consisting of two non-coding and eight coding exons, with a 302-bp 5' UTR followed by a start codon in exon 3 and a stop codon in exon 10, followed by a 621-bp 3' UTR (Sardiello et al, 2009; Palmieri et al, 2011; Settembre et al, 2011; Astanina et al, 2021; Doronzo et al, 2021; Corà et al, 2021).
At least seven different mRNA of TFEB containing alternative 5' exons have been described with restricted and differential tissue distributions (Kuiper et al, 2004; Martina et al, 2014a).
TFEB mRNA produces a 476-AA protein with a 10-AA strong transcription activation domain (AD), a 54-AA bHLH domain containing a putative nuclear localization signal (NLS) and a 22-AA leucine-zipper DNA-binding domain (LZ) (Kauffman et al, 2014).

1.3 TFEB regulation

TFEB undergoes post-translational modifications, which directly regulate its protein interactions and subcellular localization. In particular, the current understanding of TFEB biology considers phosphorylation the major driver of its regulation (Sardiello et al, 2009; Palmieri et al, 2011; Settembre et al, 2011; Cortes et al, 2019; Astanina et al, 2021; Doronzo et al, 2021; Corà et al, 2021).

Being a transcription factor, TFEB continuously shuttles between the cytosol and the nucleus and therefore its activity depends on its cellular localization. At least 3 different kinases have been shown to phosphorylate TFEB: Mechanistic target of rapamycin complex 1 (MTORC1), Extracellular signal-regulated kinase 2 (MAPK1/ERK2), and Protein kinase Cb (PRKCB). They can phosphorylate ten serine residues having distinct effects on TFEB (Settembre et al, 2013).

It has been demontrated that two serine residues are crucial in determining the subcellular localization of TFEB and are phosphorylated by mTORC1 and ERK2: Ser142 and Ser211 (Settembre et al, 2011; Settembre et al, 2012; Roczniak-Ferguson et al, 2012; Martina et al, 2012).

Generally, when TFEB is phosphorylated is considered inactive because sequestred in the cytosol and in particular at lysosome level, whereas unphosphorylated TFEB is active because is free and it can translocate into the nucleus and induce the expression of target genes.

Mutations of these serines to alanines resulted in significantly increased nuclear localization of TFEB (Settembre et al, 2011; Settembre et al, 2012).

Under nutrient-rich conditions, TFEB is temporarily recruited to lysosomes through its interaction with active RAG GTPases where it is phosphorylated

at both serines, S211 via mTORC1 and Ser142 via ERK2, and therefore its transport into the nucleus is inhibited (Martina and Puertollano, 2013; Vega-Rubin-de-Celis et al, 2017).
In particular, Ser phosphorylation enhances the detachment of TFEB from the lysosomes and connects it with the 14-3-3 family of proteins that maintain TFEB in the cytoplasm and prevent its transcriptional function (Roczniak-Ferguson et al, 2012; Martina et al, 2012; Martina and Puertollano, 2013).
Moreover, phosphorylated S142 and S211 induce the degradation of TFEB through ubiquitin-proteasome pathway (Sha et al, 2017).

Conversely, under starvation conditions, when mTORC1 is inactive and therefore de novo TFEB phopshorylation is inhibited, unphosphorylated TFEB separates from the 14-3-3 and rapidly accumulates in the nucleus where it acts as a transcription factor (Raben and Puertollano, 2016).
In addition to nutrient deprivation, pharmacological suppression of mTOR and lysosomal stress may lead to TFEB dephosphorylation and migration to the nucleus (Sardiello et al, 2009; Palmieri et al, 2011; Settembre et al, 2011; Roczniak-Ferguson et al, 2012; Settembre et al, 2012; Cortes et al, 2019; Astanina et al, 2021; Doronzo et al, 2021; Corà et al, 2021).

It was observed that overexpression of TFEB increased mTORC1 activation whereas its depletion significantly impaired mTORC1 signalling upon nutrient stimulation both in vitro and in vivo. Thus, the activation of mTORC1 in response to nutrients is regulated by TFEB creating a regulating loop between TFEB and mTORC1 (Di Malta and Ballabio, 2017; Di Malta and Ballabio, 2018).
MiT family proteins induce mTORC1 lysosomal recruitment and activity through the direct regulation of RAGD expression, necessary for mTORC1

connection to lysosomes (Di Malta et al, 2017). In particular, TFEB has a binding site on the promoter of RAGD, so its influence on RAGD protein levels is not autophagy-mediated, but directly controlled by the transcription factor (Di Malta and Ballabio, 2017).
Therefore, mTORC1 and TFEB are part of a complex mutual regulatory loop that governs cell response to nutrient availability or adaptation to starvation. The discovery that MiT family members are positive regulators of mTORC1 signaling led to the identification of a novel pathogenetic mechanism in cancer. In particular, tumors associated with hyperactivation of MiT-TFE proteins (melanoma, tRCC and PDAC) show constitutive induction of RAGD transcripts, correlated with hyperactivation of mTORC1 signaling and increased proliferation (Perera et al, 2019).

Other important cellular kinases have been seen to influence TFEB localization and stability: AKT acting on S467 (Palmieri et al, 2017) and GSK3β phosphorylating Ser134 and Ser138 (Li et al, 2016; Di Malta et al, 2019).

More recently, MAP4K3 (GLK) was found to be a regulator of TFEB, linking amino acid supply to TFEB activation status. It phosphorylates TFEB on Ser3, and this phosphorylation event is required for mTORC1 to phosphorylate TFEB on Ser211 to insure its complete inactivation via cytosolic sequestration with chaperone-like cytosolic protein 14-3-3 (Hsu et al, 2018).

In contrast, PRKCB-induced phosphorylation of Ser461, Ser466, and Ser468 is suggested to stabilize TFEB and increases its activity (Ferron et al, 2013).
As already said, TFEB subcellular localization is dynamically controlled by

its continuous shuttling between the cytosol and the nucleus; the nuclear export represents a limiting step. TFEB nuclear export is mediated by CRM1 and is modulated by nutrient availability via mTOR-dependent phosphorylation of Ser142 and Ser138, which are localized in proximity of a nuclear export signal (NES) (Napolitano et al, 2018).

The transcription-regulating activity of TFEB is dependent on its phosphorylation modification, but the phosphatases involved in TFEB dephosphorylation have remained elusive (Tong and Song, 2015).
Nevertheless, it has been demonstrated that lysosomal calcium release through MCOLN1 (mucolipin1) activates calcineurin, an endogenous serine/threonine phosphatase, which dephosphorylate TFEB at Ser211 and Ser142 promoting its nuclear translocation (Medina et al, 2015; Tong and Song, 2015; Martina and Puertollano, 2018).
More recently, the protein phosphatase 2A (PP2A) has been shown to dephosphorylate TFEB upon induction of acute oxidative stress by sodium arsenite (Martina et al, 2018; Di Malta et al, 2019).

The links between WNT signalling and MiT family are profound and variegated, producing sometimes contrasting effects in different conditions. The first evidences suggesting a connection between the two pathways focused on MITF. In fact, MITF was found to interact with LEF1, a mediator of WNT signalling, ensuring efficient propagation of WNT signals in different types of cells (Yasumoto et al, 2002).
As already reported, it is important to underline that TFEB but also MITF have different phosphorylation sites, that permit the regulation of their activity, on which acts GSK3-β, part of the destruction complex of WNT (Ploper et al, 2015). It has been demonstrated that GSK-3β inhibition brings to TFEB nuclear translocation and the following autophagy and lysosome

network induction (Marchand et al, 2015).

Interesting was the discovery of a positive feedback loop among GSK3-β and MiT-TFE members. Different works considered that complex regulation: summarizing, MITF, TFE3 and TFEB expression increases the number of multivesicular bodies that sequester the destruction complex composed by different proteins including GSK3-β, enabling the enhancement of WNT signaling and therefore the induction of different processes such as proliferation, survival, invasion and metastasis (Blitzer and Nusse, 2006; Yamamoto et al, 2006; Taelman et al, 2010; Ploper et al, 2015; Ploper et al, 2015b). This phenomenon was found to be important during the proliferative stages of melanoma (Ploper et al, 2015).

Moreover, kidney-specific TFEB overexpression in mice induces the establishment of renal carcinomas due to the activation of the WNT pathway. Confirming that point, WNT inhibition brings the normalization of the proliferation rate and rescues the disease phenotype in vivo (Calcagnì et al, 2016).

A recent work put a new piece in this intriguing puzzle: it seems that TFEB is part of the destruction complex of WNT. In fact, the authors claim that about 27% of Wnt3a-induced genes are TFEB dependent, but that these TFEB-mediated WNT target genes are different from canonical TFEB target genes involved in autophagy and lysosomal biogenesis. They found a new transcription factor complex composed by PARsylated TFEB and β-catenin-TCF/LEF1 that can induce these particular genes (Kim et al, 2021).

TFEB also regulates its own expression through a starvation-induced autoregulatory loop. The TFEB promoter contains multiple CLEAR elements to which the transcription factor binds to induce further TFEB expression (Settembre et al, 2013b).

1.4 Canonical functions of TFEB: the CLEAR network

TFEB is known to be a transcription factor. It can form homodimers or heterodimers with the other members of the MiT family (Hemeseath et al, 1994; Pogenberg et al, 2012).
It is characterized by a basic region that can bind a palindromic DNA sequence (CACGTG) located in the proximal promoter of its target genes (Sardiello et al, 2009; Palmieri et al, 2011).
This sequence, called E-box, belongs to the CANNTG motif that is recognized by other members of the helix-loop-helix leucine-zipper family of transcription factors. DNA binding in the HLH-LZ family is influenced by sequences immediately flanking the E-box: TFEB prefers the GTCACGTGAC consensus sequence that is known as a Coordinated Lysosomal Expression and Regulation, the CLEAR motif (Sardiello et al, 2009; Palmieri et al, 2011; Puertollano et al, 2018).

Lysosomes are the principal digestive compartment of the cell. In fact, they are able to degrade structurally different molecules such as proteins, glycosaminoglycans, nucleic acids and complex lipids into their building blocks, which are then recycled in biosynthetic pathways or further degraded to generate energy (Sardiello and Ballabio, 2009b).
For cellular clearance, the tight interaction between lysosomal function and the autophagic pathway is fundamental.
Autophagy is a complex catabolic process enabling the degradation of intracellular components in order to maintain cellular homeostasis getting rid of long-lived or damaged proteins, protein aggregates and exhausted or dysfunctional organelles (Sardiello and Ballabio, 2009b).
Autophagy is a fundamental function of eukaryotic cells and is well conserved from yeast to humans (Nakatogawa et al, 2009).

Three main types of autophagy have been described: macroautophagy, microautophagy, and chaperon-mediated autophagy. Macroautophagy involves the formation of a double-membrane vesicle, the autophagosome, which incorporates cytoplasmic molecules and then fuses with lysosomes to generate autophagolysosomes, structures in which cargo substrates are degraded by lysosomal enzymes (Di Malta et al, 2019).

As a major cellular degradative system, the autophagic process is strictly controlled. In normal conditions, autophagy takes place constitutively at basal levels but is strongly induced by different extracellular and intracellular stimuli and stressors, such as nutrient or growth factor limitation, oxidative stress, and accumulation of damaged organelles or misfolded proteins (Tong and Song, 2015; Corà et al, 2021).

Autophagy is made by subsequential key events that carry out the self-degradative process (Glick et al, 2010):

1 - control of phagophore formation by Beclin-1/VPS34 at the endoplasmic reticulum in response to stress signalling pathways;

2 - ATG5-ATG12 conjugation and interaction of the complex with ATG16L for subsequent multimerization at the phagophore;

3 - processing of LC3-I to LC3-II and insertion into the rising phagophore membrane;

4 - incorporation of targets for degradation;

5 - complete formation of the autophagosome;

6 - fusion of the autophagosome with the lysosome;

7 - degradation by lysosomal enzymes of engulfed molecules.

TFEB can bind a DNA sequence known as a Coordinated Lysosomal Expression And Regulation, the CLEAR motif, present on the promoter of different genes involved in lysosomal function as well as endocytosis,

autophagy and phagocytosis (Sardiello et al, 2009; Palmieri et al, 2011).
TFEB modulates the expression of at least 471 downstream targets genes that contain the CLEAR regulatory motif in their promoter: the so called “CLEAR network” (Palmieri et al, 2011; Settembre and Medina, 2015; Corà et al, 2021).
These genes encode for proteins that govern the expression, localization, entrance, influx, and performance of lysosomal and non-lysosomal enzymes participating in the destruction of cellular macromolecules such as proteins, glycosaminoglycans (GAG), lipids, glycogen, hemoglobin and chitin. Other molecular pathways regulated by the CLEAR network include the transcriptional PPAR-γco-activator-1 (PGC1), involved in mitochondrial biogenesis and respiration and in hepatic gluconeogenesis, and the AMP-activated protein kinase (AMPK) signaling, regulator of cellular energy in response to numerous stress conditions (Bahrami et al, 2020).
Example of direct targets of TFEB are ATG9, LC3, SQSTM1, and LAMP1, genes involved in the sequential steps of autophagy, from cargo recognition and autophagosome formation to vesicle fusion and substrate degradation (Palmieri, 2011).
TFEB coordinates a transcriptional program able to control the main cellular degradative pathways and to promote intracellular clearance (Napolitano and Ballabio, 2016; Corà et al, 2021) enhancing lysosome number, activity and autophagy activation (Martina and Puertollano, 2017).
For these reasons TFEB is considered the master regulator of lysosome biogenesis, autophagy and energy metabolism (Sardiello et al, 2009; Settembre et al, 2011; Settembre et al, 2013).
The transcription factor is also involved in lysosomal exocytosis, a Ca^{2+}-regulated process characterized by the recruitment of lysosomes to the cell surface and their fusion with the plasma membrane (PM), and the release of their content outside the cell. TFEB regulates lysosomal exocytosis

increasing the pool of lysosomes in the proximity of the PM and promoting their fusion with PM by raising intracellular Ca^{2+} levels through the activation of the lysosomal Ca^{2+} channel MCOLN1 (Medina et al, 2011).

A lot of cellular stresses in addition to starvation, including lysosomal, mitochondrial, ER stress and also reactive oxygen species can improve TFEB nuclear localization and so its transcriptional activity in order to respond to environmental conditions and lead to homeostasis (Napolitano and Ballabio, 2016).
Treatment with ER stressors causes translocation of TFEB to the nucleus in a process that is dependent on pERK and calcineurin but not on mTORC1. Activated TFEB and TFE3 enhance cellular response to stress by inducing direct transcriptional upregulation of ATF4 and other UPR genes. Under conditions of prolonged ER stress, TFEB contributes to cell death (Martina et al, 2016).
In general, any sort of stress could potentially activate TFEB. It does not regulate the basal transcription of its targets but rather enhances their transcriptional levels to respond to environmental cues (Napolitano and Ballabio, 2016).
In fact, cells maintain homeostasis in stressful situations through lysosomal status enhancing the transcription of genes necessary to correct perturbations, a process known as lysosomal adaptation. Through such communication between the lysosome and nucleus, TFEB regulates metabolism and cellular clearance (Martini-Stoica et al, 2016).

Underlining this function, TFEB is linked to the main pathways of the cell governing energy homeostasis: mTOR and AMPK (Settembre et al, 2012; Sakamaki et al, 2018)

1.5 Other roles of TFEB in cellular homeostasis

Besides its traditional role as master regulator of lysosomal and autophagosomal biogenesis that permits adaptation to various types of stress, recent findings have demonstrate new implications of TFEB in the cellular biology.

In fact, it is clearly implicated in different functions such as metabolism, immunity, angiogenesis, inflammation, proliferation, and drug resistance. Moreover, it seems to influence other cellular pathways such as migration, invasiveness, stemness, cell death and EMT (Astanina et al, 2020; Doronzo et al, 2021).

Conditional TFEB KO mice in liver show severe alterations of lipid metabolism, bringing to obesity and diabetes. Similarly, TFEB absence in the skeletal muscle results in impaired glucose homeostasis and mitochondrial biogenesis with decreased fatty acid oxidation and oxidative phosphorylation (Puertollano et al, 2018). Generally, gain- and loss-of-function experiments in mouse muscle demonstrated a pivotal role for TFEB in controlling energy balance in this tissue (Napolitano and Ballabio, 2016).

Another tissue-specific function of TFEB has been described in osteoclasts suggesting a role in bone resorption (Napolitano and Ballabio, 2016). In fact, TFEB deletion specifically in osteoclasts alters osteoclast function and increases bone mass (Ferron et al, 2013).

Moreover, it has been seen that TFEB is able to influence the immune response both indirectly, through its traditional coordination of the autophagy-lysosome system, and directly by the transcriptional activation of immune-related genes (Nabar and Kehrl, 2017).

In macrophages, depletion of TFEB results in impaired expression and secretion of several pro-inflammatory cytokines (Napolitano and Ballabio, 2016).

Two different studies underlined how endothelial TFEB influences the process of atherosclerotic plaque formation (Lu et al, 2017) and the post-ischemic angiogenesis (Fan et al, 2018).

Lu et al. demonstrated that TFEB is fundamental in modulating the inflammatory status and enhancing the antioxidative capacity of endothelial cells. TFEB could therefore be modulated in people at risk to develop vascular disease in order to reduce the incidence of atherosclerosis and its correlated adverse events (Lu et al, 2017).

Similarly, Fan et al. suggested that TFEB could be a novel molecular target for post-ischemic treatment in order to limit the tissue damage and improve the blood flow recovery. In fact, they saw that TFEB overexpression in ECs in mice after ischemic injury increased angiogenesis, promotes endothelial tube formation and migration through autophagy and the activation of AMPKα signaling pathway (Fan et al, 2018).

Influence of TFEB in cellular proliferation has been documented in different tissues and cancer types, but the topic will be exhaustively discussed later, as TFEB involvement in other cellular pathways such as metabolism, angiogenesis and migration.

Different works correlate TFEB function with p53 activity. In fact, they both translocate to the nucleus under cellular stresses and it seems that they cooperate in order to give the best response to genotoxic insults (Brady et al, 2018; Zhang et al, 2017).

An increasing number of observations suggests a fundamental role of TFEB in vascular biology.

TFEB null mice die at embryonic day 9.5-10.5. At day 9.5 knockdown embryos are indistinguishable from their wild type littermates concerning size, appearance and cellular conditions. Nevertheless, the day after they undergo developmental arrest and cell death can be seen in several tissues

resulting in autolysis of the embryo. While TFEB is present at low levels in the embryo, it is expressed at high levels in the labyrinthine trophoblast cells of the placenta. The labyrinth layer is quite normal in the TFEB mutant placenta but fails to express VEGF-A, required to normal vasculogenesis. The embryonic vasculature is unable to invade the placenta, halting the exchange of nutrients and causing severe hypoxia and embryonic lethality (Steingrímsson et al, 1998).

During atherogenesis, the lysosomal stress induced by the accumulation of cholesterol activates a TFEB response, which triggers an anti-inflammatory (Lu et al, 2017; Song et al, 2019) and anti-atherogenic response (Emanuel et al, 2014).

It has been demonstrated that laminar shear stress, which protects against atherogenesis, increases TFEB abundance and its translocation into the nucleus in human umbilical vein endothelial cells (HUVECs). Endothelial inflammation and oxidative stress are important factors that lead to endothelial dysfunction and consequent atherosclerotic plaque formation. TFEB is able to limit leukocyte recruitment, suppressing the expression of adhesion molecules by endothelium, and reduce the amount of intracellular ROS, promoting the expression of antioxidant factors (Lu et al, 2017).

The overexpression of TFEB in endothelial cells (ECs) promotes post-ischemic angiogenesis through the activation of autophagic flux. It has been discovered that TFEB is able to modulate EC migration, tube formation and apoptosis, but not proliferation, improving post-ischemic blood flow recovery. In contrast, EC-TFEB KO mice fail to restore blood perfusion. TFEB is normally overexpressed in the mouse ischemic skeletal muscle at day 3 after ischemia and it translocates to the nucleus to respond to nutrient deprivation. It has been found an interplay between TFEB, mTOR and AMPKα that demonstrate the importance of autophagy in endothelial cells after ischemia (Fan et al, 2018).

Finally, Doronzo et al. demonstrated that the specific loss of TFEB in ECs alters the mid and late phase of vascular development in mouse. In fact, embryos lacking TFEB in ECs died between E10.5 and E11.5, displaying defects of the vascular tree. In particular, they saw a reduction in larger caliber vessels and in the capillary network (Doronzo et al, 2019).
The effect of TFEB may begin after the formation of primitive vascular plexus because its deletion did not affect the hemangioblasts. Moreover, post-natal vascular maturation in the retina and kidney was altered in TFEB mutants (Doronzo et al, 2019).

1.6 TFEB in neurodegenerative diseases

TFEB is highly expressed in the central nervous system (CNS) and is active in both neurons and astrocytes. Given that the autophagy-lysosome system is involved in the degradation of long-lived or damaged proteins, its deficits in the CNS result in protein aggregation, generation of toxic protein species, and accumulation of dysfunctional organelles (Martini-Stoica et al, 2016)
For this reason, TFEB represents an appealing therapeutic target for lysosomal storage diseases (LSDs) and neurodegenerative diseases (Napolitano and Ballabio, 2016).
LSDs are characterized by genetic defects in specific lysosomal genes that lead to accumulation of substrates in the cell (Parenti et al, 2015). Therefore, overexpression of TFEB in cellular and mouse models of several LSDs have been shown to be beneficial in reducing substrate accumulation, improving the severity of cellular and tissue phenotypes (Napolitano and Ballabio, 2016).
More recently, TFEB activity and localization have been found to be altered in neurodegenerative disorders such as Alzheimer's disease, Parkinson's disease, and Huntington's disease, implicating impaired TFEB function in

the defective cellular clearance phenotypes linked pathogenesis. Moreover, recent genome-wide association studies linked an intronic region variant of TFEB to late-onset Alzheimer's disease risk in African-American populations. (Cortes and La Spada, 2019).

2. Role of MiT family and TFEB in tumours

Mutated or aberrantly regulated, MiT family proteins can promote or support tumor development and growth.
In fact, genomic amplifications of MITF are found in about 20% of melanomas, while translocations and rearrangements of TFE3 and TFEB are present in pediatric renal cell carcinoma (RCC) and alveolar soft part sarcoma (ASPS) (Perera et al, 2019).
Moreover, an boost in the autophagic flux has been found in pancreatic ductal adenocarcinoma (PDAC) cell lines and patient cancers due to an increase of TFEB, MITF and TFE3 expression (Astanina et al, 2020).

The majority of MITF current knowledge derives from studies in melanocytes and melanomas, in which the MITF-M isoform is considered the master gene regulator of the melanocytic lineage required for the development, growth and survival of melanocytes. MITF functions as a lineage addiction oncogene for melanoma (Steingrimsson et al, 2004; Garraway et al, 2005; Ploper and De Robertis, 2015).

2.1 MiT family in melanoma

Over a dozen rodent models with germline loss-of-function mutations of the MITF gene show various pigmentation defects such as albinism, ocular

defects and deafness. In humans, heterozygous MITF mutations are responsible for the Waardenburg Syndrome IIA, a developmental disorder characterized by melanocyte deficiency and phenotypic manifestations similar to those observed in mice (Kauffman et al, 2014; Bahrami et al, 2020).

These observations were the starting point that permitted to consider the microphthalamia-associated transcription factor (MITF) as an important piece of the puzzle in melanocyte biology: MITF is essential for melanocyte cell-fate determination during commitment from pluripotent precursor cells in the neural crest and therefore critical for the development of the melanocyte lineage itself (Widlung and Fisher, 2003).

Being a melanocyte lineage determinant, if overexpressed, together with S0X10 and PAX3, MITF can directly reprogram human and mouse fibroblasts into functional melanocytes (Perera et al, 2019).

Then, Garraway et al identified a melanoma amplification involving MITF gene that was prevalent in metastatic disease and correlated with decreased overall patient survival. They named MITF as “lineage survival” or “lineage addiction” oncogene required for both tissue-specific cancer development and tumour progression (Garraway et al, 2005).

MITF exists in different isoforms but the MITF-M is exclusive to the melanocytes because is expressed through a unique melanocyte-restricted promoter/enhancer (Widlung and Fisher, 2003).

MITF, and in particular MITF-M, is now considered a master regulator of melanocytes and a major melanoma oncogene being amplified in 30 to 40% of melanomas (Ploper et al, 2015).

MITF-associated tumors are usually caused by gene amplifications but also rare somatic mutations have been reported. These mutations are generally located in the MITF transactivation domain, suggesting that increased transcriptional activity of MITF is sufficient to trigger tumorigenesis (Perera

et al, 2019).
For example, MITFE318K has been found in patients with familial melanoma and a small fraction of sporadic cases: the mutant MITF protein obtained cannot be properly SUMOylated and has increased transcriptional activity representing a gain of function of MITF activity (Perera et al, 2019).
The ability of MITF to promote oncogenesis is not restricted to the melanocyte lineage, since the MITFE318K mutant also predisposes to renal cell carcinoma (Ploper and De Robertis, 2015).

MITF is the master regulator of the melanin synthesis pathway through direct transcriptional regulation of melanogenic enzymes such as PMEL, tyrosinase (TYR), TRP-1 and -2, and DCT (Ostrowski and Fisher, 2021).
But this is not sufficient to explain why melanocytes and melanoma cells absolutely require the expression of this factor for their development and growth. In fact, several lines of evidences suggest its absolute importance for the melanocytic compartment: first, inactivating MITF by mutations does not permit to mouse embryonic melanocytes to mature and survive; second, depleting MITF in vitro brings to complete and stable eradication of melanoma cells; third, MITF is overexpressed in most melanomas (Vachtenheim and Ondrušová, 2015).
MITF directly influences the expression of various other target genes that are important for the survival of melanocytes and melanoma cells, such as the antiapoptotic proteins BCL2 and BCL2A1, and the cell cycle regulator CDK2 and CDK4 (Ostrowski and Fisher, 2021).
It also regulates genes involved in DNA replication, mitosis, motility and DNA repair (Wellbrock and Arozarena, 2015; Ploper and De Robertis, 2015).
Moreover, MITF controls oxidative metabolism and allows melanoma cells to adapt to local nutrient conditions (Wellbrock and Arozarena, 2015).
Further supporting its contribution in melanogenesis, MITF expression is

strongly activated by the Melanocortin 1 receptor (MC1R) via its ligand, the alpha-melanocyte stimulating hormone (Bahrami et al, 2020).
MITF expression is really variable among tumor cell subpopulations and this confers marked heterogeneity and plasticity in the tumor tissue (Vachtenheim and Ondrušová, 2015).
M-MITF is expressed in more than 80% of melanomas and detectable throughout all stages of cancer development being essential for the survival of melanocytes and melanoma cells (Wellbrock and Arozarena, 2015).
The current idea is that low MITF levels promote senescence, intermediate/high levels cause proliferation and cell growth, whereas very high levels stimulate differentiation and growth arrest (Ploper and De Robertis, 2015).
Fine-tuning of MITF levels and activity in melanoma likely involves the integration of microenvironmental cues, epigenetic states and activities of different upstream signaling pathways (Perera et al, 2019).

As already treated in a previous paragraph, melanoma relies on the endolysosomal pathway for growth more strongly than other cancers and lysosomal are more highly expressed in melanomas compared to other tumor types.
It has been seen that in melanoma cell lines MITF levels correlate with the expression of a large subset of lysosomal genes such as Rab7, LAMP1, and CD63 and that the vescicular structures, called multivescicular bodies (MVBs), are increased in number when MITF is overexpressed (Ploper et al, 2015).
Nevertheless, these numerous MVBs that accumulate in melanoma cells are not functional lysosomes as they are less active in proteolysis and fail to conclude properly the autophagic flux. However, they are able to capture Axin1, phospho-LRP6, phospho-β-catenin and GSK3, parts of the

degradation complex of Wnt, in the presence of Wnt ligands (Ploper et al, 2015).
The relocalization of the desruption complex components in the MVBs significantly enhances Wnt signaling and stabilizes MITF protein that is no longer phosphorylated and inhibited by GSK3 (Ploper et al, 2015).
In the presence of Wnt ligand, therefore, a positive feedback loop is generated, in which MITF stabilized by Wnt increases MVB biosynthesis which in turn potentiates Wnt signaling enhancing, as a final result, melanoma cell proliferation (Ploper and De Robertis, 2015).
It is likely that other tumors that overexpress TFEB and TFE3 may also rewire the endolysosomal pathway similar to what happens in melanoma with MITF alteration (Ploper and De Robertis, 2015).
Moreover, depletion of MITF in melanoma cells and melanocytes attenuates the response to starvation-induced autophagy, whereas its overexpression increases the number of autophagosomes but is not sufficient to induce autophagic flux (Möller et al, 2019).

Another evidence confirming the role of MITF in regulating autophagy in melanoma is the finding that the autophagy-related protein 5 (ATG5) is downregulated in melanomas compared to nevi and melanocytes, the healthy counterpart, bringing to a general inhibition of autophagy. When ATG5 is ectopically expressed in melanoma cells, the autophagic flux increases, whereas the inhibition of proliferation takes place in parallel to the induction of senescence. Interestingly, high MITF expression levels correlate with very low ATG5 protein quantity: autophagy leads to cell senescence and melanomas with impaired autophagy and reduced ATG5 levels may escape this homeostatic mechanism. Therefore high levels of MITF might contribute to proliferation by inhibiting senescence (Ploper and De Robertis, 2015).

2.2 TFEB and melanoma

It is now clear thar also MITF-related transcription factors, TFEB and TFE3, influence the transcription of target genes responsible for the biogenesis of melanosomes, lysosome-associated organelles, important in melanoma (Bahrami et al, 2020).

In melanocytes and melanoma cells, MITF binds the CLEAR-box element in the promoters of lysosomal and autophagosomal genes but, interestingly, they are different from the lysosomal and autophagosomal genes induced by TFEB and TFE3. This point suggests that MITF, TFEB and TFE3 have specific roles in regulating the starvation-induced autophagy response in melanoma and that their presence is only in part redundant (Möller et al, 2019).

Even if TFEB expression in melanoma samples and cell lines is strongly lower compared to MITF transcript, recently it has been demonstrated that MITF and TFEB proteins, but not TFE3, directly affect each other's mRNA and protein expression. In fact, MITF positively regulates the expression of TFEB by the direct control of its promoter activity through the binding to intron 1. Moreover, both subcellular localizations of MITF and TFEB are in part regulated by the mTOR signaling pathway, which therefore influences their cross-regulatory relationship at the transcriptional level (Ballesteros-Álvarez et al, 2020).

Moreover, in BRAF-mutated melanomas, the use of BRAF inhibitors dampens ERK activity of TFEB regulation resulting in an increase in autophagy and a decrease of tumor growth. Accordingly, the expression of the dominant active TFEBS142A in A375 melanoma cells increased their in vivo tumorigenic activity (Li et al, 2019; Astanina et al, 2021).

2.3 TFEB contribution in different tumours

Several evidences suggest TFEB involvement in tumor biology with differences among tumor types, grades and tissue of origin.
Its influences can depend not only on its conclamate role as master gene of autophagy but also on other functions exerted by the transcription factor directly or indirectly.

TFEB iperactivation

Renal cell carcinoma (RCC) is the most common form of kidney cancer originating from the renal tubular epithelium. There are various subtypes of RCC different from each other for their histopathological conformation; the most frequent are clear cell renal cell carcinoma (65-70%), papillary renal cell carcinoma (15-20%) and cromophobe renal cell carcinoma (5-10%) (Amin et al, 2002).
In sporadic RCCs, about 5% of the cases are classified in a rare subgroup called translocation-RCC (tRCC), characterized by translocations and rearrangements involving MiT-TFE transcription factors. In particular, translocations involving TFE3 were the first discovered and were ones of the earliest gene fusions associated to cancer (Perera et al, 2019).
TFEB and TFEC translocations have been rarely reported as compared to those of TFE3 (Perera et al, 2019) while MiTF has been associated with hereditary RCC susceptibility (Kauffman et al, 2014).
The World Health Organization (WHO) classification has included the new category of MiT family translocation renal cell carcinoma in 2016. The behaviour of the tumors is very variable, but in general TFE3-driven cancers are more aggressive, whereas TFEB-driven ones show an indolent clinical course (Caliò et al, 2019).
tRCC mainly affects children, representing 20–50% of all pediatric RCC

cases, but is also reported in adults (Kauffman et al 2014).

Most common TFE3 gene fusions found and characterized at the mRNA transcript level in RCC tumors are PRCC-TFE3, ASPSCR1-TFE3, SFPQ-TFE3, NONO-TFE3, CLTC-TFE3. The exon structure in the different tumors is very heterogeneous, even for the same fusion partners (Kauffman et al, 2014).

Traditional TFEB rearrangement in tRCCs concerns the gene fusion between TFEB and the intronless MALAT1 genes, the best known t(6;11), that generally entails the full retention of TFEB under the control of the strong MALAT1 promoter (Davis et al, 2003).

A comprehensive genomic analysis of 161 primary papillary RCCs was performed and new fusion partners for both TFE3 and TFEB were found, even if they are very uncommon and sporadic compared to the traditional ones that are rare as well: RBM10 and DVL2 for TFE3 and COL21A1 and CADM2 for TFEB (Perera et al, 2019).

The mechanisms explaining tRCCs have not been fully understood yet.

The dysregulated activity is the most considered model: being the promoter of fusion gene very active, it permits the overexpression of TFE3 or TFEB (Perera et al, 20109). In that way, the intrinsic pro-oncogenic features of MiT-TFE transcription factors is enhanced (Bahrami et al, 2020).

TFEB-associated tRCCs are mainly characterized by t(6;11)(p21;q13), the gene fusion between TFEB on chromosome 6p21 and the Metastasis Associated Lung Adenocarcinoma Transcript 1 gene, known as MALAT1 on chromosome 11q12 (Davis et al. 2003).

MALAT1 is also called Alpha, an intronless gene with unknown function ubiquitously expressed. It encodes a single transcript of ~7.5 kb from a single exon, but it does not produce a functional protein (Kuiper et al, 2003). Alpha-TFEB gene restrains all coding exons of TFEB linked to the upstream regulatory sequences of the Alpha gene. This promoter substitution leads to

an upregulation of TFEB transcription and translation: in fact, Alpha-TFEB gene transcripts are up to 60-fold overexpressed in primary tumor cells as compared with wild-type TFEB mRNA levels in normal kidney samples (Kuiper et al, 2003).

Moreover, the balance between MiT proteins is altered: in tumor cells, TFEB transcripts account for about 90% of the total amount of MiT-TFE mRNAs, compared to about 22% in normal renal cortex samples (Kuiper et al, 2003).

Other fusion partners for TFEB are COL21A1 (Collagen type XXI alpha 1 chain), CADM2 (Cell adhesion molecule 2) and ASPSCR1 (Alveolar soft part sarcoma critical region 1) (Bahrami et al, 2020).

t(6;11) renal cell carcinoma is an extremely rare variant, accounting for 0.02% of all renal carcinomas (Caliò et al, 2019).

At the beginning, it was discovered in children, but there are also adult patients, with mean age of presentation of 34 years. Clinical course is usually indolent with a favorable clinical prognosis. An aggressive behavior is observed in about 15-20% of the cases: bigger masses and age seem to be parameters correlated with aggressiveness (Caliò et al, 2019).

More recently, another TFEB genetic alteration has been found in RCC: the 6p amplification that causes TFEB overexpression (Williamson et al, 2017). It results in enhanced cell proliferation and and increased invasive ability of RCC with parallel reduction of apoptosis (Zhan et al, 2018).

Amplification of TFEB locus is associated with aggressive behavior, multidrug resistance and unfavorable prognosis (Bahrami et al, 2020).

TFEB amplification can be independent or in association with TFEB translocation. Both TFEB gene rearrangement, as in tRCC, and amplification increase TFEB expression, but TFEB-amplified renal cell carcinomas are different from t(6;11) renal cell carcinomas (Caliò et al, 2019).

TFEB amplification can bring Vascular Endothelial Growth Factor A

(VEGFA) gene amplification, because the two genes are both located on the short arm of chromosome 6 (Caliò et al, 2019b).

Summarizing, we can say that TFEB translocation carcinoma preferentially affect children and young adults, has a favourable prognosis and only 78 cases from 1996 to 2019 have been reported, whereas TFEB-amplified carcinoma is more aggressive, concerns older people and 54 cases have been studied since 2014, some of them in concomitance with t(6;11) (Wyvekens et al, 2019).

TFEB and cancer autophagy

Processes strictly linked to cellular metabolism are autophagy and the lysosomal function that can influence the proteome, the organelle numbers and quality, altering cell functions in different ways (Amaravadi et al, 2016).

The role of autophagy in cancer is complex and dynamic, depending on the tissue of origin, the tumor type and the stage (Santana-Codina et al, 2017), but also on the nutrient availability, the microenvironment stress and the presence of the immune system (Amaravadi et al, 2016).

In cancer, autophagy can be neutral, tumor-suppressive, or tumor-promoting (Amaravadi et al, 2016).

Simplifying, it is considered to constrain tumor initiation in normal tissues by maintaining cellular and genomic integrity, regulating DNA damage and oxidative stress (Santana-Codina et al, 2017), but also getting rid of oncogenic protein substrates, toxic unfolded proteins and damaged organelles (White, 2012).

On the contrary, established cancer cells rely on autophagy for progression and maintenance because it helps to face metabolic stress providing substrates for metabolism, controlling the functional pool of mitochondria and removing damaged organelles (White, 2012; Santana-Codina et al, 2017).

During periods of growth, when external nutrients are absent or limiting, lysosome-mediated degradation and recycling of different molecules can satisfy the need of building blocks to fuel the generation of new proteins, membrane lipids, DNA and RNA (Perera et al, 2019).

In general, autophagy can be seen as the Roman God Janus in the decision of the fate of cancer cells: survival or death (Liu et al, 2013).

Different works revealed a role for TFEB in mediating anti-cancer treatment efficacy. In fact, its upregulation as a response to therapy can induce lysosomal biogenesis and an increase in autophagy that lead to resistance to different drugs (Zhitomirsky and Assaraf, 2015; Fang et al, 2017; Zhao et al, 2020).

Pancreatic ductal adenocarcinoma (PDAC) is the clearest example of tumor relying on autophagy and MiT-TFE expression.

In fact, Yang et al demonstrated that pancreatic cancer primary tumors and cell lines show a constitutively activated autophagy and profoundly depend on this process for growth. Genetically or pharmacologically inhibition of autophagy in those cell causes increased reactive oxygen species, elevated DNA damage and metabolic defects leading to decreased mitochondrial oxidative phosphorylation (Yang et al, 2011).

It was then observed that in PDA cell lines and patient-derived samples, MITF, TFE3 and TFEB are upregulated compared to normal tissues and to other tumor types, with levels only exceeded in melanoma and kidney cancers, where we have already analyzed that MiT proteins are known oncogenes. Their knockdown causes downregulation of different CLEAR genes and subsequent inhibition of cell growth. In particular, it has been demonstrated that MiT-TFE are master regulators of metabolic reprogramming in pancreatic cancer, able to maintain the cellular amino acid pool (Perera et al, 2015; Klein et al, 2016).

Moreover, MiT-TFE proteins are constitutively active and localized in the

nucleus regardless of nutrient availability and therefore bypassing the mTORC1-mediated control (Perera et al, 2019).

Curiously, TFEB loss is not sufficient to suppress autophagy but its expression is increased after KRAS knock-down, suggesting a link between the two proteins in PDAC growth as part of compensation programs to face cellular stresses (Klein et al, 2016).

On the contrary, testing the efficacy of Alantolactone in pancreatic cancer, He et al found that the drug inhibits cancer cell proliferation and increases apoptosis in vivo and in vitro through the reduction of TFEB levels (He et al, 2018).

TFEB-induced autophagy seems to have a function also in other cancer types.

For example, androgens promote prostate cancer growth in part through autophagy and TFEB silencing decreases androgen-mediated proliferation of cancer cells (Blessing et al, 2017). Similarly, intense TFEB expression and lysosomal biogenesis have been found in about 25% of early breast carcinomas and relate with poor prognosis (Giatromanolaki, 2017).

TFEB and invasive phenotype

Different studies underlined a putative correlation between TFEB expression and cancer infiltration, metastasis and survival.

Colorectal cancer (CRC) progression is linked to TFEB. In fact, Liang et al demonstrated a significantly positive correlation between the transcription factor in cancer tissues and aggressive clinical features, such as deep infiltration, lymphatic metastasis rate and poor survival. Moreover, they observed in multivariate analysis that TFEB levels in patients could be a predictor of survival and its silencing in vitro inhibited cell proliferation and migration. They concluded that TFEB expression could be used as a prognostic factor and exploited as a potential treatment target in CRC (Liang

et al, 2018).

Following the idea of TFEB as a promoter of critical oncogenic characteristics, different works show a connection between high TFEB levels and invasive phenotype: it seems that the MiT family member can stimulate migration and infiltration in cancer cells. That is true for CRC (Liang et al, 2018), pancreatic cancer (He et al, 2019), oral squamous cell carcinoma (Sakamoto et al, 2018), lung cancer (Kundu et al, 2018) and NSCLC (Giatromanolaki et al, 2015).

TFEB may be also able to modulate epithelial-mesenchymal transition (EMT), a key process in neoplastic transformation and in metastatic process. In fact, it has been shown that it can influence E-cadherin, WT1 and Snail expression, proteins involved in EMT regulation (Astanina et al, 2020).

In PDAC, it seems that TFEB could also promote migration and invasion being linked to TGF-β signalling. In particular, SMAD activation by TGF-β causes an elevation of TFEB transcription and nuclear translocation that in turn increases the autophagy rate. Autophagy induces RAB5A-dependent endocytosis of Itgα5β1 and the focal adhesion disassembly that, as a result, raises the invasive feature of pancreatic cancer cells (He et al, 2019).

It seems that the connection between TGF-β and TFEB is reciprocal. In fact, after BRAF inhibition in melanoma it has been seen that autophagy is increased as a consequence of TFEB nuclear translocation: being ERK2 activity decreased, TFEB phosphorylation is reduced and therefore its translocation to the nucleus is facilitated. Blocking TFEB expression after BRAF inhibition brings no benefit, but on the contrary an enhanced tumor progression takes place: EMT-transdifferentiation, metastatic dissemination, and chemoresistance, associated with elevated TGF-β levels and enhanced TGF-β signaling. Only shutting down TGF-β signaling restores tumor differentiation and drug responsiveness (Li et al, 2019).

3. Tumour proliferation: the role of TFEB

3.1 Cell cycle

Growth and reproduction of all organisms depend on duplication and distribution of their chromosomes to newly formed daughter cells in a process called cell cycle (Harashima et al, 2013).

It is composed of three phases strictly interconnected. The gap 1 (G1) phase enables cells to grow before the synthesis (S) phase where they duplicate their DNA. They can continue to grow in the second gap (G2) phase and then reach the mitosis (M) phase in which sister chromatids are separated. The cell cycle ends with the cytokinesis that completes the cell division with the formation of two daughter cells separated by a plasma membrane (Harashima et al, 2013).

Due to its importance, the process is strictly controlled: its misregulation can bring to several pathological conditions from cancer to degenerative diseases.

Fundamental regulators, called “checkpoints”, are cyclin proteins and cyclin-dependent kinases (CDKs), which form complexes and control the progression of the program. As cyclins are synthesized and destructed systematically during the cycle, different CDKs are activated at different times. In their activated form, they are able to phosphorylate specific substrates that drive events of the cell division. Cell cycle checkpoints are responsible for ensuring that each earlier process has been correctly completed before the cell moves on to the next phase of the cycle (Wenzel & Singh, 2018).

Four cyclins (D, E, A, B) and four CDKs (4, 6, 2, 1) are necessary for the correct execution of the cycle.

CDK4, as all CDKs, is a serine/threonine kinase whose activity depends on a regulatory subunit, a cyclin. The cyclin provides domains essential for enzymatic activity and its expression levels are subjected to regulation during cell cycle (Malumbres, 2014).

In response to several mitogenic stimuli or other signals, CDK4, associated with D-type cyclins, is able to promote the entry into cell cycle from G0 phase. CDK4 is a key regulator of G1-S transition and drives cell cycle progression. CDK4 and CDK6 with D-type cyclins promote the transition from G0 into G1 by phosphorylating the retinoblastoma (Rb) protein and therefore preventing it to bind and inhibit the E2F transcription factor (Wenzel & Singh, 2018). In fact, it phosphorylates the tumor suppressor protein Rb, or one of the two other Rb-family members, p130 and p107, on Ser 807 and Ser811 inactivating it and permitting the detachment of E2F from Rb. Acting as a transcription factor, E2F induces its early taget genes, including proteins required for DNA synthesis and mitosis. In the G1 phase, Rb is continuously phosphorylated on other residues, in total 13, and also E2F late genes are expressed (Malumbres, 2014).

Subsequently, CDK2, in complex with cyclins E and A, controls the S-G2 phase, whereas CDK1 with cyclins A and B the G2-M phase (Harashima et al, 2013). In addition to Rb, another tumor-suppressor gene plays an important role in the whole process: p53.

The Rb-CDK4-cyclinD-p16 axis has been seen altered in several cancers: Rb and p16 are tumor suppressor whereas CDK4 and cyclinD can be considered onco-proteins (Sherr et al, 2016).

The progression through cell cycle is accompanied by dramatic reorganization of gene expression: it has been evaluated that about 20% of the genome is periodically transcribed during this time frame. The program appears as a continuum of transcriptional activation and deactivation of particular gene clusters committed to regulated the single phases (Haase &

Wittenberg, 2014).

3.2 MAPK pathway and cell proliferation

Cells are able to catch extracellular stimuli through the activation of surface receptors and react to them inducing an appropriate biological response after integrating the extent and timing of the various microenvironmental clues (Roux and Blenis, 2004; Chambard et al, 2007).

The MAPK (Mitogen-Activated Protein Kinases) pathway, present in all eukaryotic cells, plays a pivotal role in the cell signaling transduction network (Guo et al, 2020).

Four MAPK cascades have been identified in mammals, named accordingly to their MAPK tier component: ERK (extracellular signal-related kinase), JNK (c-Jun amino-terminal kinase or stress-activated protein kinase - SAPK), p38-MAPK and ERK5. Each of these enzymes exists in several isoforms: ERK1 to ERK8, p38-α, -β, -γ, and -δ and JNK1 to JNK3 (Kim and Choi, 2010; Sun et al, 2015).

MAPKs can be activated by a wide range of extracellular and intracellular stimuli such as growth factors, cytokines, hormones and cellular stressors, but, in general, ERK preferentially responds to growth factors whereas JNK and p38 are more sensitive to stress stimuli including ionizing radiations and cytokines (Roux and Blenis, 2004; Kim and Choi, 2010).

Each family of MAPKs is composed of a set of at least three sequentially acting serine/threonine kinases: a MAPK, a MAPK kinase (MAPKK or MAP2K), and a MAPKK kinase (MAPKKK or MAP3K). The MAPKKKs are often activated through phosphorylation as a result of their interaction with a small GTP-binding protein of the Ras/Rho family. MAPKKKs phosphorylate and activate MAPKKs, which in turn phosphorylate and activate MAPKs. Once activated, MAPKs phosphorylate target substrates,

including phospholipases, transcription factors and cytoskeletal proteins (Roux and Blenis, 2004; Kim and Choi, 2010).

The ERK/MAPK axis is the most studied MAPK signaling pathway and is very important for the correct functioning of the cell due to its implication in fundamental processes such as proliferation, cell cycle control, differentiation, migration, survival, senescence and death (Sun et al, 2015; Guo et al, 2020).

The signaling cascade is induced by growth factors, polypeptide hormones, neurotransmitters, chemokines and phorbol esters, usually through the RTKs (receptor tyrosine kinases) or the GPCRs (G protein-coupled receptors). The upstream components of the ERK/MAPK pathway are the RAS GTPase and the protein kinases RAF, MEK and ERK (Mendoza et al, 2011).

As already said, ERK has different isoforms: ERK 1, 2, 3, 5 and 6, but ERK1 and ERK2 are the most important members, with molecular weights of 44 and 42 kDa, respectively (Guo et al, 2020).

ERK1/2 is activated by MEK1/2 through the phosphorylation of Tyr204/187 and Thr202/185: the modifications of both tyrosine and threonine is required for the total enzyme activation (Roskoski, 2012).

MEK1/2 is in turn activated by a RAF isoform: A-RAF, B-RAF or RAF-1. The kinase RAF is activated upstream by the small GTPase RAS after the receptor triggering (Kim and Choi, 2010).

The only RAF substrates are MEK1/2 and the only MEK1/2 substrates are ERK1/2. On the opposite, ERK1/2 catalyze the phosphorylation of many cytoplasmic and nuclear substrates including transcription factors and regulatory molecules (Roskoski, 2019).

The target specificity of active ERK is controlled by different factors such as substrate availability, scaffolding and subcellular localization. That means

that cell type, cell cycle phase and extracellular environment influence ERK activity (Mendoza et al, 2011).
ERK is generally located in the cytoplasm but after its activation, it transfers to the nucleus where regulates gene expression: c-FOS, c-JUN, ELK-1, c-MYC and ATF2 are all transcription factors regulated by ERK (Guo et al, 2020).

Deviation from the strict control of MAPK signaling pathways is implicated in the development of many human diseases including Alzheimer's disease, Parkinson's disease, amyotrophic lateral sclerosis, developmental disorders, inflammation and various types of cancers (Kim and Choi, 2010; Guo et al, 2020)
The activity of the RAS-RAF-MEK-ERK cascade is increased in about one-third of all human cancers (Roskoski, 2012).

As already treated, cell cycle entry and the following G1/S transition are promoted by the formation of an active cyclinD1-CDK4/6 complex. The process is strictly controlled by different factors among which ERK plays an important role. In fact, ERK regulates cyclin D1 transcription induction, the assembly of cyclin – CDK complexes and the repression of some anti-proliferative genes (Chambard et al, 2007).
Moreover, ERK is also implicated in the regulation of the G2/M transition (Chambard et al, 2007).

3.3 Altered proliferation in melanoma: focus on MAPK and PTEN pathway

As already reported, the RAS/RAF/MEK/ERK pathway is fundamental for the cell and plays a pivotal role in different steps of tumorigenesis being

implicated in processes such as cell proliferation, differentiation, invasion and death: the MAPK cascade is perhaps considered the most important oncogenic driver (Roskoski, 2019).

It is, in fact, of central importance for the pathogenesis of many forms of human cancer, in particular lung adenocarcinoma, colorectal adenocarcinoma and melanoma (Ostrowski and Fisher, 2021).

Some components of the cascade, such as RAS of BRAF, are mutated or aberrantly expressed in tumours but more interesting, even in the absence of conclamate genetic mutations, the pathway is frequently activated in different cancer types (McCubrey et al, 2007).

Being MAPKs crucial for melanocyte proliferation, it is comprehensible that the ERK signaling is essential for melanoma instaurance and progression; therefore activating mutations of this pathway are the most frequent driving mutations in melanoma (Savoia et al, 2019).

Strong activation of the MAPK pathway is detected in more than 90% of melanomas: about 50% of patients carry mutations in BRAF whereas 28% of them in NRAS (Wellbrock and Arozarena, 2016).

In particular, BRAF is mutated in about 7% of all cancers, but especially in melanoma (27-70%), papillary thyroid cancer (36-53%), colorectal cancer (5-22%) and ovarian cancer (30%) (McCubrey et al, 2007).

Among recurrent activating mutations in BRAF in cutaneous melanoma, the most common is the substitution of valine at codon 600 with glutamic acid, bringing to the so called BRAFV600E. Less frequent mutations include other substitutions at codon 600 such as the V600K, as well as other rare mutations such as the G469R. BRAFV600E mutations are typical of nevus-associated melanoma, truncal location and younger patients, whereas BRAFV600K mutations are more commonly linked to chronic UV exposure in areas of the head and neck chronically exposed to sun (Ostrowski and Fisher, 2021).

Oncogenic BRAF mutations bring to constitutive BRAF activity and downstream activation of MEK and ERK without the need for the upstream signaling engagement (Perera et al, 2019; Ostrowski and Fisher, 2021).
The discovery of the implication of MAPK pathway in the formation and biology of melanoma have opened a new era in the treatment of this tumor (Savoia et al, 2019).
Nowadays, the blockade of this signalling module by targeted inhibitors is an important anti-tumor strategy that is so far only approved for the treatment of melanoma although numerous other cancers are driven by MAPK activation (Roskoski, 2019).
However, despite the positive results of BRAF inhibitors, the average duration of the response is short, due to the onset of resistance mechanisms. The combination therapy with MEK inhibitors is an excellent strategy to circumvent drug resistance, but is not sufficient.: the recent development of RAS and ERK inhibitors could mark a turning point for the fight against the acquired resistance to target therapy in melanoma (Savoia et al, 2019).

Another gene found mutated in 10 to 30% of cutaneous melanoma is PTEN (phosphatase and tensin homologue) (Savoia et al, 2019; Ostrowski and Fisher, 2021).
Various somatic alterations of the PTEN gene are present in 5-20% of primary melanomas and in about 30-50% of melanoma cell lines (Němejcová et al, 2020). Moreover, loss or decrease in PTEN expression is associated with an aggressive tumour behaviour (Němejcová et al, 2020).
PTEN has different cytoplasmic and nuclear functions and is implicated in the tumorigenesis of melanoma: in general, cytoplasmic PTEN negatively regulates the PI3K/AKT/mTOR signalling pathway, while nuclear PTEN works as a tumour suppressor (Němejcová et al, 2020).

PTEN is able to inhibit migration and stem cell self-renewal, induce cell cycle arrest, regulate chromosome stability, DNA repair and apoptosis (Němejcová et al, 2020).
Loss of function of PTEN by deletion, mutation or epigenetic dysregulation leads to hyperactivation of the AKT signalling and the MAPK pathway (Savoia et al, 2019; Ostrowski and Fisher, 2021).
PTEN absence is commonly associated with BRAFV600E mutation in melanoma and tumors carrying both alterations display a worse outcome for patients (Němejcová et al, 2020).

As seen, the function of MITF in melanoma development is complex and controversial. This is partly due to its dynamic regulation by different signaling pathways: among them, the MAPK pathway plays an important role (Wellbrock and Arozarena, 2015).
Ectopic MITF expression in conjunction with the BRAF(V600E) mutant leads to the malignant transformation of primary human melanocytes (Garraway et al, 2005).
Moreover, MITF gene amplification is also found in patients relapsed on MAPK inhibitor therapy, suggesting that it provides a growth or survival advantage even when the MAPK pathway is inhibited (Wellbrock and Arozarena, 2015).
The relationship between the transcription factor and the signaling patway is mutual and multifaceted: MITF is essential for the maintenance of oncogenic BRAF-driven melanoma in vivo and the level of MAPK pathway activation appears to be critical for MITF abundance and function in melanoma cells (Wellbrock and Arozarena, 2015).
MITF is controlled by the RAS/RAF/MEKERK pathway at various levels including its transcription and its protein turnover and function. For example, MITF is modulated by phosphorylation on serine S73 by ERK2: this

phosphorylation event increases MITF activity but accelerate MITF protein degradation (Vachtenheim and Ondrušová, 2015).

MAPK pathway plays a major role in coordinating the balance between melanocyte differentiation and proliferation through MITF (Wellbrock and Arozarena, 2016).

Increase of intracellular cAMP levels induce the differentiation process because is followed by a brief and weak activation of ERK that leads to a transient increased activity of MITF that positively acts on the promoter of TYR. In fact, ERK is only transiently activated during early stages of cAMP signalling in melanocytes due to DUSP1-mediated feedback regulation. On the other hand, activation of the MAPK pathway through growth factors stimulates strong sustained ERK activation leading to melanocyte proliferation due to the reduction of MITF protein levels (Wellbrock and Arozarena, 2015; Wellbrock and Arozarena, 2016).

BRAFV600E can influence TFEB transcriptional programs through the inhibiting phosphorylation triggered by ERK. The use of a BRAF inhibitor reverses this condition, activates autophagy and reduces in vivo tumor growth whereas TFEB overexpression increased the tumorigenic activity of melanoma cells (Astanina et al, 2020).

Moreover, oncogenic BRAF through ERK induces BRN2 expression that in turn activates the MITF promoter in human melanoma cells (Wellbrock and Arozarena, 2015).

In this way, MAPK pathway can both increase or decrease MITF activity depending on the duration of its activation induced by different stimuli.

3.4 TFEB and proliferation

In cancer, the influence of TFEB on cell proliferation has been extensively investigated and it has been mainly connected with its effect on the

autophagic flux.

Knockdown of TFEB decreases the proliferation rate of prostate cancer (Blessing et al, 2017), pancreatic cancer (Perera et al, 2015) and colorectal cancer (Liang et al, 2018).

In particular, in the prostate cancer, Blessing et al demonstrated that TFEB is a direct target of the androgen receptor and that TFEB silencing is sufficient to block androgen-mediated tumor growth (Blessing et al, 2017).

PDAC, that was exhaustively analyzed before, is under strictly control of MiT proteins for autophagy and the consequent increase of proliferation (Yang et al, 2011; Perera et al, 2015). In fact, pancreatic cancer cells have predominant nuclear localization of TFEB while normal pancreatic epithelial cells had cytoplasmic TFEB, suggesting a role for the transcription factor in supporting their growth (Ploper and De Robertis, 2015).

In CRC TFEB is generally expressed at low levels but Liang et al found a correlation between the transcription factor and CRC progression. In fact, they saw that silencing TFEB entailed a decrease in proliferation and migration. Conversely, TFEB over-expression enhanced the proliferation rate rescuing tumor growth (Liang et al, 2018).

Interestingly, in tumor types known to be particularly affected by TFEB, such as RCC, PDAC and melanoma, it has been shown that the crosstalk between TFEB/TFE3 and mTORC1 is fundamental for tumor proliferation through RagD induction (Di Malta et al, 2017).

Moreover, the increased cell proliferation observed in renal cell carcinoma carrying the t(6;11)(p21:q13) translocation, which leads to a TFEB promoter substitution with the 5’ upstream regulatory sequence of the alpha intronless gene, indirectly supports the important role of TFEB in cell growth (Calcagnì et al, 2016). The lack of promoter-mediated physiological control of TFEB expression promotes clonogenic cell growth (Haq and Fisher, 2011).

In some other cases, such as oral squamous cell carcinoma (Sakamoto et

al, 2018), non-small cell lung cancer (Giatromanolaki et al, 2015; Kundu et al, 2018) and breast cancer (Giatromanolaki et al, 2017), TFEB does not directly control proliferation but its expression is correlated with poor prognosis and/or enhanced migratory phenotype.

The studies considered before demonstrated that TFEB can influence cell proliferation, but none of these showed a direct control of the transcription factor on a particular protein involved in traditional pathways responsible for cell growth and proliferation.
In contrast, Doronzo et al observed that TFEB depletion halts proliferation at the G1-S transition by inhibiting the CDK4/CyclinD1/Rb pathway in human endothelial cells. In particular they demonstrated that the phosphorylation of the retinoblastoma protein, Rb, was decreased and that the protein expression of the CDK4/CyclinD1/Rb complex targets, such as E2F and PCNA, was altered after TFEB silencing. So, they predicted a TFEB binding region on the promoter of the CDK4 gene and finally they proved that TFEB can directly induce the expression of that protein, fundamental for cell proliferation (Doronzo et al, 2019).

4. TFEB and metabolism

4.1 Cancer metabolism

Metabolic needs of proliferating cells are fundamentally different from those of nonproliferating ones. In fact, the onset of proliferation introduces a big challenge: generating two daughter cells through cell cycle requires the energy to sustain the process and to double the total biomass (DeBerardinis et al, 2008).

It is therefore clear that cancer cell proliferation and metabolism are strictly linked: in order to obtain sufficient amounts of metabolites and energy for high rates proliferation, tumor cells undergo metabolic reprogramming (Kim et al, 2021b).
This reprogramming consists in activating or enhancing metabolic pathways able to produce the metabolic precursors for cell anabolism, to satisfy energy request for cell maintenance and biosynthesis and to control redox balance (Vazquez et al, 2016).
Moreover, transformed cells adapt their metabolism to enable tumor initiation and progression. In fact, peculiar metabolic activities influence directly malignant transformation or support the biological processes that lead to tumor growth (Vander Heiden and DeBerardinis, 2017).
Proliferative signals usually contribute to metabolic reorganization that allows quiescent cells to begin to proliferate (DeBerardinis et al, 2008).

Otto Warburg was the pioner in the field of cancer metabolism reporting already in the 1920s that cancer cells harbor different metabolic behaviours compared to healthy cells. In fact, normal cells in presence of oxygen follow the so called Pasteur effect, abolishing glucose fermentation and preferentially conveying pyruvate to mitochondria to fuel oxidative phosphorylation. On the contrary, most tumor cells are able to maintain high rates of glycolysis converting glucose to lactate even in the presence of oxygen, a phenomenon known as “aerobic glycolysis” that has also been termed “Warburg effect” (Danhier et al, 2017).
Glucose catabolism followed by oxidative phosphorylation has a high energy yield in the form of ATP, therefore cancer cells undergoing areobic glycolysis have a wasteful form of metabolism requiring a high glucose consumption rate to satisfy their energy and anabolic demands (Vazquez et al, 2016).

Warburg explained lactate secretion from tumor cells as an indication that their oxidative metabolism was damaged and the increase in glycolytic flux as a compensatory mechanism (Vander Heiden and DeBerardinis, 2017).
This theory was then demonstrated to be wrong and it has been proved that glycolysis provides several advantages for proliferating cells.
In fact, if glycolytic flux is sufficiently high, the percentage of cellular ATP can exceed that produced from oxidative phosphorylation. Moreover, glycolysis intermediates can be used as building blocks for biosynthetic pathways: ribose sugars for nucleotides, glycerol and citrate for lipids, nonessential amino acids and NADPH through the oxidative pentose phosphate pathway. The Warburg effect can therefore benefit both bioenergetics and biosynthesis (DeBerardinis et al, 2008).
Later, the Warburg effect has also been found in non-transformed cells as a reversible status, suggesting that it reflects proliferation-associated changes in metabolism rather than a feature of malignancy (Vander Heiden and DeBerardinis, 2017).

In the same way, also TCA cycle has a key role in proliferating cells as a hub for biosynthesis. In fact, most part of the carbon that enters the cycle is used in biosynthetic pathways that consume rather than produce ATP: the efflux of its intermediates (cataplerosis) is essential to synthesize lipids, proteins and nucleic acids (DeBerardinis et al, 2008).
As cancer cells usually synthesize lipids de novo for their membranes rather than scavenged from the extracellular environment, citrate can be exported from the cycle for lipid synthesis and therefore the fraction of mitochondrial citrate that is oxidized is decreased (DeBerardinis et al, 2008).
Similarly, pyruvate can be converted into acetyl-CoA in the mitochondria but rather being incorporated in TCA cycle, it can be exported to the cytosol for lipid synthesis as well (Vander-Heiden et al, 2011).

On the other hand, oxaloacetate and α-ketoglutarate supply intracellular pools of nonessential amino acids for the synthesis of proteins and nucleotides (DeBerardinis et al, 2008).
Therefore, TCA truncation supports cell proliferation (DeBerardinis et al, 2008).

Glucose is not the only substrate contributing in cell metabolic functions like energy formation, biomass assimilation and redox control. Such alternative nutrients include glutamine, acetate, different fatty acids, lactate, branched chain amino acids, serine and glycine (Vander Heiden and DeBerardinis, 2017).
The ability to use different molecules represent an advantage for cancer cells because plasticity is fundamental for surviving and proliferating in unfavorable conditions.
In particular, glutamine, the most abundant amino acid in the plasma of mammals, strongly contributes to anaplerosis providing carbon to fuel TCA cycle (DeBerardinis et al, 2008).
In fact, under in vitro cell culture conditions, it is the second most consumed nutrient after glucose and its consumption exceeds its demand for protein synthesis (Vazquez et al, 2016).
A great part of consumed glutamine, transported into the cell via the glutamine receptor Solute Carrier Family 1 Member 5 (SLC1A5), is generally transformed to glutamate by several amidotransferases or by glutaminases and exported to the extracellular medium or converted into α-ketoglutarate that fuels TCA cycle (Vazquez et al, 2016).
Glutamate conversion to α-ketoglutarate is catalyzed by either Glutamate Dehydrogenase 1 (GDH) or mitochondrial Alanine and Aspartate Aminotransferase (GOT2 and GPT2, respectively) (Fischer et al, 2018).
Glutamine can be exploited through oxidative metabolism following

traditional TCA cycle progression for ATP generation or to produce malate which is then converted to pyruvate and decarboxylated to obtain acetyl-CoA exported to the cytosol for lipid synthesis (Vander-Heiden et al, 2011). Moreover, it can be used as a primary nitrogen donor in nucleotide and amino acid biosynthesis and for redox balance through NADPH production (Kim et al, 2021b).

This route of glutamine metabolism is called glutaminolysis (Vander-Heiden et al, 2011).

Conversely, glutamine can also be used to generate cytosolic acetyl-CoA by direct conversion of α-ketoglutarate to citrate in a reductive pathway, called reductive carboxylation, that is TCA cycle pushed in the opposite way (Vander-Heiden et al, 2011).

Reverse TCA cycle flux to supply acetyl-CoA provides a perfect illustration of the metabolic versatility of cancer cells (Filipp et al, 2012).

The synthesis of citrate from α-ketoglutarate through reductive carboxylation has been reported to be essential for growth of cancer cells with mitochondrial defects (Vazquez et al, 2016).

Glutamine is therefore important for both bioenergetics and biosynthesis (DeBerardinis et al, 2008).

4.2 Metabolism in melanoma

Melanomas are metabolically heterogeneous and able to adapt their fuel utilization for their maintenance, progression and metastasis induction (Fischer et al, 2018).

Metabolic reprogramming as an adaptation to tumor microenvironment-dependent stress is driven by oncogenic stimuli such as activity of the MAPK pathway, HIF1α, Myc and MITF: they are responsible for the control of the balance between non-oxidative and oxidative branches of carbon

metabolism (Ratnikov et al, 2017).

This important connection between oncogenic activation and energetic metabolism confers remarkable metabolic plasticity to melanoma cells that can use both cytosolic and mitochondrial compartments to produce energy even if their energetic demand mainly depends on glycolysis, whose upregulation is strictly linked to constitutive activation of BRAF/MAPK pathway affected by BRAFV600E mutation (Ruocco et al, 2019).

Like other cancer cells, the majority of rapidly proliferating melanoma cells undergo the “Warburg effect”, metabolizing glucose into lactate regardless of oxygen levels. In fact, in normoxic conditions, only 25% of pyruvate enters the mitochondria, where it is converted to acetyl-CoA by pyruvate dehydrogenase (PDH) (Fischer et al, 2018).

This phenomenon of lactate production from glucose is obviously increased under hypoxic conditions through the transcriptional program induced by hypoxia inducible factors (HIFs) (Ratnikov et al, 2017).

Accumulation of HIF1α allows its interaction with HIF1β and their following activation that promotes the transcritpion genes involved in glucose uptake and utilization increasing glycolytic rates (Fischer et al, 2018).

Furthermore, the concomitant induction of lactate dehydrogenase A (LDHA) and the activation of pyruvate dehydrogenase kinase 1 (PDK1), which inhibits PDH, preventing pyruvate from entering the TCA cycle, decrease mitochondrial respiration (Ratnikov et al, 2017).

MYC and the PI3K/AKT/mTOR signaling pathways also promote increased glycolytic activity inducing glucose uptake and glycolytic gene induction (Fischer et al, 2018).

Activation of the MAPK pathway increases transcription and stabilization of HIF1α even in normoxia, but Warburg phenotype is also achieved through MAPK inhibition of MITF (Fischer et al, 2018).

Both MITF and PGC1α levels were found to be inversely proportional to

MAPK pathway activity. In fact, MITF induces the expression of metabolic genes involved in oxidative phosphorylation through the upregulation of PGC1α that is known to act on mitochondrial biogenesis. Elevated MITF and PGC1α levels have also been found in biopsies from melanoma patients treated with BRAF/MEK inhibitors suggesting energetic adaptation of melanoma cells via MITF and PGC1α induction (Ratnikov et al, 2017).

Oxidative phosphorylation also plays a critical role with a subset of melanomas relying extensively on this pathway to meet their bioenergetic needs. However, functional mitochondria are critical for all melanoma cells by providing intermediates for biosynthetic and redox reactions (Fischer et al, 2018).

Metabolic profiling studies using tracers showed that glycolysis is decoupled from TCA cycle, not in a dysfunctional way but rather as an versatile metabolic rewiring important for energy production, biosynthesis and redox balance (Filipp et al, 2012).

The replenishment of TCA intermediates used as biosynthetic precursors (anaplerosis) is mainly satistied by glutamine as an alternative carbon source. In fact, as previously reported, glutamine addiction is a hallmark of oncogenic transformation, melanoma included (Ratnikov et al, 2017).

Glutaminolysis can potentially contribute to fatty acid synthesis, but melanoma cells demonstrate a strong reductive carboxylation of α-ketoglutarate with lipids produced mainly through a reverse TCA cycle (Filipp et al, 2012).

4.3 TFEB role in cell metabolism

Numerous studies have provided evidence suggesting that TFEB exerts an important function in cellular metabolic control and therefore in the

maintenance of cellular physiological and pathological processes (Puertollano et al, 2018).

According its role in regulating autophagosomal compartment and the different molecules that can be degraded through this process, it has obviously the potential to participate indirectly in many aspects of energy production and biosynthesis management, including mitochondrial activities, but this is not the only contribution: TFEB has been seen to take part in a more direct and specific way in cell metabolism and metabolic adaptation (Perera et al, 2019; Astanina et al, 2020).

In particular, TFEB plays a crucial role in the regulation of lipid homeostasis linking autophagy to energy metabolism at the transcriptional level and its procatabolic activity occurs in most cells with specificity in the different tissues and organs (Perera et al, 2019; Yu et al, 2020).

Moreover, it seems that TFEB and TEF3 can cooperatively regulate whole-body energy metabolism in a compensatory rather than redudant way (Pastore et al, 2017).

In the liver, in response to fasting, TFEB promotes the expression of genes implicated in autophagy and different types of lipid catabolism including fatty acid oxidation, lipophagy and ketogenesis, via activation of a gene expression program that includes the master metabolic transcription factors Peroxisome Proliferator-Activated Receptor Gamma Coactivator 1-Alpha (PPARGC1A also called PGC1A) and Peroxisome Proliferator-Activated Receptor Alpha (PPARA) (Martina et al, 2014a).

This mechanism has been demostrated to be conserved in Caenorhabditis elegans suggesting a pivoltal role for TFEB in the evolution of the adaptive response to food deprivation (Settembre et al, 2013b).

Liver-specific TFEB deletion results in defective degradation of lipids during starvation rendering mice hypersensitive to the effects of a high-fat diet,

whereas TFEB overexpression reverts obesity limiting lipid accumulation and the following metabolic syndrome (Perera et al, 2019).
On the other way, PPARGC1A induces TFEB to maintain mitochondrial quality control during high-energy production: besides driving mitochondrial biogenesis and coactivating the expression of target genes required for metabolic pathways that ensure high levels of ATP, PPARGC1A controls ROS production inducing anti-oxidant genes. Therefore, increasing TFEB expression provides PPARGC1A another mean to regulate cellular homeostasis (La Spada, 2012).
Another example of molecule regulating TFEB is the fasting-induced hormone fibroblast growth factor 21 (FGF21) that governs lysosome homeostasis. FGF21 deficiency in mice impairs hepatic lysosomal function by blocking TFEB. In this case, FGF21 controls TFEB indirectly inducing the mobilization of calcium from the endoplasmic reticulum and activating the protein phosphatase PP2A which dephosphorylates TFEB (Chen et al, 2017).

PGC1A influences different aspects of skeletal muscle functionality and the expression of metabolic genes that govern insulin sensitivity and was previously seen to be directly regulated by TFE3 (Salma et al, 2015).
As already seen in liver, also in muscle and in particular during exercise, PGC1A and TFEB are able to influence and activate each other resulting in mitochondrial biogenesis (Erlich et al, 2018)
Nevertheless, in the adaptive metabolic response to physical exercise, TFEB acts as a central coordinator of skeletal muscle insulin sensitivity, glucose homeostasis, lipid oxidation and mitochondrial function also independently from PGC1A. In fact, TFEB controls the expression of glucose transporters, glycolytic enzymes and pathways related to glucose homeostasis, but also genes involved in mitochondrial biogenesis, fatty acid

oxidation and oxidative phosphorylation, suggesting a central role for the transcription factor in governing the muscle metabolic flexibility during physical exercise (Mansueto et al, 2017).

Also in cardiomyocytes TFEB exerts a strong influence on different metabolic pathways fundamental for the correct functioning of the cells. High-fat and high-sucrose diet can cause cardiomyocyte injury by inhibiting TFEB; in the same way, loss of TFEB renders the heart prematurely susceptible to nutrient overload-induced injury, suggesting that lipid deposition and TFEB loss are concomitant molecular events. The effects observed are not only due to a suppression of the correct lysosomal function as shown by the analysis of differentially expressed genes (DEGs) after TFEB deletion: genes involved in macroautophagy, mitophagy and lysosome function are only a small portion of DEGs which are mainly part of other pathways such as nutrient metabolism, DNA damage and repair, cell death and cardiac function. Therefore, in cardiomyocite, the non-canonical effect of TFEB to reprogram energy metabolism is more evident than the canonical action of TFEB on lysosomal function and autophagy (Trivedi et al, 2020).

TFEB and TFE3 also establish an interplay in adipogenesis and mature adipose tissue control directly binding to consensus E-boxes within the Peroxisome Proliferator-Activated Receptor Gamma 2 (PPARG) transcriptional regulatory region both *in vitro* and *in vivo* (Salma et al, 2017). Recently, it has been seen that mice with TFEB overexpression specific in adipocytes were protected from diet-induced obesity, insulin resistance and metabolic syndrome. The transcriptional characterization permitted to find out that DEGs involved in adipose tissue browning are more compared to those involved in autophagy. In particular, it seems that TFEB is able to induce adipose tissue browning through its direct control on PGC1A (Evans

et al, 2019).

The influence of TFEB on lipid metabolism was observed also in macrophages suggesting a crosstalk between lipid metabolism and the innate immune response that converges on the lysosome (Schilling et al, 2013).

Also epithelial cells of different origin are subjected to TFEB influence concerning metabolism regulation.
For example, TFEB overexpression is able to reduce the oxidative stress in podocytes exposed to high glucose increasing the expression of superoxide dismutase 2 (SOD2) and heme oxygenase 1 (HO1) antioxidant enzymes. Moreover, it can promote mitochondrial biosynthesis in part through PGC1A and reduce glucose-induced podocyte apoptosis by activating the AKT/BAD pathway (Kang et al, 2019).
Another study demonstrated that retinal pigment epithelial cells increase their level of TFEB and MITF in response to nutrient deprivation and lysosomal stress and that TFEB overexpression also induces the expression of CLEAR network genes suggesting a role for the transcription factor in regulating the metabolic adaptive response after different stress stimuli (Pan et al, 2019).

Last but not least, a recent study analyzed TFEB role in glucose metabolism *in vivo*. In particular, using EC-selective TFEB knockout and EC-selective TFEB transgenic mice fed a high-fat diet, they observed that TFEB deletion brings to impaired glucose tolerance whereas TFEB presence improves glucose tolerance through AKT signaling pathway (Sun et al, 2021).

Given the pleiotropy of effects induced by TFEB in different studies, it can

be speculated that its influence on metabolism might depend on specific tissue commitments and defined metabolic conditions (Astanina et al, 2020).

4.4 TFEB role in cancer metabolism

According to the role of TFEB in regulating autophagy, it is not surprising that it can potentially participate indirectly in nearly all aspects of cancer cell metabolism (Astanina et al, 2020).

As already extensively reported, given their accelerated rates of growth, cancer cells have an increased demand for energy and biosynthtetic precursors.

When metabolic sources are limiting due to different reasons, tumors may switch to non conventional ways of nutrient scavenging pathways involving autophagy and lysosomes (Perera et al, 2019).

Glycogen can be hydrolyzed to carbohydrates for glycolysis, proteins provide amino acids for TCA cycle or for protein synthesis, nucleotides can be degraded to obtain ribose-phosphate, which can either be converted to glycolytic intermediates in the pentose phosphate pathway to generate ATP or be used anabolically for DNA replication and repair (Santana-Codina et al, 2017).

Degrading and recycling cellular materials to feed cellular metabolic pathways permit cancer cells to gain tremendous metabolic plasticity, particularly relevant to face several stresses (Kimmelman and White, 2017).

Generally, one of the most important metabolic effects observed after autophagy inhibition is the decrease of mitochondrial respiration and ATP production due to a reduced protein turnover and altered supply of intermediates to the TCA cycle (Santana-Codina et al, 2017).

Autophagy can also target substrates selectively; for example, mitophagy degrades defective mitochondria to prevent oxidative stress and to maintain

mitochondrial metabolic processes whereas lipophagy acts on lipid stores or lipid droplets for the release of free fatty acids that support fatty acid β-oxidation and the TCA cycle (Santana-Codina et al, 2017).
Therefore MiT family of transcription factors, controlling transcriptional programs for autophagy and lysosome biogenesis, have emerged as regulators of energy metabolism in cancer (Perera et al, 2019).

TFEB can therefore sustain tumor growth influencing cell metabolism indirectly through autophagy, but it can potentially partecipate in a more direct way, transcriptionally regulating metabolic genes.
A clear example of that was recently provided by Kim et al. In fact, they demonstrated that TFEB plays an important role in PDAC metabolism given that its genetic suppression inhibits both glutamine and mitochondrial metabolism. In particular, they observed the suppression of PDAC growth both *in vitro* and *in vivo* after TFEB silencing even with no effect on the autophagic flux. They concluded that TFEB transcriptionally regulates glutaminase (GLS) expression by directly binding its promoter (Kim et al, 2021b).
The connection among TFEB, glutamine metabolism and autophagy through TFEB in PDAC had already been explored. In fact, Seo et al observed that PDAC cells require both autophagy and typical glutamine transporters to maintain intracellular glutamine levels and that glutamine deprivation brings to the activation of TFEB and therefore autophagy (Seo et al, 2016).

RESULTS

Experimental design

Using mouse and cellular models, we investigated the physiological role of Tfeb in the regulation of melanoma development by loss-of-function approach.

The experiments were performed on different melanoma cell lines characterized by the most important mutations found in melanoma patients: D4M (BrafV600E/wt, Pten-/-), YUMM 1.7 (BrafV600E/wt, Pten-/-, Cdkn2-/-), YUMM 1G1 (BrafV600E/wt, Pten-/-, Cdkn2-/-, Mc1r e/e), YUMM 3.3 (BrafV600E/wt, Cdkn2-/-), YUMM 4.1 (Pten-/-, Cdkn2-/-), YUMM 5.2 (BrafV600E/wt, p53-/-) (Jenkins et al, 2014; Meeth et al, 2016).

Basal level of *Tfeb* was assessed through transcriptional analysis (Fig S1A) reporting different amount of the transcription factor in the different murine melanoma cell lines considered.

We predominantly focused on the murine D4M cell line, presenting the activating Braf V600E mutation that supports the iperactivation of MAPK pathway and the deletion of the *Pten* gene, alterations frequently present in human melanomas.

In all experiments, melanoma cells in which endogenous *Tfeb* was silenced by a specific short hairpin (sh-)RNA lentivirus (sh-*Tfeb*) were compared with untreated control cells (ctrl) or cells carrying a control sh-RNA (scr-shRNA). Quantitative PCR was performed at different time points to confirm *Tfeb* deletion maintenance *in vitro* for the whole time in which following experiments were carried out in D4M cells *in vitro* and *in vivo* (Fig S1B).

Tfeb silencing dampens melanoma proliferation in vivo

To perform allograft mouse tumour studies in order to investigate Tfeb contribution in melanoma development, ctrl, scr-shRNA and sh-*Tfeb* D4M cells were injected subcutaneously in the flank of immunocompetent C57BL/6 mice.

From the seventh day after D4M inoculation, we measured tumour volume with a calibre at different time points to monitor tumour expansion. The resulting growth curve clearly showed a slower development of tumours raised from sh-*Tfeb* D4M compared to both ctrl and scr-shRNA D4M tumours (Fig 1A).

This result was confirmed at day 22, when the tumor explant took place: sh-*Tfeb* tumors were smaller compared to both ctrl and scr-shRNA D4M masses (Fig 1B).

Given that the resulting tumour size depends on different factors including tumour cell proliferation per se and the influence exerted by tumour microenvironment elements, we decided to better characterize D4M tumours.

First of all, we evaluated cell proliferation rate in tumour samples by the quantification of Ki-67 protein that is expressed in the nucleus during all active phases of cell cycle (G1, S, G2 and mitosis), but absent in resting cells (G0), making it an excellent marker for determining the proliferative fraction of tumor cell masses. The analysis of Ki-67^{+} nuclei in D4M tumors indicated that the percentage of proliferating cells over total nuclei decreased from 39% in ctrl and 47% in scr-shRNA tumors to 22% in sh-*Tfeb* samples (Fig 1C) suggesting an alteration of cell proliferation resulting from *Tfeb* silencing in D4M cells.

Interestingly, sh-*Tfeb* D4M tumours compared to both ctrl and scr-shRNA D4M tumours were also characterized by the alteration of tumour

angiogenesis as evidenced by the reduction of the $CD31^+$ vascular area (Fig 1D). On the contrary, no big differences were apparently found in the recruitment of immune cells in the tumour masses as evidenced by the quantification of $CD45^+$ area among the three tumour conditions (Fig 1E).
Taken together, these data suggest that the volume decrease of sh-*Tfeb* D4M tumors was probably correlated to a reduction of cell proliferation linked to a smaller vascular area, even if a better characterization of immune markers should be performed to exclude quality changes in the recruitment of immune cells.

Tfeb deletion in vitro inhibits melanoma cell cycle progression

The effect of *Tfeb* deletion on melanoma cell proliferation was further investigated *in vitro*.
$Ki67^+$ nuclei immunostaining of D4M cells confirmed a reduction by 64% of sh-*Tfeb* proliferating cells compared to scr-shRNA D4M cells (Fig 2A).
This evidence was supported by the crystal violet assay quantification: the colorimetric staining showed a lowering by 41% of the proliferative rate of sh-*Tfeb* compared to scr-shRNA D4M cells (Fig 2B).
To confirm the role of Tfeb on melanoma growth we repeated the experiment in different YUMM cell lines with different mutational landscapes: YUMM 1.7, 1G1, 3.3, 4.1 and 5.2. Similarly to D4M cells *Tfeb* silencing reduced the cellular proliferation rate as evidenced by crystal violet assay quantification in all five YUMM cells tested (Fig 3A).
In all melanoma cells considered (D4M, YUMM 1.7 and YUMM 3.3), *Tfeb* silencing specifically restrained the G1-S cell cycle transition as previously described in human endothelial cells (Doronzo et al, 2019). In fact, the count of 5-ethynyl-2'-deoxyuridine (EdU) positive cells clearly evidenced an increased percentage of cells blocked in the G1 phase and a decreased

percentage of those progressing in S phase (Fig 2C, 3B).

For these reason we investigated the role of the transcription factor in the regulation of different molecules involved in cell cycle progression and in particular in the G1-S transition phase.

In human endothelium, it was previously described CDK4 as a TFEB direct target gene (Doronzo et al, 2019). On the basis of this regulation, in endothelium TFEB silencing leads to the downmodulation of CDK4 transcription and protein expression (Doronzo et al, 2019). We confirmed this phenomenon in melanoma cells: Cdk4 mRNA (Fig 2D) and protein amount (Fig 2E) were reduced in sh-*Tfeb* compared to scr-shRNA D4M; also in YUMM 1.7, 3.3 and 4.1 cells, but not in YUMM 1G1 and 5.2 cells we appreciated a decrease in the transcript of *Cdk4* after *Tfeb* inhibition (Fig 3C).

CDK4 forms a complex with Cyclin D1 protein regulating G1-S cell cycle transition (Malumbres, 2014). Although no data suggest Cyclin D1 as a direct target of TFEB, it was downregulated in sh-*Tfeb* D4M compared to control cells both in the transcription (Fig 2D) and in the protein expression (Fig 2E).

Moreover, YUMM 1.7, 1G1 and 3.3 cells, but not YUMM 4.1 and 5.2 cells, bring the same transcriptional alteration after *Tfeb* silencing (Fig 3C).

G1-S phase transition of cell cycle is mediated not only by the expression of Cdk4-Cyclin D1 complex but also by its activity. In fact, Cdk4 assembled with Cyclin D1 is able to phopshorylate and inhibit the Rb protein. Unphosphorylated Rb binds E2F transcription factor limiting its nuclear translocation and function (Merkey et al, 2002).

Sh-*Tfeb* compared to scr-shRNA D4M cells showed a reduced ratio of pRb/Rb protein amount (Fig 2E) suggesting an alteration of its activation via Cdk4-Cyclin D1 complex phosphorylation. As a consequence, E2F transcriptional activity was reduced: the transcript (Fig 2F) and the protein

expression (Fig 2E) of Pcna, one of E2F-responsive gene that is necessary for DNA synthesis (Thacker et al, 2003), was significantly decreased in sh-*Tfeb* compared to scr-shRNA D4M cells.

Taken together, these results support the idea that Tfeb can influence melanoma proliferation, in particular regulating G0/G1-S transition of cell cycle through the regulation of Cyclin D1-Cdk4 protein expression and E2F activation.

Tfeb silencing does not influence Gsk3β expression and activity but MAPK signaling pathway

Cyclin D1 amount and function is finely controlled by different mechanisms. In particular, Glycogen Synthase Kinase 3-beta (Gsk3β) and MAPK pathways, fundamental for cell survival and growth in physiological and pathological conditions, are able to regulate Cyclin D1 expression and degradation (Chambard et al, 2007; Takahashi-Yanaga and Sasaguri, 2008; Luo, 2009; Gao et al, 2014; Sun et al, 2015; Zhan et al, 2017; Guo et al, 2020).

For this reason, we decided to focus on the two signaling cascades in order to better characterize Cyclin D1 regulation after *Tfeb* silencing in D4M melanoma cells.

Gsk3β is one of the most important and versatile enzyme forming the “disruption complex” that phosphorylates and sends to degradation a lot of proteins modulating their intracellular level and so their activity (Gao et al, 2014; Zhan et al, 2017).

Gsk3β’s canonical target is the transcription factor Beta-Catenin (β-Cat or Ctnnb1), but it has also a role in the inhibitory phosphorylation of a lot of other proteins, including Cyclin D1 (Takahashi-Yanaga and Sasaguri, 2008; Luo, 2009). Moreover, Cyclin D1, as well as other proteins such as c-Myc,

are directly controlled in their expression by β-Cat (Zhan et al, 2017).
A link between Gsk3β, β-Catenin and Cyclin D1could be assumed after *Tfeb* silencing. Cyclin D1 could undergo a faster recycling due to an increase in its phosphorylation exerted by Gsk3β as well as be less synthetized due to a decrease in β-Catenin. Nevetheless, Gsk3β and β-Catenin protein expression analysis did not confirm our hypothesis (Fig 4A).
Different studies suggest that the persistent activation of MAPK pathway causes the activation of G1-S transition phase of cell cycle via the induction of Cyclin D1 expression and the Cyclin D1-Cdk4 complex formation, one of the earliest cell cycle-related events (Chambard et al, 2007; Sun et al, 2015; Guo et al, 2020).
After *Tfeb* silencing the transcription of *Kras*, *Raf1*, *Mek1*, *Mek2*, *Erk1* and *Erk2* was downregulated (Fig 5A). The observation was confirmed looking their protein amount: in sh-*Tfeb* D4M cells compared to control we appreciated a decrease in total Braf, Mek1/2 and Erk1/2 protein expression (Fig 5B).
The functioning of MAPK cascade is nevertheless driven by subsequent phosphorylations; for this reason, we decided to focus on them. We observed a decrease in phosphorylation only on the last actor of the signaling cascade, Erk1/2, and not of Braf and Mek1/2 as evidenced by the ratio of phospho-protein vs total protein (Fig 5C).
These evidences suggest a role for Tfeb in directing melanoma cell cyce progression not only via Cdk4-Cyclin D1 complex but also via MAPK signaling regulation.

Tfeb influences melanoma metabolism in vivo

Cell cycle progression and cell proliferation are not only under the control of cyclins, ciclin-dependent kinases/inhibitors or transcription factors but are

also in synchrony with the fine regulation of the metabolic cellular programs. Alternative activation and inhibition of metabolic enzymes and cyclins, cyclin-dependent kinases/inhibitors or transcription factors are modulated according to cell cycle progression. The different metabolic pathways not only support the proliferative program by improving ATP production, DNA replication, lipid synthesis but they are also able to modulate the expression and activation of key molecules of G1-S cell cycle transition (Icard et al, 2019).

On the basis of these assumptions we decided to look for Tfeb putative modulation of tumour metabolism.

First of all, we evaluated Tfeb role in the regulation of the activity of different enzymes involved in the main energy-producing pathways of the cell: glycolysis, TCA cycle and oxidative phosphorylation.

Compared to control D4M tumors, in sh-*Tfeb* D4M masses we observed a decrease in the activity of different key proteins involved in glycolysis such as Phosphofructokinase (PFK -53.5%), Aldolase (ALDO -50.3%), Glyceraldehyde-3-Phosphate Dehydrogenase (GAPDH -69.3%), Enolase (ENO -78.2%), Piruvate Kinase (PK -69.4%), Lactate Dehydrogenase (LDH -68.5%) (Fig 6A).

Interestingly, looking at TCA cycle, the second part of the process was downmodulated. In fact, Citrate Synthase (CS), Aconitase (ACO1) and Isocitrate Dehydrogenase (IDH) seemed to be stable in their activity, whereas Oxoglutarate Dehydrogenase (OGDH) and Succinate Dehydrogenase (SDH) were less operative (-68.9% and -64.3%, respectively) (Fig 6B).

All the complexes of the oxidative phosphorylation were downregulated in their function (complex I -50.6%, complex II -65.6%, complex III -63.3%, complex IV -63.6%) (Fig 6C) and therefore the mitochondrial ATP synthesis was reduced by 55.6% (Fig 6D).

Moreover, we reported an increase in indexes of mitochondrial damage and malfunctioning such as TBARS (indicative of increased ROS and lipid peroxidation, +170%) and Superoxide Dismutase 2 (SOD2 +131%) (Fig 6E).

Taken together, these observations suggest strong metabolic impairments after *Tfeb* silencing *in vivo*.

Tfeb affects melanoma metabolism in vitro

Given the promising data obtained in sh-*Tfeb* D4M tumours, we decided to better analyze the metabolic profile of scr-shRNA and sh-Tfeb D4M cells *in vitro*.

In sh-*Tfeb* compared to scr-shRNA D4M cells we confirmed a reduction in glycolysis: we evaluated the impairment in the activity of different enzymes of the cascade (GLUT -37.5%, PFK -63.7%, ALDO -65.4%, GAPDH -55.8%, ENO -60.9%, PK -68.9%, LDH -56%) (Fig 7A), that correlated with the decrease in lactate production (-49.6%) (Fig 7B).

We found a reduction of TCA cycle flux (-48.7%) (Fig 7C) in sh-Tfeb compared to scr-shRNA D4M cells; similar to tumours, a block of the second part of TCA cycle sustained by glutamine (OGDH -37.6%, SDH -62.4%) (Fig 7D) was evident.

Glutaminase (Gls) and Glutamic Dehydrogenase (Glu-DH) are key enzyme of glutaminolysis producing glutamate and α-ketoglutarate that can fuel TCA cycle: we verified their activity and showed that in sh-Tfeb compared to scr-shRNA D4M cells there was a reduction of Gls activity (-58.4%) while Glu-DH functionality was not modified (Fig 8A). On the contrary, no modulation of Gls transcription (Fig 8B) and protein expression (Fig 8C) was evidenced after *Tfeb* silencing.

We also considered the regulation of glutamine synthesis and demonstrated

that Glutamine Synthetase (Gs) activity was impaired (-61.9%) (Fig 8A), its mRNA was weakly reduced (Fig 8B) while its protein amount (Fig 8C) was not altered after *Tfeb* silencing in D4M cells.

To better undestand the molecular mechanism sustaining this phenomenon, we checked whether Tfeb could modulate glucose and glutamine uptake. After exogenous administration of [14C-6] glucose or [14C] glutamine we reported that the glucose quantity in sh-*Tfeb* compared to scr-shRNA D4M cells was reduced by 37.5% as well as glutamine quantity by 62.4% (Fig 8D).

Moreover, after glutamine addiction, the resulting intracellular amount of [14C] glutamate was reduced by 54.2% (Fig 8E).

The study of the TCA flux after exogenous implementation of [14C-6] glucose or [14C] glutamine confirmed a block of glucose and glutamine uptake: *Tfeb* silencing correlated with an inhibition by 50.8% of glucose-mediated and 72% of glutamine-mediated TCA flux (Fig 8F).

In order to rescue the putative block of cell proliferation mediated by the alteration of glutamine uptake, we feed D4M cells with different concentrations of glutamine. Glutamine deprivation has a negative impact on proliferation for both scr-shRNA and sh-*Tfeb* cells respectively compared to scr-shRNA and sh-*Tfeb* D4M with the normal glutamine concentration ([Q]=2mM) in the culture medium (Fig 8G), sustaining a strong role for glutamine in melanoma proliferation.

Assuming that a partial block in glutamine entry could be compensated by the increase of its supplementation, we grew cells in a five-fold more quantity of glutamine ([Q]=10mM) as usual ([Q]=2mM): sh-*Tfeb* D4M cells in 10mM-glutamine medium did not proliferate more compared to sh-Tfeb D4M cells in 2mM-glutamine medium (Fig 8G), underlining again the block of glutamine uptake.

Sh-*Tfeb* D4M cells compared to scr-shRNA cells were also characterized by

the reduction of oxidative phosphorylation (complex I -26.5%, complex II -52.8%, complex III -59.7%, complex IV -27.9%) (Fig 7E), mitochondrial ATP synthesis (-61.4%) (Fig 7F) and total quantity of ATP in cells (-40.7%) (Fig 7G).

Mitochondria seemed to be altered after *Tfeb* silencing as well as suggested by the increased of oxidative damage indexes: activity of mitochondrial transition pore (mPTP, +188.5%), TBARS (+53.9%), SOD2 (+123.4%) (Fig 7H).

These results suggest a global impairment of the metabolic activity of sh-*Tfeb* D4M cells and the inhibition of glycolysis and glutaminolysis seems to have a crucial role after *Tfeb* silencing.

Tfeb silencing alters lipid metabolism

Studying deeper the metabolic alterations caused by *Tfeb* silencing in D4M, we wonder whether it could affect lipid metabolism.

We found that cholesterol synthesis is decreased both *in vitro* (Fig 9A) and *in vivo* (Fig 9C) (-48.1% and -41.1%, respectively), whereas fatty acid beta-oxidation is increased again both *in vitro* (Fig 9B) and *in vivo* (Fig 9D) (+98.3% and +246%, respectively).

These evidences support the idea that Tfeb has an important role in regulating different metabolic pathways of the cell, including lipid management.

Tfeb deletion has similar effects on endothelial cell metabolism

In order to better characterize Tfeb contribution and specificity in cell metabolism, we decided to perform metabolic assays in a completely different cellular model: the human endothelial cells (HUVECs).

Even if the alterations are less marked, we saw a situation similar to that observed in D4M cells regarding energy production: glycolysis (Fig 10A), TCA cycle (Fig 10C) and oxidative phosphorylation (Fig 10D) are all downmodulated in sh-TFEB ECs. Interestingly, the enzymes affected in TCA cycle are different to those altered in melanoma cells.

Also in this case, lactate production (Fig 10B) and the mitochondrial ATP synthesis (Fig 10E) are decreased after TFEB silencing (-21.1% and -52.8%, respectively). In parallel, data show an increase in the oxidative damage indexes as observed in D4M cells, suggesting mitochondrial damage and malfunctioning: mPTP by 858%, TBARS by 67%, SOD2 by 119% (Fig 10F).

Concerning glutamine and lipid metabolism, glutaminase activity is reduced in sh-TFEB ECs by 33.6% (Fig 11A) as well as cholesterol synthesis by 51.6% (Fig 11B). On the contrary, fatty acid beta-oxidation is increased by 44.6% after TFEB silencing (Fig 11C).

Taken together, these results further support the observation that TFEB plays a pivotal role in regulating metabolism in different cell types and contexts.

FIGURE S1

A)

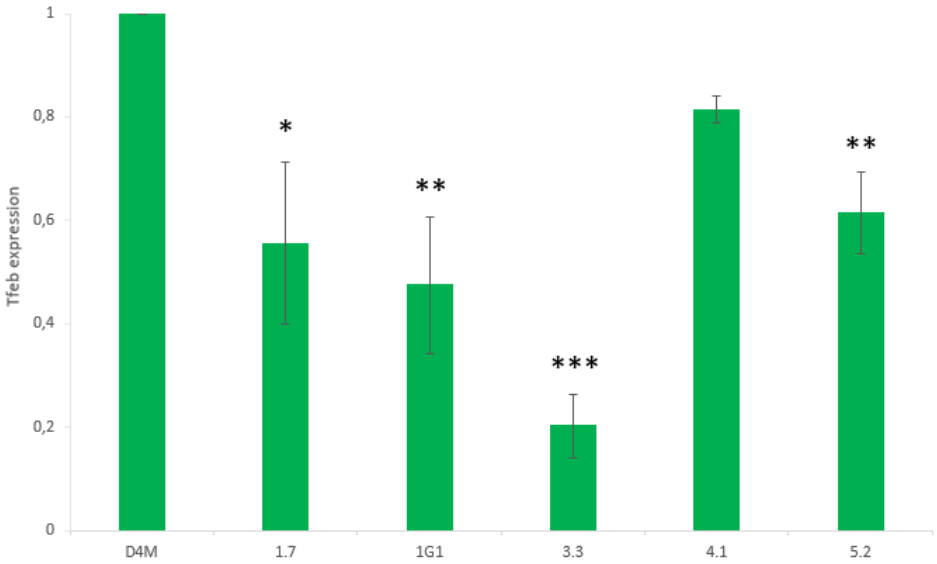
Tfeb expression
1
0,8
0,6
0,4
0,2
0
*
**
***
**
D4M
1.7
1G1
3.3
4.1
5.2

B)

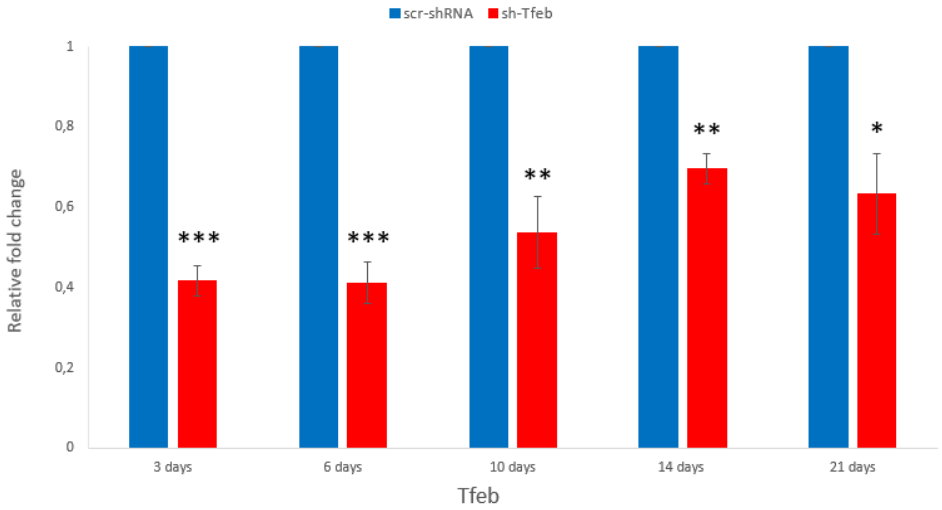
scr-shRNA
sh-Tfeb
Relative fold change
1
0,8
0,6
0,4
0,2
0
***
***
**
**
*
3 days
6 days
10 days
14 days
21 days
Tfeb

Figure S1. *Tfeb* expression

A) qPCR of *Tfeb* expression in the different murine melanoma cell lines at basal level. Data are expressed as relative fold-change compared to the expression of *Tfeb* in D4M samples after normalization with the housekeeping gene *Tbp* (exp n=3, mean +- SEM; *P<0.05, **P<0.01, ***P<0.001 vs D4M cells by Student's t-test).

B) qPCR of *Tfeb* expression in scr-shRNA and sh-*Tfeb* D4M cells at different time points after infection with the specific lentivirus. Data are expressed as relative fold-change compared to the expression of scr-shRNA samples after normalization with the housekeeping gene *Tbp* (exp n=3, mean +- SEM; **P<0.01, ***P<0.001 vs scr-shRNA cells by Student's t-test).

FIGURE 1

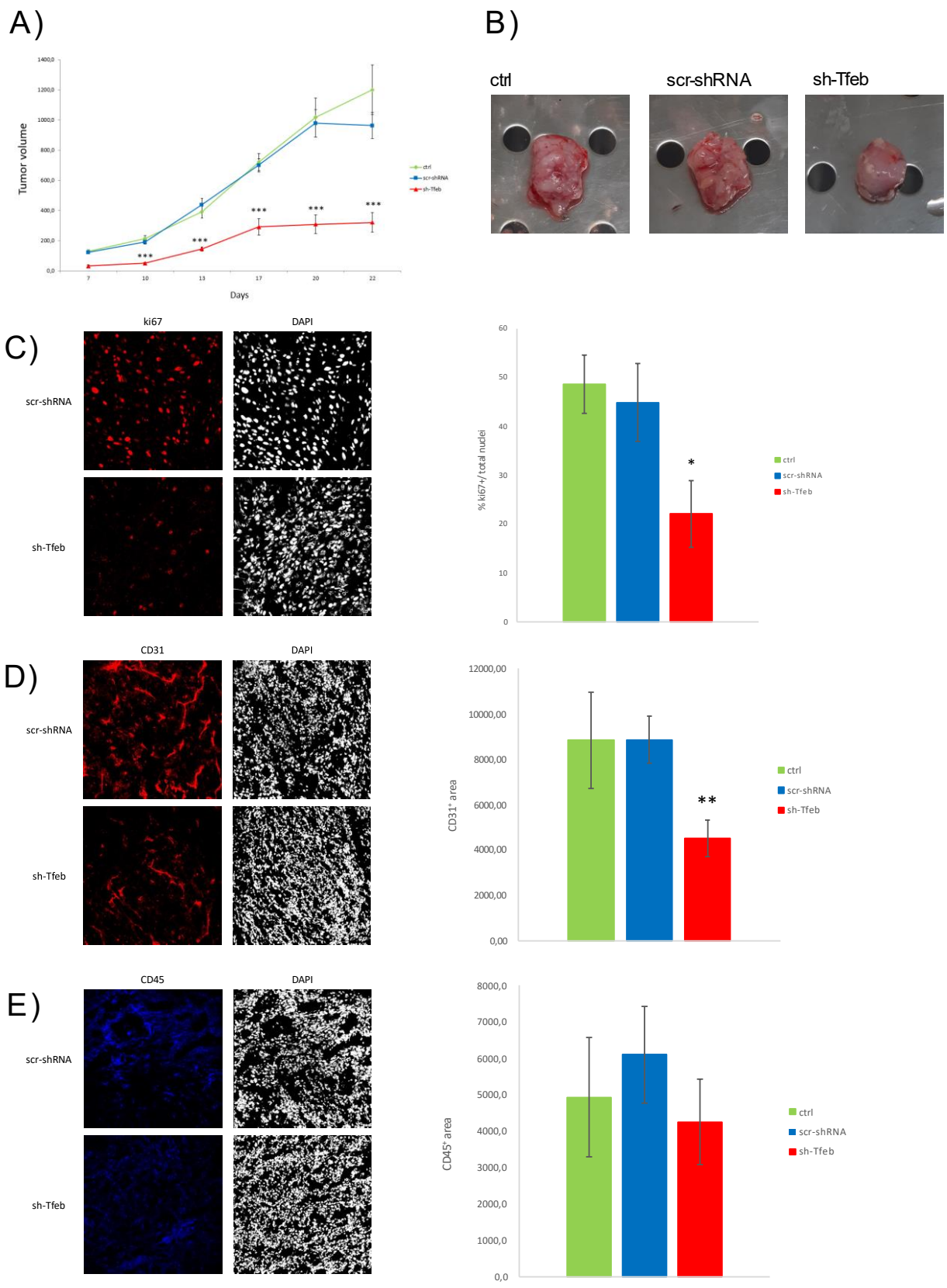
A)
Tumor volume
Days
ctrl
scr-shRNA
sh-Tfeb
B)
ctrl
scr-shRNA
sh-Tfeb
C)
ki67
DAPI
scr-shRNA
sh-Tfeb
% ki67+/ total nuclei
D)
CD31
DAPI
scr-shRNA
sh-Tfeb
CD31+ area
E)
CD45
DAPI
scr-shRNA
sh-Tfeb
CD45+ area

Figure 1. Tumour growth after *Tfeb* deletion

A) Growth curve of ctrl, scr-shRNA and sh-*Tfeb* D4M tumours (exp n=7, mean +- SEM; ***P<0.001 vs ctrl or scr-shRNA tumours by Student's t-test).
B) Representative images of ctrl, scr-shRNA and sh-*Tfeb* D4M tumours explanted from mice 22 days after cancer cell injection.
C) Ki67 staining of D4M tumour samples: representative images and quantification of positive area over total area (exp n=7, mean +- SEM; *P<0.05 vs scr-shRNA tumours by Student's t-test).
D) CD31 staining of D4M tumour samples: representative images and quantification of positive area over total area (exp n=7, mean +- SEM; **P<0.01 vs scr-shRNA tumours by Student's t-test).
E) CD45 staining of D4M tumour samples: representative images and quantification of positive area over total area (exp n=7, mean +- SEM).

FIGURE 2

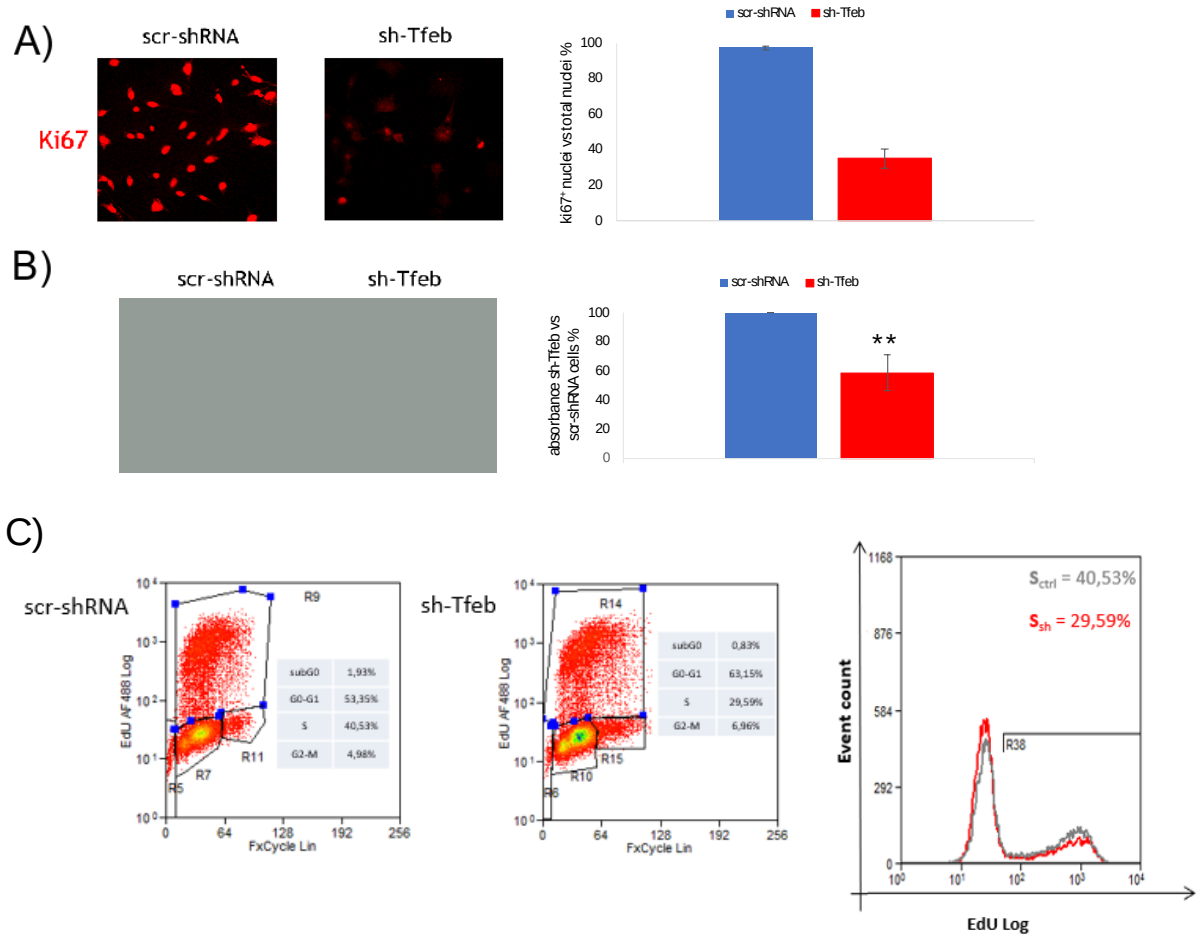
A)
scr-shRNA
sh-Tfeb
Ki67
scr-shRNA
sh-Tfeb
ki67+ nuclei vs total nuclei %
B)
scr-shRNA
sh-Tfeb
scr-shRNA
sh-Tfeb
absorbance sh-Tfeb vs scr-shRNA cells %
**
C)
scr-shRNA
sh-Tfeb
EdU AF 488 Log
FxCycle Lin
R9
R11
R7
R5
R14
R15
R10
R8
subG0 1,93%
G0-G1 53,35%
S 40,53%
G2-M 4,98%
subG0 0,83%
G0-G1 63,15%
S 29,59%
G2-M 6,96%
S_ctrl = 40,53%
S_sh = 29,59%
Event count
R38
EdU Log
D)
scr-shRNA
sh-Tfeb
Relative fold change
***
**
Ccnd1
Cdk4
E)
scr-shRNA
sh-TFEB
Cyclin D1
Cdk4
pRb
Rb
Pcna
alpha -actin
F)
scr-shRNA
sh-Tfeb
Relative fold change
***
Pcna

Figure 2. Cell proliferation after *Tfeb* silencing *in vitro*

A) Ki67 staining of D4M cells 3 days after infection: representative images and quantification of positive area over total area (exp n=3, mean +- SEM; ***P<0.001 vs scr-shRNA cells by Student's t-test).

B) Crystal violet staining of D4M cells 8 days after infection (exp n=4, mean +- SEM; **P<0.01 vs scr-shRNA cells by Student's t-test).

C) Cell cycle progress analysis of D4M cells 3 days after infection. DNA incorporation of EdU and propidium iodide staining detected through Fluorescence-Activated Cell Sorter: representative experiment out of 2 with similar results.

D) qPCR of *Cyclin D1* and *Cdk4* expression in scr-shRNA and sh-*Tfeb* D4M cells. Data are expressed as relative fold-change compared to the expression of scr-shRNA samples after normalization with the housekeeping gene *Tbp* (exp n=6, mean +- SEM; **P<0.01, ***P<0.001 vs scr-shRNA cells by Student's t-test).

E) Representative western blots of total lysates from scr-shRNA and sh-*Tfeb* D4M cells probed with specific Abs.

F) qPCR of *Pcna* expression in scr-shRNA and sh-*Tfeb* D4M cells. Data are expressed as relative fold-change compared to the expression of scr-shRNA samples after normalization with the housekeeping gene *Tbp* (exp n=6, mean +- SEM; ***P<0.001 vs scr-shRNA cells by Student's t-test).

FIGURE 3

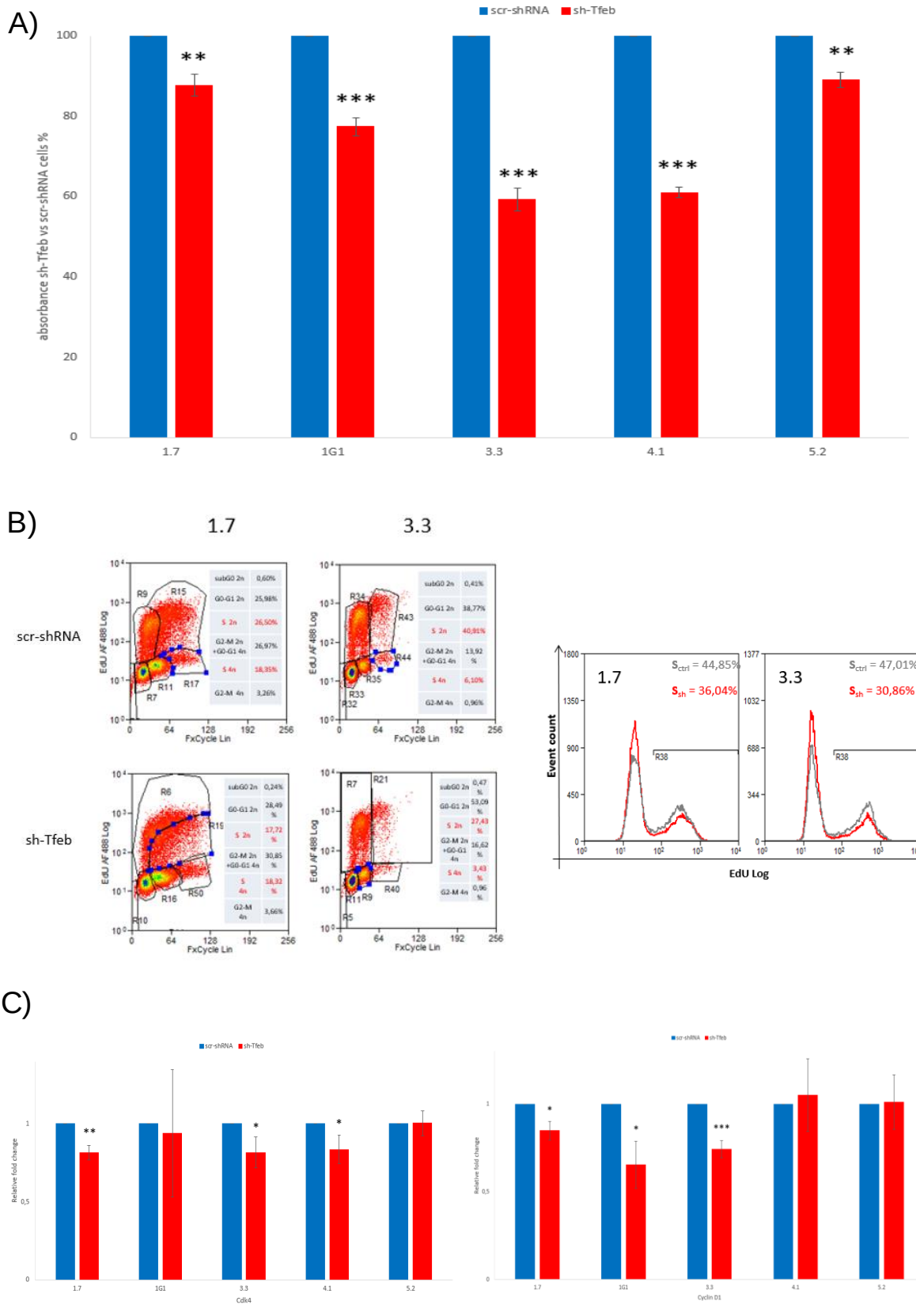
A)
scr-shRNA
sh-Tfeb
absorbance sh-Tfeb vs scr-shRNA cells %
1.7
1G1
3.3
4.1
5.2
B)
1.7
3.3
scr-shRNA
sh-Tfeb
EdU AF 488 Log
FxCycle Lin
Event count
EdU Log
S_ctrl = 44,85%
S_sh = 36,04%
S_ctrl = 47,01%
S_sh = 30,86%
R38
C)
Relative fold change
Cdk4
Cyclin D1

Figure 3. Tfeb effect on YUMM cell proliferation

A) Crystal violet staining of different YUMM cell lines 3 days after infection (exp n=3, mean +- SEM; **P<0.01, ***P<0.001 vs scr-shRNA cells by Student's t-test).

B) Cell cycle progress analysis of 1.7 and 3.3 YUMM cell lines 3 days after infection. DNA incorporation of EdU and propidium iodide staining detected through Fluorescence-Activated Cell Sorter: representative experiment out of 2 with similar results.

C) qPCR of *Cyclin D1* and *Cdk4* expression in scr-shRNA and sh-*Tfeb* YUMM cells. Data are expressed as relative fold-change compared to the expression of scr-shRNA samples after normalization with the housekeeping gene *Tbp* (exp n=3, mean +- SEM; *P<0.05, **P<0.01, ***P<0.001 vs scr-shRNA cells by Student's t-test).

FIGURE 4

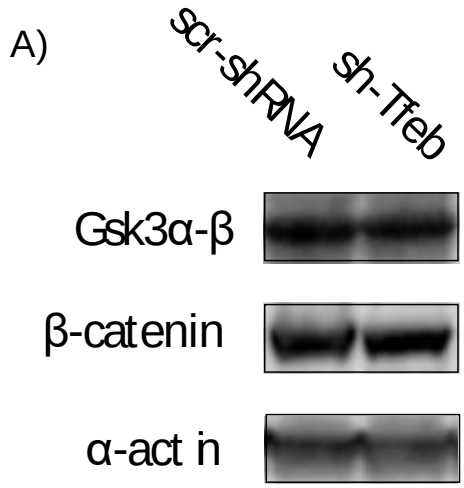

Figure 4. Gsk3β after *Tfeb* inhibition

A) Representative western blots of total lysates from scr-shRNA and sh-*Tfeb* D4M cells probed with specific Abs.

FIGURE 5

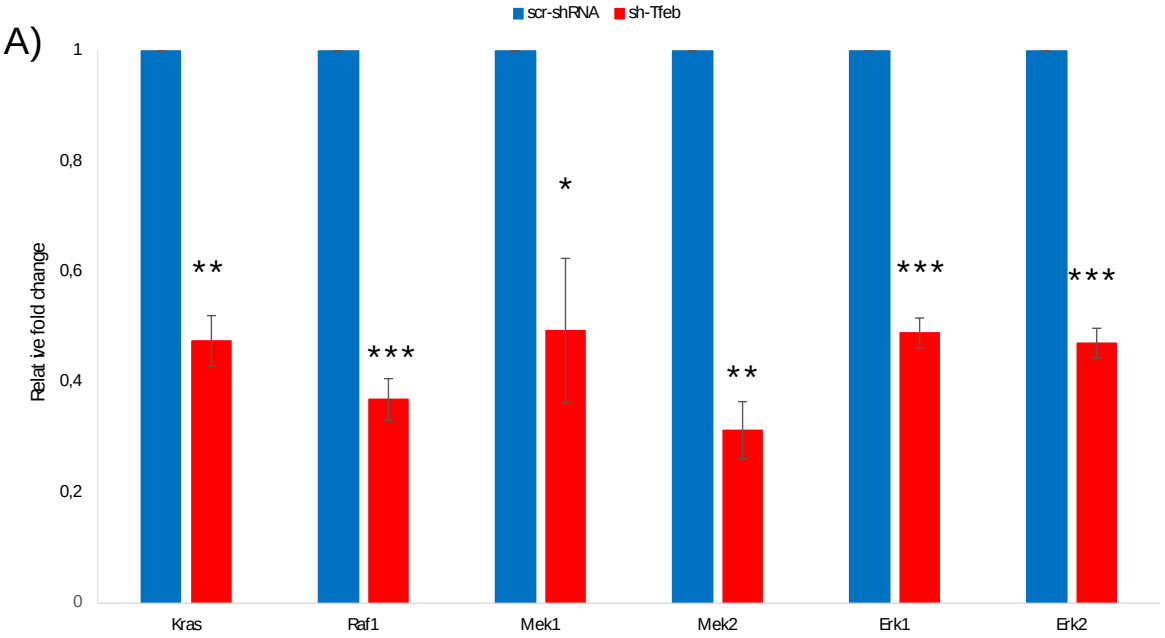
A)
scr-shRNA
sh-Tfeb
Relat ive fold change
1
0,8
0,6
0,4
0,2
0
**
***
*
**
***
***
Kras
Raf1
Mek1
Mek2
Erk1
Erk2

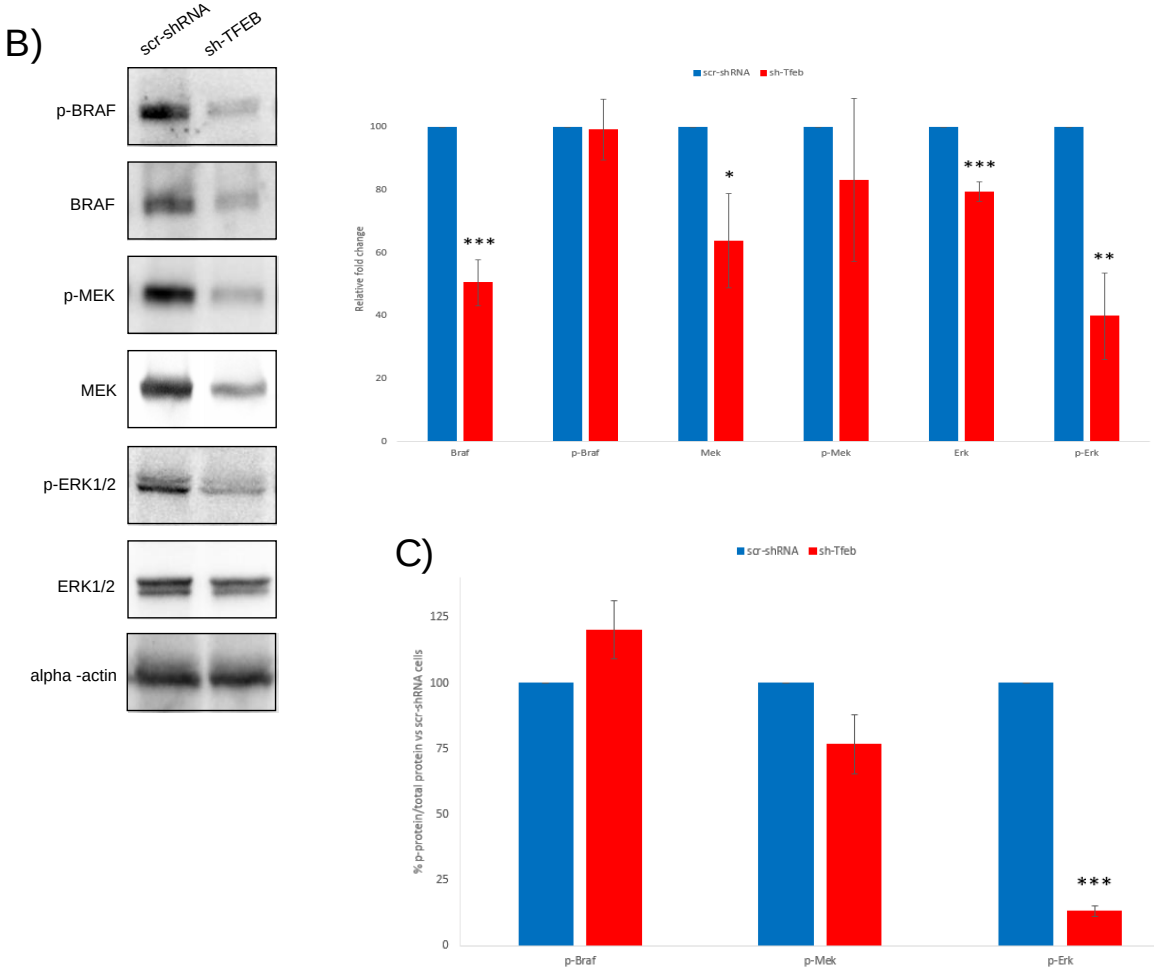
B)
scr-shRNA
sh-TFEB
p-BRAF
BRAF
p-MEK
MEK
p-ERK1/2
ERK1/2
alpha -actin
scr-shRNA
sh-Tfeb
Relative fold change
100
80
60
40
20
0
***
*
***
**
Braf
p-Braf
Mek
p-Mek
Erk
p-Erk
C)
scr-shRNA
sh-Tfeb
% p-protein/total protein vs scr-shRNA cells
125
100
75
50
25
0
***
p-Braf
p-Mek
p-Erk

Figure 5. Tfeb influence on MAPK pathway

A) qPCR of *Kras, Raf1, Mek1, Mek2, Erk1* and *Erk2* expression in scr-shRNA and sh-*Tfeb* D4M cells. Data are expressed as relative fold-change compared to the expression of scr-shRNA samples after normalization with the housekeeping gene *Tbp* (exp n=3, mean +- SEM; *P<0.05, **P<0.01, ***P<0.001 vs scr-shRNA cells by Student's t-test).

B) Representative western blots of total lysates from scr-shRNA and sh-*Tfeb* D4M cells probed with specific Abs and relative densitometric analysis expressed as ratio between protein of interest and α-actin (exp n=3, mean +- SEM; *P<0.05, **P<0.01, ***P<0.001 vs scr-shRNA cells by Student's t-test).

C) Ratio between p-protein and total protein vs scr-shRNA D4M cells (exp n=3, mean +- SEM; ***P<0.001 vs scr-shRNA cells by Student's t-test).

FIGURE 6

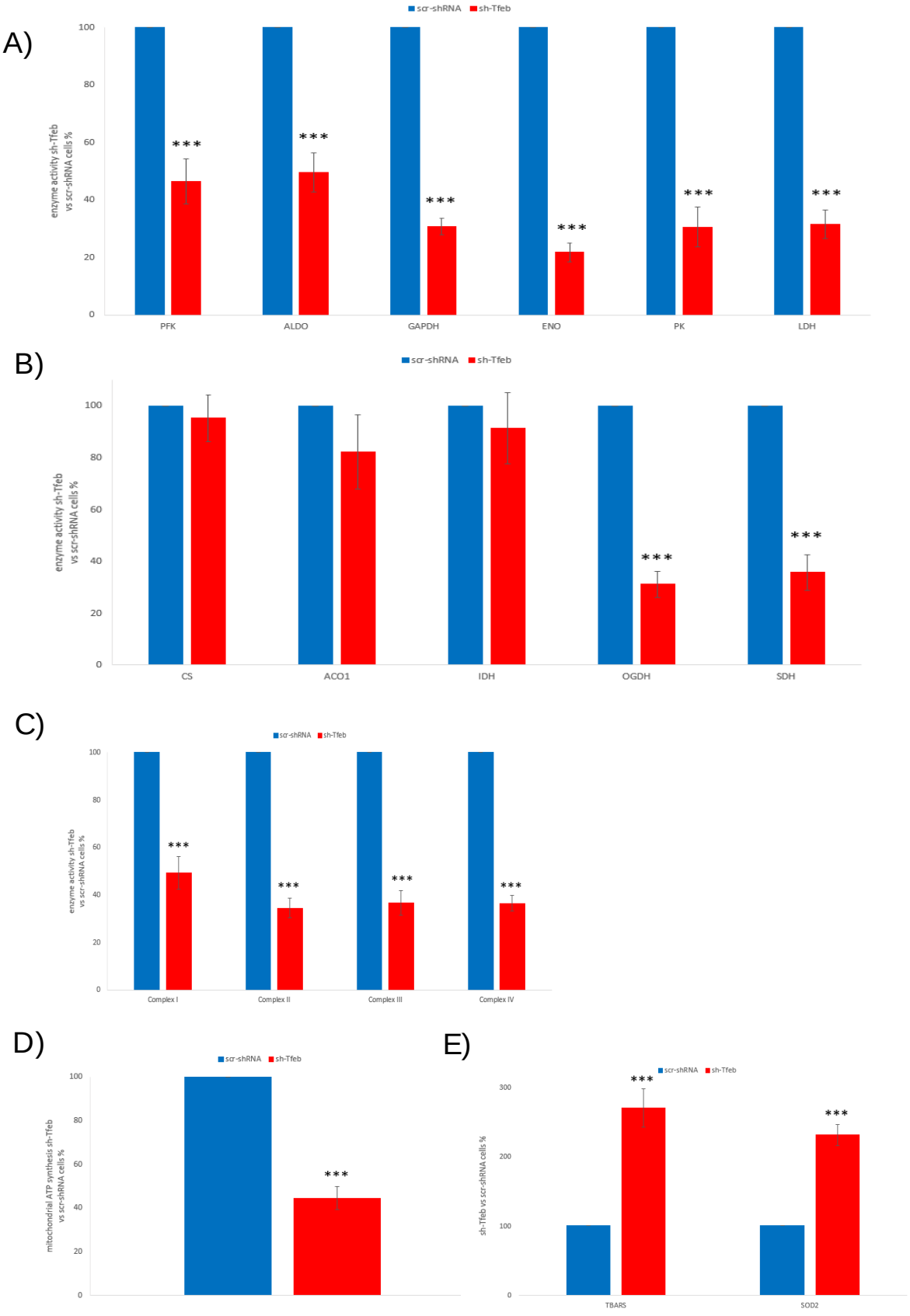
A)
scr-shRNA
sh-Tfeb
enzyme activity sh-Tfeb vs scr-shRNA cells %
PFK
ALDO
GAPDH
ENO
PK
LDH
B)
CS
ACO1
IDH
OGDH
SDH
C)
Complex I
Complex II
Complex III
Complex IV
D)
mitochondrial ATP synthesis sh-Tfeb vs scr-shRNA cells %
E)
sh-Tfeb vs scr-shRNA cells %
TBARS
SOD2

Figure 6. Tfeb role in tumour metabolism *in vivo*

A) Activity of different enzymes of the glycolytic pathway (nmoles NAD/min/mg prot for PFK, ALDO, GAPDH, ENO, LDH or nmoles pyruvate/mg prot for PK) in percentage compared to scr-shRNA D4M tumour samples (exp n=7, mean +- SEM; ***P<0.001 vs scr-shRNA cells by Student's t-test).

B) Activity of different enzymes of the TCA cycle (mU/mg mitochondrial proteins) in percentage compared to scr-shRNA D4M tumour samples (exp n=7, mean +- SEM; ***P<0.001 vs scr-shRNA cells by Student's t-test).

C) Activity of the different complexes of the oxidative phosphorylation (nanomoles of oxidized cytochrome c/min/mg mitochondrial proteins) in percentage compared to scr-shRNA D4M tumour samples (exp n=7, mean +- SEM; ***P<0.001 vs scr-shRNA cells by Student's t-test).

D) Mitochondrial ATP synthesis (nmoles ATP/mg mitochondrial proteins) in percentage compared to scr-shRNA D4M tumour samples (exp n=7, mean +- SEM; ***P<0.001 vs scr-shRNA cells by Student's t-test).

E) Quantification of oxidative stress indexes (nmol/mg mitochondrial proteins for TBARS, µmoles reduced cytochrome c/min/mg mitochondrial proteins for SOD2) in percentage compared to scr-shRNA D4M tumour samples (exp n=7, mean +- SEM; ***P<0.001 vs scr-shRNA cells by Student's t-test).

FIGURE 7

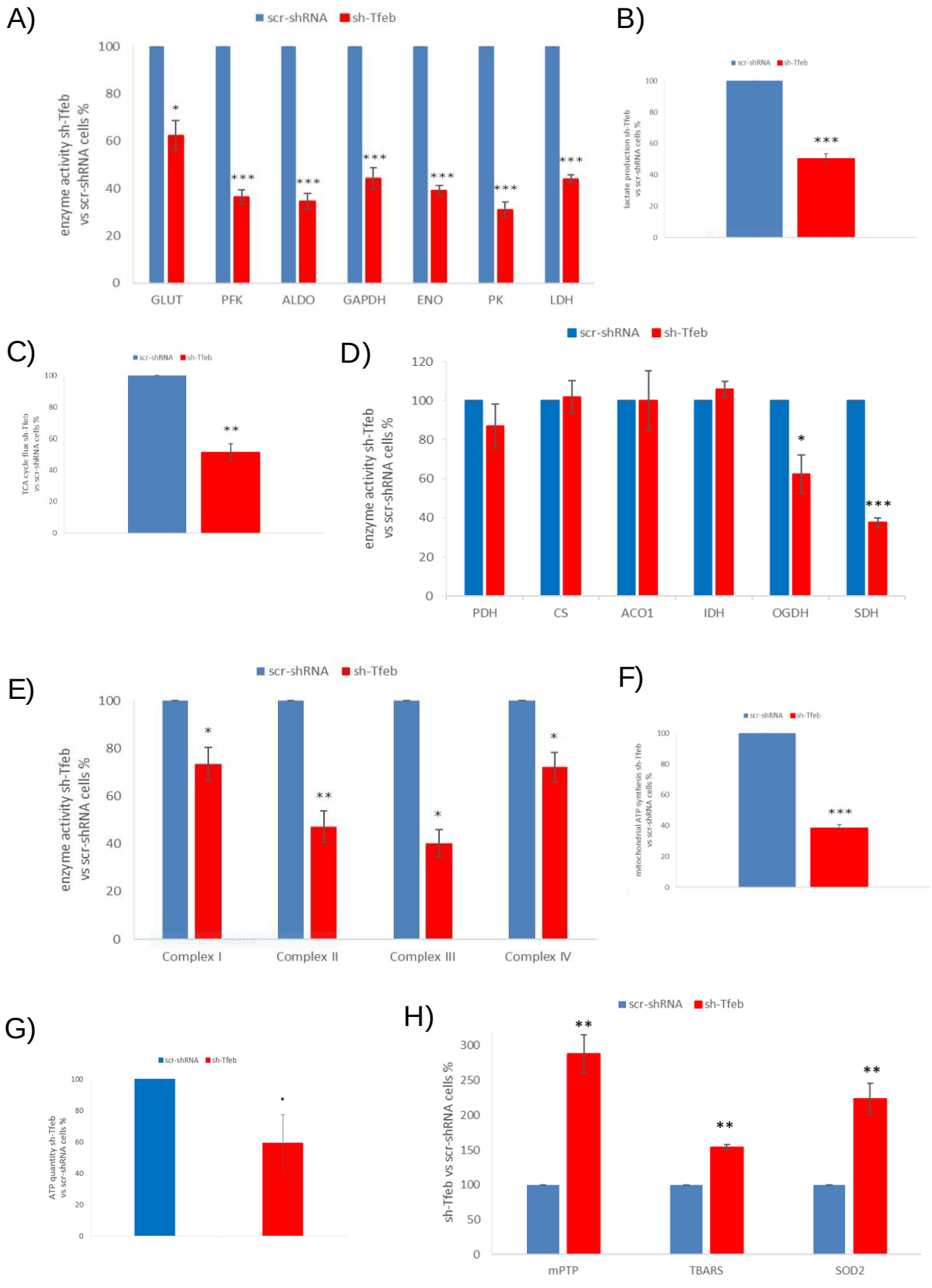
A)
scr-shRNA
sh-Tfeb
enzyme activity sh-Tfeb vs scr-shRNA cells %
GLUT
PFK
ALDO
GAPDH
ENO
PK
LDH
B)
lactate production sh-Tfeb vs scr-shRNA cells %
C)
TCA cycle flux sh-Tfeb vs scr-shRNA cells %
D)
PDH
CS
ACO1
IDH
OGDH
SDH
E)
Complex I
Complex II
Complex III
Complex IV
F)
mitochondrial ATP synthesis sh-Tfeb vs scr-shRNA cells %
G)
ATP quantity sh-Tfeb vs scr-shRNA cells %
H)
sh-Tfeb vs scr-shRNA cells %
mPTP
TBARS
SOD2

Figure 7. Tfeb influence on the major metabolic pathways *in vitro*

A) Activity of different enzymes of the glycolytic pathway (nmoles NAD/min/mg prot for GLUT, PFK, ALDO, GAPDH, ENO, LDH or nmoles pyruvate/mg prot for PK) in percentage compared to scr-shRNA D4M cells 3 days after infection (exp n=3, mean +- SEM; *P<0.05, ***P<0.001 vs scr-shRNA cells by Student's t-test).

B) Lactate production (nmoles lactate/mg cellular proteins) in percentage compared to scr-shRNA D4M cells 3 days after infection (exp n=3, mean +- SEM; ***P<0.001 vs scr-shRNA cells by Student's t-test).

C) TCA cycle flux (nmoles CO_2/h/mg proteins) in percentage compared to scr-shRNA D4M cells 3 days after infection (exp n=3, mean +- SEM; **P<0.01 vs scr-shRNA cells by Student's t-test).

D) Activity of different enzymes of the TCA cycle (mU/mg mitochondrial proteins) in percentage compared to scr-shRNA D4M cells 3 days after infection (exp n=3, mean +- SEM; *P<0.05, ***P<0.001 vs scr-shRNA cells by Student's t-test).

E) Activity of the different complexes of the oxidative phosphorylation (nanomoles of oxidized cytochrome c/min/mg mitochondrial proteins) in percentage compared to scr-shRNA D4M cells 3 days after infection (exp n=3, mean +- SEM; *P<0.05, **P<0.01 vs scr-shRNA cells by Student's t-test).

F) Mitochondrial ATP synthesis (nmoles ATP/mg mitochondrial proteins) in percentage compared to scr-shRNA D4M cells 3 days after infection (exp n=3, mean +- SEM; ***P<0.001 vs scr-shRNA cells by Student's t-test).

G) Quantification of ATP in cells (relative light units (RLU)) in percentage compared to scr-shRNA D4M cells 8 days after infection (exp n=3, mean +- SEM; *P<0.05 vs scr-shRNA cells by Student's t-test).

H) Quantification of oxidative stress indexes (relative fluorescence unit (RFU)/mg cellular proteins for mPTP, nmol/mg mitochondrial proteins for TBARS, µmoles reduced cytochrome c/min/mg mitochondrial proteins for SOD2) in percentage compared to scr-shRNA D4M cells (exp n=3, mean +- SEM; **P<0.01 vs scr-shRNA cells by Student's t-test).

FIGURE 8

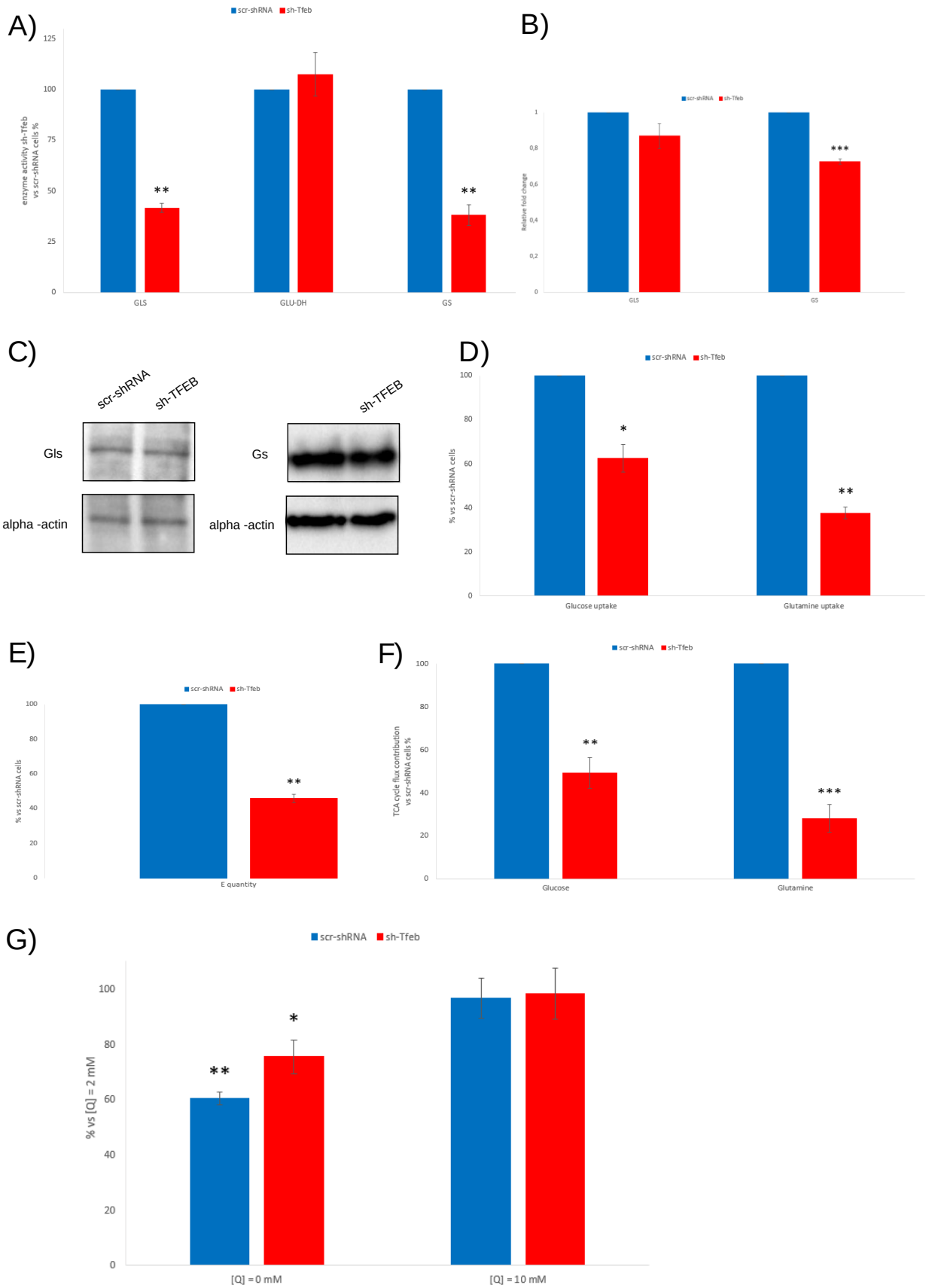
A)
scr-shRNA
sh-Tfeb
enzyme activity sh-Tfeb vs scr-shRNA cells %
125
100
75
50
25
0
**
**
GLS
GLU-DH
GS
B)
scr-shRNA
sh-Tfeb
Relative fold change
1
0,8
0,6
0,4
0,2
0
***
GLS
GS
C)
scr-shRNA
sh-TFEB
Gls
alpha -actin
sh-TFEB
Gs
alpha -actin
D)
scr-shRNA
sh-Tfeb
% vs scr-shRNA cells
100
80
60
40
20
0
*
**
Glucose uptake
Glutamine uptake
E)
scr-shRNA
sh-Tfeb
% vs scr-shRNA cells
100
80
60
40
20
0
**
E quantity
F)
scr-shRNA
sh-Tfeb
TCA cycle flux contribution vs scr-shRNA cells %
100
80
60
40
20
0
**
***
Glucose
Glutamine
G)
scr-shRNA
sh-Tfeb
% vs [Q] = 2 mM
100
80
60
40
20
0
**
*
[Q] = 0 mM
[Q] = 10 mM

Figure 8. Effects on glutamine metabolism after *Tfeb* silencing *in vitro*

A) Activity of enzymes involved in glutamine metabolism (µmol NADH/min/mg prot for GLS and GLU-DH, nmol/mg prot for GS) in percentage compared to scr-shRNA D4M cells 3 days after infection (exp n=3, mean +- SEM; **P<0.01 vs scr-shRNA cells by Student's t-test).

B) qPCR of *Glutaminase* and *Glutamine Synthetase* expression in scr-shRNA and sh-*Tfeb* D4M cells. Data are expressed as relative fold-change compared to the expression of scr-shRNA samples after normalization with the housekeeping gene *Tbp* (exp n=4, mean +- SEM; ***P<0.001 vs scr-shRNA cells by Student's t-test).

C) Representative western blots of total lysates from scr-shRNA and sh-*Tfeb* D4M probed with specific Abs.

D) Glucose and glutamine uptake (pmol/min/mg prot for glucose and µmol/mg prot for glutamine) in percentage compared to scr-shRNA D4M cells 3 days after infection (exp n=3, mean +- SEM; *P<0.05, **P<0.01 vs scr-shRNA cells by Student's t-test).

E) Quantification of glutamate in cells after [14C] glutamine supplementation in cells (µmol/mg prot) in percentage compared to scr-shRNA D4M cells 3 days after infection (exp n=3, mean +- SEM; **P<0.01 vs scr-shRNA cells by Student's t-test).

F) Glucose and glutamine contribution in TCA cycle flux (nmol CO2/h/mh prot) in percentage compared to scr-shRNA D4M cells 3 days after infection (exp n=3, mean +- SEM; **P<0.01, ***P<0.001 vs scr-shRNA cells by Student's t-test).

G) Crystal violet staining of D4M cells 4 days after infection and 1 day with different Q concentration in percentage compared to scr-shRNA D4M with [Q] = 2mM (exp n=3, mean +- SEM; *P<0.05, **P<0.01 vs scr-shRNA cells

by Student’s t-test).

FIGURE 9

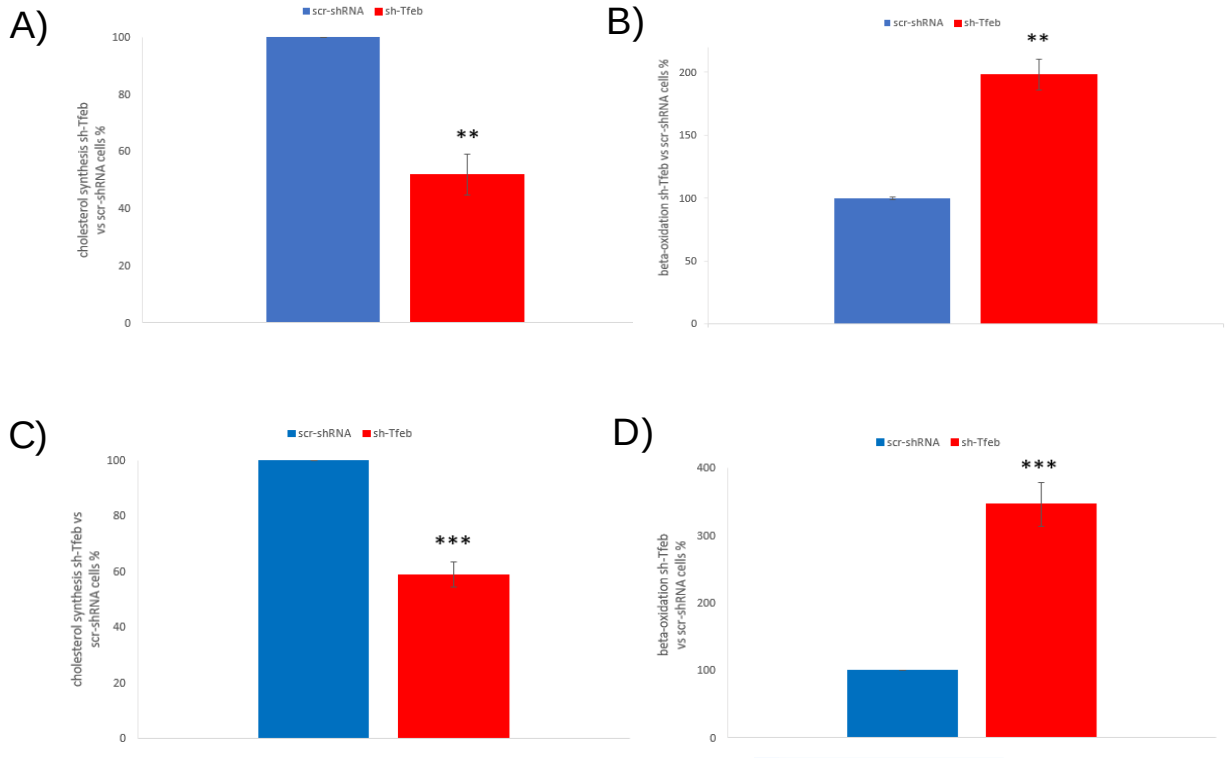
A)
scr-shRNA
sh-Tfeb
cholesterol synthesis sh-Tfeb vs scr-shRNA cells %
100
80
60
40
20
0
**
B)
scr-shRNA
sh-Tfeb
beta-oxidation sh-Tfeb vs scr-shRNA cells %
200
150
100
50
0
**
C)
scr-shRNA
sh-Tfeb
cholesterol synthesis sh-Tfeb vs scr-shRNA cells %
100
80
60
40
20
0
***
D)
scr-shRNA
sh-Tfeb
beta-oxidation sh-Tfeb vs scr-shRNA cells %
400
300
200
100
0
***

Figure 9. Tfeb involvement in lipid metabolism *in vitro* and *in vivo*

A) Cholesterol synthesis (pmoles/10^6 cells) in percentage compared to scr-shRNA D4M cells 3 days after infection (exp n=3, mean +- SEM; **P<0.01 vs scr-shRNA cells by Student's t-test).
B) Beta-oxidation (pmoles/h/mg prot) in percentage compared to scr-shRNA D4M cells 3 days after infection (exp n=3, mean +- SEM; **P<0.01 vs scr-shRNA cells by Student's t-test).
C) Cholesterol synthesis (pmoles/10^6 cells) in percentage compared to scr-shRNA D4M tumour samples (exp n=3, mean +- SEM; ***P<0.001 vs scr-shRNA cells by Student's t-test).
D) Beta-oxidation (pmoles/h/mg prot) in percentage compared to scr-shRNA D4M tumour samples (exp n=3, mean +- SEM; ***P<0.001 vs scr-shRNA cells by Student's t-test).

FIGURE 10

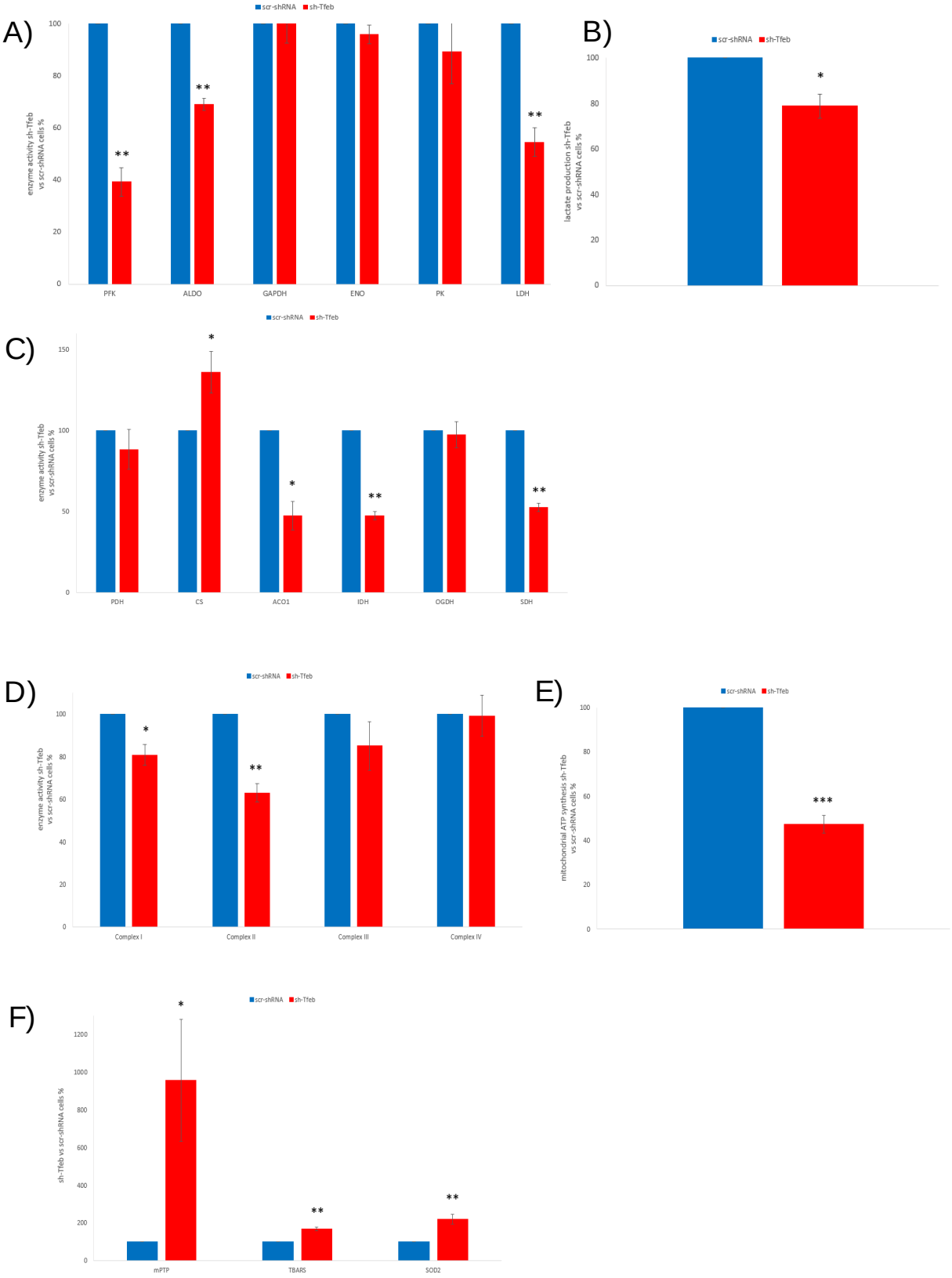
A)
scr-shRNA
sh-Tfeb
enzyme activity sh-Tfeb vs scr-shRNA cells %
PFK
ALDO
GAPDH
ENO
PK
LDH
B)
lactate production sh-Tfeb vs scr-shRNA cells %
C)
PDH
CS
ACO1
IDH
OGDH
SDH
D)
Complex I
Complex II
Complex III
Complex IV
E)
mitochondrial ATP synthesis sh-Tfeb vs scr-shRNA cells %
F)
sh-Tfeb vs scr-shRNA cells %
mPTP
TBARS
SOD2

Figure 10. TFEB influence on the major metabolic pathways in human endothelial cell *in vitro*

A) Activity of different enzymes of the glycolytic pathway (nmoles NAD/min/mg prot for PFK, ALDO, GAPDH, ENO, LDH or nmoles pyruvate/mg prot for PK) in percentage compared to scr-shRNA ECs 3 days after infection (exp n=3, mean +- SEM; **P<0.01 vs scr-shRNA cells by Student's t-test).

B) Lactate production (nmoles lactate/mg cellular proteins) in percentage compared to scr-shRNA ECs 3 days after infection (exp n=3, mean +- SEM; *P<0.05 vs scr-shRNA cells by Student's t-test).

C) Activity of different enzymes of the TCA cycle (mU/mg mitochondrial proteins) in percentage compared to scr-shRNA ECs 3 days after infection (exp n=3, mean +- SEM; *P<0.05, **P<0.01 vs scr-shRNA cells by Student's t-test).

D) Activity of the different complexes of the oxidative phosphorylation (nanomoles of oxidized cytochrome c/min/mg mitochondrial proteins) in percentage compared to scr-shRNA ECs 3 days after infection (exp n=3, mean +- SEM; *P<0.05, **P<0.01 vs scr-shRNA cells by Student's t-test).

E) Mitochondrial ATP synthesis (nmoles ATP/mg mitochondrial proteins) in percentage compared to scr-shRNA ECs 3 days after infection (exp n=3, mean +- SEM; ***P<0.001 vs scr-shRNA cells by Student's t-test).

F) Quantification of oxidative stress indexes (relative fluorescence unit (RFU)/mg cellular proteins for mPTP, nmol/mg mitochondrial proteins for TBARS, µmoles reduced cytochrome c/min/mg mitochondrial proteins for SOD2) in percentage compared to scr-shRNA ECs (exp n=3, mean +- SEM; **P<0.01 vs scr-shRNA cells by Student's t-test).

FIGURE 11

A)

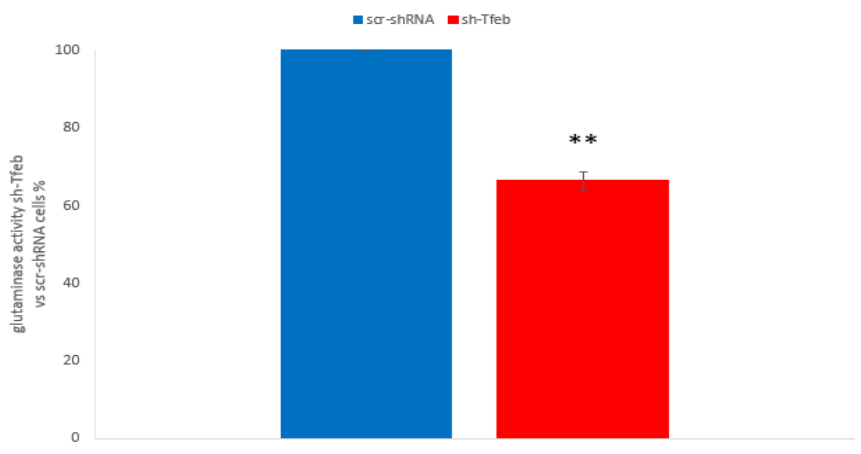

B)

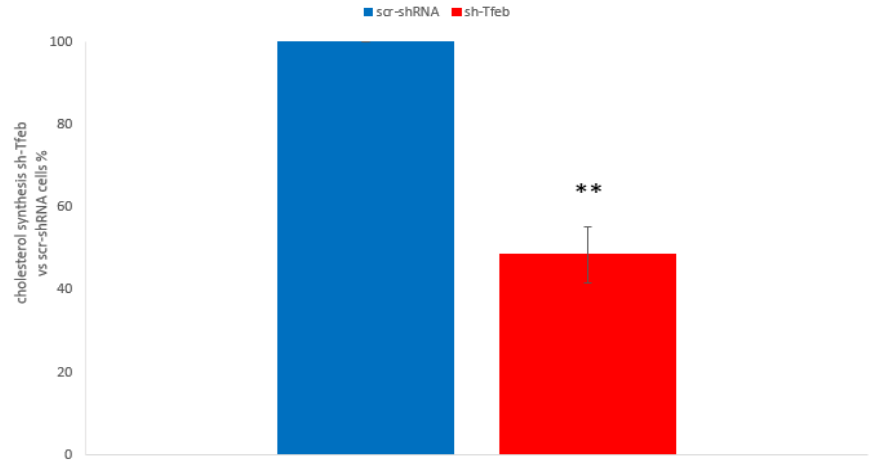

C)

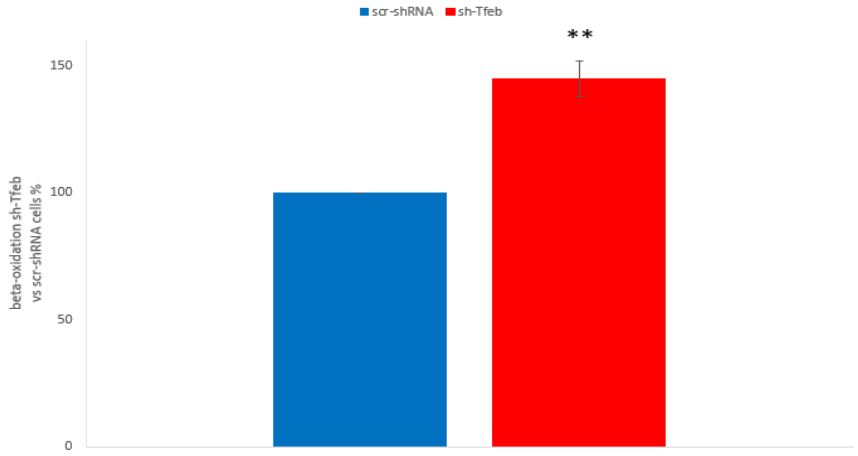

Figure 11. TFEB role in lipid and glutamine metabolism in endothelium *in vitro*

A) Glutaminase activity (µmol NADH/min/mg prot) in percentage compared to scr-shRNA ECs 3 days after infection (exp n=3, mean +- SEM; **P<0.01 vs scr-shRNA cells by Student's t-test).
B) Cholesterol synthesis (pmoles/10^6 cells) in percentage compared to scr-shRNA ECs 3 days after infection (exp n=3, mean +- SEM; **P<0.01 vs scr-shRNA cells by Student's t-test).
C) Beta-oxidation (pmoles/h/mg prot) in percentage compared to scr-shRNA ECs 3 days after infection (exp n=3, mean +- SEM; **P<0.01 vs scr-shRNA cells by Student's t-test).

DISCUSSION

Melanoma is the most frequent form of cancer found in young adults and its frequency is increasing worldwide being now the fifth most common form of cancer in men and the sixth in women in the United States (Rastrelli et al, 2014; Raimondi et al, 2020).

Although most patients have localized disease at the time of the diagnosis and are treated by surgical excision of the primary tumor, melanoma has a high risk of metastatic spread (Rastrelli et al, 2014).

In recent years, targeted therapies and immunotherapy have improved the outcomes of metastatic melanoma, but drug resistance and tumour relapse still occurs (Ostrowski and Fisher, 2021).

For this reason, challenges remain in investigating the biology of melanoma in order to find new therapeutic treatments.

In the present study, we demonstrated how the MiT-TFE family member TFEB, traditionally involved in autophagy and lysosomal clearance, plays an important role in melanoma biology.

We investigated the role of TFEB in melanoma by *in vitro* and *in vivo* experiments focusing on the murine melanoma D4M cell line, characterized by the activating mutation BRAFV600E and the deletion of *Pten* gene, mimicing the pathological molecular alterations present in a great number of human melanomas. Nevertheless, Tfeb effects were also confirmed in other murine melanoma cell lines with different mutational landscapes, suggesting a general role of Tfeb in melanoma.

In this work, we demonstrated that Tfeb is involved in melanoma development and in particular we evidenced that the silencing of cellular physiological *Tfeb* directly reduces tumour growth via the parallel regulation of cell proliferation and metabolism. Moreover, after *Tfeb* inhibition

melanoma development alteration is also supported by the reduction of tumour angiogenesis while the immune system cell recruitment seems not to be involved.

It has already been demonstrated that TFEB has a role in regulating cancer cell proliferation but its contribution has been mainly connected with its effect on the autophagic flux. In particular, knockdown of TFEB decreases the proliferation rate of prostate cancer (Blessing et al, 2017), pancreatic cancer (Perera et al, 2015) and colorectal cancer (Liang et al, 2018). Moreover, the increased cell proliferation observed in renal cell carcinoma carrying the t(6;11)(p21:q13) translocation indirectly supports the important influence of TFEB on cell growth (Calcagnì et al, 2016).

In some other cases, such as oral squamous cell carcinoma (Sakamoto et al, 2018), non-small cell lung cancer (Giatromanolaki et al, 2015; Kundu et al, 2018) and breast cancer (Giatromanolaki et al, 2017), TFEB does not directly control proliferation but its expression is correlated with poor prognosis and/or enhanced migratory phenotype.

However, these previous studies demonstrated that TFEB can influence cell proliferation, but none of these showed a direct control of the transcription factor on a particular protein involved in traditional pathways responsible for cell growth and proliferation.

In contrast, Doronzo et al observed that TFEB can directly bind to the promoter and therefore induce the expression of the CDK4 gene, fundamental for cell proliferation, in human endothelium (Doronzo et al, 2019).

Similarly, in the melanoma cells we observed an inhibition of Cdk4 transcription and protein expression after *Tfeb* silencing. Moreover, in the same condition, we demonstrated a robust reduction of both trascription and protein amount of Cyclin D1.

Cyclin D1 and Cdk4 working together are able to promote the cell cycle

transition from G1 to S phase. The Cdk4-Cyclind D1 complex is involved in the phosphorylation and inhibition of Rb protein allowing E2F transcription factor activity. E2F induces the transcription of different cyclins, cyclin-dependent kinases and other transcription factors sustaining DNA replication and cell cycle progression (Malumbres, 2014; Haase & Wittenberg, 2014).

While CDK4 is a direct target gene of TFEB in the endothelium (Doronzo et al, 2019), no direct correlation is known between TFEB and Cyclin D1 promoter; therefore we assumed an indirect regulation of this gene by the transcription factor.

Cyclin D1 amount and function is finely controlled by different mechanisms. In particular, Wnt and MAPK pathways, fundamental for cell survival and growth, are able to regulate Cyclin D1 expression and activity (Chambard et al, 2007). Interestingly, Wnt signaling seems not to be altered in our system after *Tfeb* silencing, whereas MAPK pathway undergoes important changes. In particular, we observed an important reduction in the phosphorylation of Erk, the last component of the signaling pathway that directly acts as transcription factor and regulator also of Cyclin D1 (Chambard et al, 2007).

Moreover, being the tumor suppressor Pten able to induce cell cycle arrest decreasing the level and nuclear localization of Cyclin D1 (Radu et al, 2003; Diao and Chen, 2007), it is interesting that in D4M cells, genetically lacking *Pten* and therefore having high level of active Cyclin D1, *Tfeb* silencing mimics Pten function in deregulating Cyclin D1.

On the basis of our results, in melanoma cells, the Rb-Cdk4-Cyclin D1 axis is dampened after *Tfeb* inhibition both directly through Cdk4 promoter binding and indirectly via MAPK pathway acting on Cyclin D1. The net result is the strong reduction of the phosphorylation on Rb mediated by the Cdk4-Cyclin D1 complex and consequently the block in cell cycle and decrease in

cell proliferation.

After *Tfeb* silencing in melanoma we also evidenced a complex alteration of the main metabolic pathways: glycolysis, TCA cycle, oxidative phosphorylation, cholsterol synthesis, glutamine management are, in fact, all downregulated. As a consequence, these tumours are characterized by a decrease of the total cellular ATP amount. In parallel, cells undergo an increase in beta-oxidation, lactate production and mitochondrial oxidative damage.

In melanoma, *Tfeb* inhibition leads to a block of glucose and glutamine uptake that correlates with a reduced activity of the enzymes involved in glycolysis and glutamine metabolism. As expected, also the support to TCA cycle by these pathways is dampened. In particular, TCA cycle is downmodulated both *in vivo* and *in vitro* starting from Alpha-ketoglutarate dehydrogenase (Ogdh), the point in which glutamine, transformed into glutamate by Glutaminase (Gls) and then alpha-ketoglutarate, fuels the pathway

It has been demonstrated that GLS is under the direct control on TFEB in human pancreatic cancer (PDAC) (Kim et al, 2021b). In particular, it was observed that after TFEB silencing pancreatic cancer cells have a reduction in ATP quantity, oxygen consumption, TCA cycle intermediates and a general alteration of mitochondrial metabolism (Kim et al, 2021b). Even if our data partially overlap Kim and colleagues' ones, we did not confirm the direct regulation on the trascription of *Gls* gene by Tfeb in melanoma as it happens in PDAC.

After *Tfeb* inhibition in melanoma, Gls and Glutamine Synthetase (Gs) protein synthesis is unchanged while we demonstrated a decrease in their enzyme activity: this phenomenon is probably due to the impairment of glutamine cellular uptake. In the future, on the basis of the data about endothelial endocytosis modulation and alteration of endothelial plasma

membrane structure after TFEB silencing (Doronzo et al, 2019), it would be important to understand whether the decrease in glutamine and glucose uptake is due to a general and aspecific change in the structure and functionality of melanoma cell membranes. At the same time, it will be also important to verify whether the inhibition of the metabolic uptake is connected to a more specific and direct control of Tfeb on different transporters or channels that permit the entry of solutes into the cell.

Interestingly, cholesterol cellular concentration is very important in the regulation of membrane functions (Yang et al, 2016; Fantini et al, 2019). The interaction between the transmembrane domains of proteins and plasma membranes is strongly modulated by cholesterol (Fantini and Barrantes, 2013). In particular, ASCT2, the main glutamine transporter, is characterized by cholesterol saturable sites and its transport activity is influenced by cholesterol concentration. Cholesterol does not modify the K_m for glutamine, but the transport rate and the conformational changes of the protein (Scalise et al, 2019).

Another intriguing consideration comes from the comparison between melanoma cells and human endothelial cells referring not only to the block of proliferation but also to the metabolic alterations observed after *Tfeb* silencing. In fact, in both so different conditions proliferation and the main metabolic pathways are similarly downmodulated after *Tfeb* inhibition, sustaining a constant and not cell type-dependent Tfeb effect. Nevertheless, the effects in melanoma cells are stronger than the ones reported in endothelium. We postulate that this phenomenon may be due to the fact that tumour cells are basically more active from a metabolic point of view and therefore a lack of energy and biosynthetic precursors for D4M cells causes more catastrophic events compared to the more stable endothelial cells.

Our findings suggest new implications for TFEB in tumour growth and

maintenance, not strinctly linked to its canonical function in autophagy and lysosomal clearance. Its silencing leads to a general shutdown of melanoma cells probably due to different mechanisms that still need to be explored and well characterized.

The influences exerted by Tfeb on proliferation and metabolism in melanoma cells can be seen as linked parts of the same phenomenon through the correlations between cell cycle and cell metabolism. In fact, generating two daughter cells through cell cycle requires the energy and the sufficient amounts of metabolites to sustain the process and to double the total biomass (DeBerardinis et al, 2008).

We can therefore postulate that TFEB may be considered as an oncogene because its silencing induces a block in cell proliferation and metabolism, processes necessary for tumour progression.

Given the hyperactivation of MAPK signaling in most melanoma and being MAP kinases known and frequent oncogenes driving different tumor types, the fact that Tfeb may have a role in regulating Erk activation and function paves the way for further studies using Tfeb modulation as a therapeutical tool.

Tfeb silencing is linked to the net decrease of Erk phopshorylation without any effect on its protein expression suggeting that Tfeb might sustain the regulation of the expression of one or more phosphatases acting on Erk.

Dual-specificity MAP kinase (MAPK) phosphatases (MKPs or DUSPs) are the main negative regulators of MAPK signalling in mammalian cells and tissues (Kidger and Keyse, 2016).

In particular, MKPs are a subfamily of 10 catalytically active proteins sharing a common structure and able to dephosphorylate MAPKs (Owens and Keyse, 2007). Based on the sequence homology, protein structure, substrate specificity and subcellular localization, the MKP family can be divided into three groups: Type I, Type II, and Type III (Kondoh and Nishida,

2007).

Type I group includes DUSP1/MKP-1, involved in radiation, chemotherapy and immunotherapy resistance in different cancers. In fact, it is now considered a specific target to improve the efficacy of these therapeutic treatments and to overcome drug resistance (Kidger and Keyse, 2016; Shen et al, 2016).

Since one of the most important phosphatase acting on Erk is Dusp1, it would be interesting to investigate whether it could be a direct target of Tfeb in melanoma and if it is involved in the inhibition of cell proliferation and melanoma development.

Another intriguing point could be trying to find the interaction between Tfeb modulation and different anticancer drugs acting on MAPK pathway. Exploiting this hypothetical sinergism could avoid or decrease pharmacological resistance of tumor cells due to the stronger dual treatment acting on the same hyperactivated signaling pathway but in different ways. One candidate to test with *Tfeb* silencing is the BRAFV600E inhibitor PLX4032 that reduces melanoma cell proliferation deregulating MAPK pathway (Joseph et al, 2010).

Given the decrease in the vascular area of sh-*Tfeb* tumours, another worthy point would be to better characterize tumour vasculature and verify the effect of *Tfeb* inhibition on the known anti-angiogenetic drug tumour resistance.

Nevertheless, it remains to understand whether TFEB role is specific for melanoma or our considerations can be extended to different tumour types.

In conclusion, the considerations derived by the results of our study can be addressed to test new therapeutical combinations exploiting existing drugs with the manipulation of TFEB in melanoma.

MATERIALS AND METHODS

Cells

D4M cell line obtained backcrossing the transgenic mouse model *Tyr::CreER;Braf*^{CA}*;Pten*$^{lox/lox}$ to a C57BL/6 resulting in Braf/Pten mice (Jenkins et al, 2014) were maintained in DMEM/F-12 medium supplemented with 5% FBS, 1% penicillin-streptomycin and 1% L-glutamine.

YUMM (Yale University Mouse Melanoma) cell lines obtained backcrossing different transgenic mouse model (BrafV600E/wt Pten-/- Cdkn2-/- for YUMM1.7, BrafV600E/wt Pten-/- Cdkn2-/- Mc1r e/e for YUMM 1.G1, BrafV600E/wt Cdkn2-/- for YUMM 3.3, Pten-/- Cdkn2-/- for YUMM 4.1, BrafV600E/wt p53-/- for YUMM 5.2) to a C57BL/6 (Meeth et al, 2016) were maintained in DMEM/F-12 medium supplemented with 10% FBS, 1% penicillin-streptomycin and 1% nonessential amino acids.

Silencing experiments

Loss-of-function experiments were performed with scramble control shRNA (scr-shRNA) or shRNA against *Tfeb* (TRCN0000013111) cloned in the pLKO.1-puro non-Mammalian vector. Cells were transduced with specific lentiviral particles (MOI=1) prepared according to (Follenzi et al, 2000) in the presence of 8 µg/ml polybrene. The medium was replaced after 24 h and cells stably expressing the lentivirus were selected on puromycin (1 µg/ml) for 24 h. The inhibition of Tfeb was verified by qPCR and immunoblotting analyses.

Allografts

1x10^6 ctrl, scr-shRNA and sh-*Tfeb* D4M cells 3 days after transduction with the corrisponding lentiviral particles were resuspended in PBS and Matrigel then subcutaneously injected in the flank of immunocompetent C57BL/6

mice (at least 5 mice for every group).
Tumor size was measured with a caliper and tumor volume was calculated by the modified ellipsoid formula: length × $(width)^2/2$.
Allografts were maintained for 22 days.

Tissue and cell staining and analysis

For immunofluorescence staining, cells, grown up on cover slides, or tissue slices, derived from tumours previously frozen in OCT and cut into 10 µm thick sections, were fixed in 4% paraformaldehyde for 10 min at room temperature, permeabilized (PBS 0.1% Triton X-100) and then incubated with the indicated primary Abs and the appropriate Alexa Fluor secondary Abs (ThermoFisher Scientific).
Primary antibodies used were: Ki67, CD31, CD45 (ThermoFisher Scientific). Different fields per sample section were randomly chosen for analysis. When the same molecule was evaluated in different samples, laser power, gain, and offset settings were maintained. Immunofluorescence images were acquired on a TCS SPE confocal laser-scanning microscope (Leica Microsystems).

Proliferation

For growth assay, in 6-well plates 200,000 cells per well were plated. The culture medium was not changed for 24 hours, then cells were fixed in 2.5% glutaraldehyde and stained with 0.1% crystal violet. The dye was extracted with 10% acetic acid and relative proliferation levels were determined according to the optical density at 595 nm.

Western blot

For whole-cell lysates, cells were washed twice with cold PBS and proteins were extracted with a buffer containing 0.5M Tris-HCl, pH 6.8, 5% SDS, 20%

glycerol, and quantified by the BCA protein assay kit (ThermoFisher Scientific). Equal amounts of each sample were separated by SDS-PAGE (Bio-Rad) and transferred to PVDF membranes (Bio-Rad). Membranes were incubated with specific primary antibodies and proper HRP-conjugated secondary antibodies. Immunoreactive proteins were then visualized by enhanced chemiluminescence system (ECL) (Bio-Rad), acquired using a ChemiDoc Touch Gel Imaging System (Bio-Rad) and analyzed with Image Lab software 5.2.1 (Bio-Rad).

Antibodies used were: anti-Tfeb (Bethyl - A303-673A), anti-Cyclin D1 (Abcam - ab16663), anti-Cdk4 (Abcam - ab137675), anti-Rb (Abcam - ab181616), anti-pRb ser 807/811 (Cell Signaling - cst#8516), anti-Pcna (Cell Signaling - cst2586), anti-Gsk3α/β (ThermoFisher Scientific - MA3-038), anti-β-Catenin (Cell Signaling - cst#8480), anti-pBraf ser 445 (Cell Signaling - cst#2696), anti-Braf (Santa Cruz - sc-5284), anti-pMek1/2 ser 217/221 (Cell Signaling - cst#9154), anti-Mek1/2 (Cell Signaling - cst#9126), anti-pErk1/2 (Cell Signaling - cst#9106), anti-Erk1/2 (Cell Signaling - cst#9102), anti-Gls (ThermoFisher Scientific - PA5-35365), anti-Gs (Novus Biologicals - NB110-41404) and anti-α-actin (Abcam - ab179467).

Gene expression

Total RNA was isolated from cells with Maxwell RSC miRNA Tissue kit (Promega). Quality and concentration of RNAs were assessed with a NanoDrop ND-1000 spectrophotometer (ThermoFisher Scientific).

1 µg of of the extracted RNA was converted to cDNA using High-Capacity cDNA Reverse Transcription kit and random primers (ThermoFisher Scientific).

Real-time PCR was performed using a CFX96 system (Bio-Rad) with TaqMan/Sybr PCR Universal Master Mix and specific TaqMan/Sybr assays. The experiments were performed in triplicate, and *Tbp* was used as a

reference gene.

The following TaqMan/Sybr assays were used: Tfeb (Mm00448968), Ccnd1 (Mm00432359), Cdk4 (Mm00726334), Pcna (Mm00448100), Kras (qMmuCID0005957), Raf1 (qMmuCID0005988), Mek1 (qMmuCID0022421), Mek2 (qMmuCID0006198), Erk1 (qMmuCED0025043), Erk2 (qMmuCID0025360), Gls (Mm01257297), Gs (Mm00725701) and Tbp (Mm01277042).

Cellular ATP amount quantification

The intracellular ATP level was measured using the Cell Titer-Glo Luminescent Cell Viability Assay kit (Promega) following the manifacturer's instructions. Results were expressed as relative light units (RLU).

Flow citometry

Proliferation rate and DNA content were evaluated by using Click-iT EdU Flow Cytometry Cell Proliferation Assay and propidium iodide (PI) staining according to manufacturer's protocol. Data were acquired with a CyAn ADP flow cytometer (Dako) and analyzed with FlowJo software (Tree Star, Ashland, OR, USA).

Glycolysis

Cells were washed with fresh medium, detached with trypsin/EDTA, re-suspended at 1 x 10^5 cells/ml in 0.2 ml of 100 mM TRIS 10 mM/EDTA I mM (pH 7.4), and sonicated on ice with two 10 s bursts. Tumor homogenates were resuspended in the same buffer and sonicated. Enzymatic activities were measured on 10 µl cell lysates, incubated for 5 min at 37°C. The protein content was measured using the BCA1 kit (Sigma, St. Louis, MO). The activity of phosphofructokinease-1 (PFK1) assay was measured spectrophotometrically as reported in (Sharma, 2011). Aldolase activity was

measured by using the Aldolase Activity Colorimetric Assay Kit (Bio-Vision, Milipitas, CA). The activities of glyceraldehyde 3-phosphate dehydrogenase (GAPDH), enolase and lactate dehydrogenase (LDH) were measured spectrophotometrically according to (Riganti 2002; Capello 2016). For GAPDH, cell lysate was incubated with 5 mM 3-phosphoglyceric acid, 1 U phosphoglycerate 3-kinase, 5 mM ATP and 2.5 mM NADH. For enolase, cell lysate was incubated with 10 mM $MgCl_2$, 100 mM KCl, 1 mM 2-phosphoglyceric acid, 0.4 mM ADP, 6.8 U/mL PK, 9.9 U/mL LDH, 0.2 mM NADH. Pyruvate kinase (PK) activity was measured with the Pyruvate Kinase Assay kit (Abcam, Cambridge, UK). For all assays of glycolytic enzymes, the activities were monitored measuring the absorbance variation at 340 nm using a in a Synergy HTX 96-well microplate reader (Bio-Tek Instruments). The kinetics were linear throughout the measurement. Results were expressed as nmoles NAD/min/mg prot (PFK1, aldolase, GAPDH, enolase, LDH) or nmoles pyruvate/mg prot (PK).

Lactate

Lactate production was measured with the Glycolysis Assay Kit (Sigma), following manufacturer's protocol and detecting the signals with a Synergy HTX 96-well microplate reader (Bio-Tek Instruments). Lactate level was set at 100% in the untreated condition. Results were expressed as nmoles lactate/mg cellular proteins.

Tricarboxylic acid cicle (TCA) flux

The glucose flux through TCA cycle was measured by radiolabeling 1 x 10^6 cells with 2 µCi [6-^{14}C]-glucose (55 mCi/mmol; PerkinElmer, Waltham, MA, USA) or [1-^{14}C]-acetic acid (1 mCi/ml, PerkinElmer) or [^{14}C]-L-glutamine (200 mCi/mmol, PerkinElmer). Cell suspensions were incubated for 1 h in a closed experimental system to trap the $^{14}CO_2$ developed from [^{14}C]-glucose,

[^{14}C]-acetic acid], [^{14}C]-L-glutamine. The reaction was stopped by injecting 0.5 ml of 0.8 N $HClO_4$. The amount of glucose transformed into CO_2 through the TCA cycle was calculated as described (Riganti et al., 2004) and expressed as nmoles CO_2/h/mg proteins.

TCA cycle enzymes

The enzymatic activities of pyruvate dehydrogenase (PDH), citrate synthase (CS), aconitase, isocitrate dehydrogenase (IDH), α-ketoglutarate dehydrogenase (α-kGlu-DH), succinate dehydrogenase (SDH) were measured on 10 µg mitochondrial proteins using the PDH Assay Kit (Sigma), the Citrate Synthase Assay Kit (Sigma), the Aconitase kit (Caymann Chemical, Ann Arnor, MI), the Isocitrate Dehydrogenase Activity Assay kit (Sigma),the Alpha Ketoglutarate Assay Kit (Abcam), the Succinate Dehydrogenase Activity Colorimetric Assay Kit (BioVision), as per manufacturer's instructions. Results were expressed as mU/mg mitochondrial proteins.

Mitochondrial extraction and electron transport chain (ETC)

To extract mitochondria, cells or tumor homogenayes were lysed in 0.5ml mitochondria lysis buffer (50 mM Tris-HCl, 100 mM KCl, 5 mM Mg Cl_2, 1.8 mM ATP, 1 mM EDTA, pH7.2), supplemented with Protease Inhibitor Cocktail III (Sigma), 1 mM phenylmethylsulfonyl fluoride (PMSF) and 250 mM NaF. Samples were clarified by centrifugation at 650 g for 3 min at 4°C. Supernatants were collected and centrifuged at 13000 g for 5 min at 4°C. The new supernatants, corresponding to the cytosolic fraction, were used for cytosolic ROS measurements. Pellets, containing mitochondria, were washed once with lysis buffer and resuspended in 0.25 ml mitochondria resuspension buffer (250 mM sucrose, 15 mM K_2HPO_4, 2 mM $MgCl_2$, 0.5 mM EDTA). 50 µl aliquots were sonicated and used for the measurement of

protein content by the BCA Protein Assay kit (Sigma) and for quality control: 10 µg of each sonicated sample were analyzed by SDS-PAGE and immunoblotting with an anti-porin antibody (Abcam) to confirm the presence of mitochondrial proteins in the extracts. The remaining 200 µl were used for the metabolic assays reported below (Wibom, 2002). To measure complex I activity, 20 µg of non-sonicated mitochondrial samples were re-suspended in 0.2 ml buffer 1A (5 mM KH_2PO_4, 5 mM $MgCl_2$, 5% w/v BSA), incubated 1 min at room temperature followed by 7 min in 0.1 ml buffer 1B (25% w/v saponin, 50 mM KH_2PO_4, 5 mM $MgCl_2$, 5% w/v BSA, 0.12 mM oxidized ubiquinone, which acts as electrons shuttle from complex I to complex III, 2.5 mM antimycin A, which inhibits complex III, 0.2 mM NaN_3, which blocks complex IV; pH 7.5). 1.5 mM NADH, as electron donor was added to the mix. The rate of NADH oxidation was followed for 5 min at 37°C, reading the absorbance at 340 nm. The results were expressed as nanomoles of NAD^+/min/mg mitochondrial proteins.

Complex II activity was measured as rate of electrons transfer between complex II and complex III. 20 µg of non-sonicated mitochondrial samples were re-suspended in 0.1 ml buffer 2A (50 mM KH_2PO_4, 7.5 mM $MgCl_2$, 25% w/v saponin, 20 mM succinic acid; pH 7.2) and incubated for 30 min at room temperature. 0.2 ml buffer 2B (50 mM KH_2PO_4, 7.5 mM $MgCl_2$, 5% w/v BSA, 30 mM succinic acid as substrate of complex II, 0.12 mM oxidized ubiquinone as electrons shuttle from complex II to complex III, 0.12 mM oxidized cytochrome c as acceptor of electrons flowing from complex II to complex III, 5 mM rotenone to prevent electron flux from complex I, 0.2 mM NaN_3, to block complex IV) were added. The rate of reduction of cytochrome c was measured for 5 min at 37°C, reading the absorbance at 550 nm. The results were expressed as nanomoles of reduced cytochrome c/min/mg mitochondrial proteins.

The activity of complex III was measured in the same samples where the

electron flux from complex I to complex III was evaluated. After 1 min from the addition of NADH, as inducer of electrons flow, 5 mM rotenone, which blocks the activity of complex I, was added. The rate of reduction of cytochrome c, which is dependent on the activity of complex III only in the presence of rotenone, was followed for 5 min at 37°C, reading the absorbance at 550 nm. The results were expressed as nanomoles of reduced cytochrome c/min/mg mitochondrial proteins.

To measure the activity of complex IV, the rate of oxidation of cytochrome c (reduced form, generated by complex III) was measured. 20 µg of non-sonicated mitochondrial samples were re-suspended in 0.1 ml buffer 4A (50 mM KH_2PO_4, 20 mM succinic acid, 25% w/v saponin; pH 7.2) and incubated 30 min at room temperature. 0.2 ml buffer 4B (50 mM KH_2PO_4, 5 mM rotenone, which prevents electron flux from complex I to complex III, 30 mM succinic acid as substrate of complex II and electrons generator, 0.03 mM reduced cytochrome c as acceptor of electrons flowing from complex III to complex IV) were added. The rate of oxidation of cytochrome c was followed for 5 min at 37°C, reading the absorbance at 550 nm. The results were expressed as nanomoles of oxidized cytochrome c/min/mg mitochondrial proteins.

Mitochondrial ATP

The ATP levels in mitochondria extracts were measured with the ATP Bioluminescent Assay Kit (Sigma-Aldrich, St. Louis, MO USA). ATP was quantified as relative light units (RLU) and converted into nmoles ATP/mg mitochondrial proteins, according to the calibration curve previously set.

Mitochondrial permeability transition pore (mPTP) activity

The activity of the mPTP, considered an index of damaged mitochondria, was measured using the Mitochondrial Permeability Transition Pore Assay

Kit (Biovision), as per manufacturer's instructions. The intracellular fluorescence was measured at λ excitation 488 nm using a in a Synergy HTX 96-well microplate reader (Bio-Tek Instruments). Results were expressed as relative fluorescence unit (RFU)/mg cellular proteins.

Mitochondrial TBARS

The extent of oxidative damage was measured in in mitochondrial extracts by using the Lipid Peroxidation (4-HNE) Assay Kit (Abcam) that evaluates the 4-hydroxy-nonenale, one of the thiobarbituric reactive substance that is an index of lipid peroxidation. Results were expressed as nmol/mg mitochondrial proteins.

Superoxide dismutase (SOD) activity

Mitochondria separation was performed then the activity of SOD2 was measured in mitochondrial extracts. 10 µg proteins of the extract were incubated with 50 µmol/L xanthine, 5 U/mL xanthine oxidase, 1 µg/mL oxidized cytochrome c at 37°C. The rate of cytochrome c reduction, which is inhibited by the presence of SOD, was monitored for 5 min by reading the absorbance at 550 nm with a Lambda 3 spectrophotometer (PerkinElmer). Results were expressed as µmoles reduced cytochrome c/min/mg mitochondrial proteins.

Fatty acid β-oxidation (FAO)

Cells were washed with fresh medium, detached with trypsin/EDTA, re-suspended at 1 x 10^5 cells/ml in 0.2 ml of 100 mM TRIS 10 mM/EDTA and 50 µl aliquots were sonicated and used for protein measurements and normalization using the BCA1 kit (Sigma). Tumor homogenates were resuspended in the same buffer and sonicated. The remaining samples were centrifuged 13000 g for 5 min at room temperature and re-suspended

in 0.5 ml Hepes 20 mM (pH 7.4), containing 0.24 mM fatty acid-free BSA, 0.5 mM L-carnitine, 2 µCi [1-^{14}C]palmitic acid (3.3 mCi/mmol, PerkinElmer,) and transferred into test tubes that were tightly sealed with rubber caps. In each experimental set, cells were pre-incubated for 30 min with the carnitine palmitoyltransferase inhibitor etomoxir (1 µM) or with the AMP-kinase activator 5-aminoimidazole-4-carboxamide ribonucleotide AICAR (1 mM), as negative and positive controls, respectively. After 2 h incubation at 37°C, 0.3 ml of a 1:1 v/v phenylethylamine/methanol solution was added to each sample using a syringe, followed by 0.3 mL 0.8 N $HClO_4$. Samples were incubated for a further 1 h at room temperature, then centrifuged at 13,000 g for 10 min. Both the supernatants, containing $^{14}CO_2$, and the precipitates, containing ^{14}C-acid soluble metabolites (ASM), i.e. the main products of fatty acid β-oxidation, were collected. The radioactivity of each supernatant and precipitate was counted by liquid scintillation, according to (Gaster 2004), and expressed as pmoles/h/mg prot.

Cholesterol and isoprenoid synthesis

The *de novo* synthesis of cholesterol, farnesyl pyrophosphate (FPP), geranyl pyrophosphate (GGP) and ubiquinone was measured by radiolabeling 1 x 10^6 cells (after overnight starvation) with 1 µCi [^{3}H]acetate (3600 mCi/mmol; Amersham Bioscience, Piscataway, NJ) for 24 h (Castella et al, 2011). Cells were washed twice with PBS and scraped in 200 µl PBS. Methanol (0.5 ml) and hexane (1 ml) were added to the cell suspension, which was stirred at room temperature for 1 h and centrifuged at 2,000 x g for 5 min. The upper phase containing hexane was transferred to a new test tube, the lower phase was supplemented with 1 ml hexane and stirred overnight. After a 5-min centrifugation at 2,000 g, the upper phase was added to the previous one and the solvent was allowed to evaporate at room temperature for 24 h. Cellular lipid extracts produced by this separation were

re-suspended in 30 µl chloroform and then subjected to thin layer chromatography (TLC), using a 1:1 (v/v) ether/hexane solution as mobile phase. Each sample was spotted on pre-coated LK6D Whatman silica gels (Merck, Darmstadt, Germany) and allowed to run for 30 min. Solutions of 10 µg/ml cholesterol, GGPP and ubiquinone were used as standards. The plates were exposed for 1 h to an iodine-saturated atmosphere, and the migrated spots were cut out. Their radioactivity was measured by liquid scintillation, using a Tri-Carb Liquid Scintillation Analyzer (PerkinElmer, Waltham, MA). Cholesterol, GGPP and ubiquinone synthesis was expressed as pmoles/10^6 cells, according to the titration curves prepared previously.

Glutamine catabolism and synthesis

Glutamine catabolism was measured as reported (Curthoys and Weiss, 1974), with minor modifications. Cells were washed with PBS, detached by gentle scraping, centrifuged at 13,000 x g for 5 min at 4°C, re-suspended in 250 µL of buffer A (150 mmol/L KH_2PO_4, 63 mmol/L Tris/HCl, 0.25 mmol/L EDTA; pH 8.6) and sonicated. A volume of 100 µL of the whole cell lysates was incubated for 30 min at 37°C in a quartz cuvette, in the presence of 50 µL of 20 mmol/L L-glutamine and 850 µL of buffer B (80 mmol/L Tris/HCl, 20 mmol/L NAD^+, 20 mmol/L ADP, 3% v/v H_2O_2; pH 9.4). The absorbance of NADH was monitored at 340 nm using a Lambda 3 spectrophotometer (PerkinElmer). The kinetics was linear throughout the assay. The results were expressed as µmol NADH/min/mg cell proteins and were considered as an index of the activity of glutaminase (GLS) plus L-glutamic dehydrogenase (GDH). In a second series of samples, 20 µL of the GLS inhibitor bis-2-(5-phenylacetamido-1,3,4-thiadiazol-2-yl)ethyl sulfide BTPES (30 µmol/L) was added after 15 min. This concentration was chosen as it produced 100% inhibition of GLS activity in our system (not shown). The

absorbance of NADH was monitored for 15 min as described previously. The results, considered as an index of the activity of GDH, were expressed as µmol NADH/min/mg cell proteins. GLS activity was obtained by subtracting the rate of the second assay from the rate of the first one. The enzymatic activity of glutamine synthetase (GLUL) was measured spectrophotometrically, using the Glutamine Synthetase Microplate Assay Kit (Cohesion Biosciences Ltd, London, UK). Results were expressed as mU/mg cellular proteins.

Glutamine/glutamate uptake and metabolism

To measure glutamine uptake and metabolism, $1x10^6$ cells were labeled with 1 µCi [14C]-L-glutamine (PerkinElmer) for 30 min, washed five times with ice-cold PBS, detached with trypsin/EDTA, rinsed with 0.5 ml ice-cold PBS and sonicated. A 50 µl aliquot was used to quantify intracellular proteins. [14C]-L-glutamate and [14C]-L-glutamine present within cell lysates were separated by ion exchange chromatography in a 2 ml column (Tassone et al, 2017). The radioactivity of the eluate containing [14C]-L-glutamate and [14C]-Lglutamine was counted by liquid scintillation and expressed as µmol/mg cellular proteins. The ratio between [14C]-L-glutamate/[14C]-L-glutamine was considered an index of glutamine consumption. In the case of glutamate uptake, $1x10^6$ cells were labeled with 1 µCi [14C]-L-glutamate (PerkinElmer).Cells were processed as reported above and the intracellular amount of [14C]-L-glutamate was measured by liquid scintillation. Results were expressed as µmoles/mg cellular proteins.

Glutamine/glutamate efflux

$1x10^6$ cells were labeled with 1 µCi [14C]-L-glutamine or [14C]-L-glutamate (PerkinElmer) for 30 min, washed five times with ice-cold PBS, and rinsed with fresh medium for 1 h. After this incubation time, 1 ml of supernatants

was collected. The amount of [14C]-L-glutamine or [14C]-L-glutamate was measured by liquid scintillation. Results were expressed as µmoles/mg cellular proteins.

Statistical analysis

All statistical analyses were performed using Excel (Microsoft) software. Pooled data are expressed as the mean ± SEM. n represents the number of independent biological replicates. Significance was determined by using unpaired Student's t-test (two tailed), assuming a normal distribution. $P < 0.05$ was considered significant. Specific details for each experiment can be found in the corresponding figure legend.

REFERENCES

Amaravadi R., Kimmelman A.C., White E. (2016) Recent insights into the function of autophagy in cancer. **Genes Dev 30:** 1913-1930

Amin M.B., Amin M.B., Tamboli P., Javidan J., Stricker H., de-Peralta Venturina M., Deshpande A., Menon M. (2002) Prognostic impact of histologic subtyping of adult renal epithelial neoplasms: an experience of 405 cases. **Am J Surg Pathol 26:** 281-291

Argani P., Antonescu C.R., Illei P.B., Lui M.Y., Timmons C.F., Newbury R., Reuter V.E., Garvin A.J., Perez-Atayde A.R., Fletcher J.A., Beckwith J.B., Bridge J.A., Ladanyi M. (2001) Primary renal neoplasms with the ASPL-TFE3 gene fusion of alveolar soft part sarcoma: a distinctive tumor entity previously included among renal cell carcinomas of children and adolescents. **Am J Pathol 159:** 179-192

Argani P., Hicks J., De Marzo A.M., Albadine R., Illei P.B., Ladanyi M., Reuter V.E., Netto G.J. (2010) Xp11 translocation renal cell carcinoma (RCC): extended immunohistochemical profile emphasizing novel RCC markers. **Am J Surg Pathol 34:** 1295-1303

Astanina E., Bussolino F., Doronzo G. (2021) Multifaceted activities of transcription factor EB in cancer onset and progression. **Mol Oncol. 15:** 327-346

Bahrami A., Bianconi V., Pirro M., Orafai H.M., Sahebkar A. (2020) The role of TFEB in tumor cell autophagy: Diagnostic and therapeutic opportunities.

Life Sci 244: 117341

Ballesteros-Álvarez J., Dilshat R., Fock V., Möller K., Karl L., Larue L., Ögmundsdóttir M.H., Steingrímsson E. (2020) MITF and TFEB cross-regulation in melanoma cells. **PLoS One 15:** e0238546

Beckmann H., Su LK, Kadesch T. (1990) TFE3: a helix-loop-helix protein that activates transcription through the immunoglobulin enhancer muE3 motif. **Genes Dev 4:** 167-179

Betschinger J., Nichols J., Dietmann S., Corrin P.D., Paddison P.J., Smith A. (2013) Exit from pluripotency is gated by intracellular redistribution of the bHLH transcription factor Tfe3. **Cell 153:** 335-347

Blessing A.M., Rajapakshe K., Reddy Bollu L., Shi Y., White M.A., Pham A.H., Lin C., Jonsson P., Cortes C.J., Cheung E., La Spada A.R., Bast R.C. Jr., Merchant F.A., Coarfa C., Frigo D.E. (2017) Transcriptional regulation of core autophagy and lysosomal genes by the androgen receptor promotes prostate cancer progression. **Autophagy 13:** 506-521

Blitzer J.T., Nusse R. (2006) A critical role for endocytosis in Wnt signaling. **BMC Cell Biol 7:** 28

Brady O.A., Jeong E., Martina J.A., Pirooznia M., Tunc I., Puertollano R. (2018) The transcription factors TFE3 and TFEB amplify p53 dependent transcriptional programs in response to DNA damage. **Elife 7:** e40856

Calcagnì A., Kors L., Verschuren E., De Cegli R., Zampelli N., Nusco E., Confalonieri S., Bertalot G., Pece S., Settembre C., Malouf G.G., Leemans

J.C., de Heer E., Salvatore M., Peters D.J., Di Fiore P.P., Ballabio A. (2016) Modelling TFE renal cell carcinoma in mice reveals a critical role of WNT signaling. **Elife 5:** e17047

Caliò A., Segala D., Munari E., Brunelli M., Martignoni G. (2019) MiT Family Translocation Renal Cell Carcinoma: from the Early Descriptions to the Current Knowledge. **Cancers (Basel) 11:** 1110

Caliò A., Brunelli M., Segala D., Pedron S., Doglioni C., Argani P., Martignoni G. (2019b) VEGFA amplification/increased gene copy number and VEGFA mRNA expression in renal cell carcinoma with TFEB gene alterations. **Mod Pathol 32:** 258-268

Capello M., Ferri-Borgogno S., Riganti C., Chattaragada M.S., Principe M., Roux C., Zhou W., Petricoin E.F., Cappello P., Novelli F. (2016) Targeting the Warburg effect in cancer cells through ENO1 knockdown rescues oxidative phosphorylation and induces growth arrest. **Oncotarget 7(5):** 5598-5612

Carr C.S., Sharp P.A. (1990) A helix-loop-helix protein related to the immunoglobulin E box-binding proteins. **Mol Cell Biol 10:** 4384-4388

Castella B, Riganti C, Fiore F, Pantaleoni F, Canepari ME, Peola S, Foglietta Palumbo M., Bosia A., Coscia A., Boccadoro M., Massaia M. (2011) Immune modulation by zoledronic acid in human myeloma: an advantageous cross-talk between Vγ9Vδ2 T cells, αβ CD8+ T cells, regulatory T cells, and dendritic cells. **J Immunol 187(4):** 1578-1590

Chambard J.C., Lefloch R., Pouysségur J., Lenormand P. (2007 ERK

implication in cell cycle regulation. **Biochim Biophys Acta 1773:** 1299-1310

Chen L., Wang K., Long A., Jia L., Zhang Y., Deng H., Li Y., Han J., Wang Y. (2017) Fasting-induced hormonal regulation of lysosomal function. **Cell Res 27(6):** 748-763

Christopherson W.M., Foote F.W. Jr, Stewart F.W. (1952) Alveolar soft-part sarcomas; structurally characteristic tumors of uncertain histogenesis. **Cancer 5:** 100-111

Corà D., Bussolino F., Doronzo G. (2021) TFEB Signalling-Related MicroRNAs and Autophagy. **Biomolecules 11(7):** 985

Cortes C.J., La Spada A.R. (2019) TFEB dysregulation as a driver of autophagy dysfunction in neurodegenerative disease: Molecular mechanisms, cellular processes, and emerging therapeutic opportunities. **Neurobiol Dis 122:** 83-93

Curthoys N.P., Weiss R.F. (1974) Regulation of renal ammoniagenesis. Subcellular localization of rat kidney glutaminase isoenzymes. **J Biol Chem 249(10):** 3261-3266

Danhier P., Bański P., Payen V.L., Grasso D., Ippolito L., Sonveaux P., Porporato P.E. (2017) Cancer metabolism in space and time: Beyond the Warburg effect. **Biochim Biophys Acta Bioenerg 1858(8):** 556-572

Davis I.J., Hsi B.L., Arroyo J.D., Vargas S.O., Yeh Y.A., Motyckova G., Valencia P., Perez-Atayde A.R., Argani P., Ladanyi M., Fletcher J.A., Fisher

D.E. (2003) Cloning of an Alpha-TFEB fusion in renal tumors harboring the t(6;11)(p21;q13) chromosome translocation. **Proc Natl Acad Sci USA 100:** 6051-6056

DeBerardinis R.J., Lum J.J., Hatzivassiliou G., Thompson C.B. (2008) The biology of cancer: metabolic reprogramming fuels cell growth and proliferation. **Cell Metab 7(1):** 11-20

Di Malta C., Siciliano D., Calcagni A., Monfregola J., Punzi S., Pastore N., Eastes A.N., Davis O., De Cegli R., Zampelli A., Di Giovannantonio L.G., Nusco E., Platt N., Guida A., Ogmundsdottir M.H., Lanfrancone L., Perera R.M., Zoncu R., Pelicci P.G., Settembre C., Ballabio A. (2017) Transcriptional activation of RagD GTPase controls mTORC1 and promotes cancer growth. **Science 356:** 1188-1192

Di Malta C., Ballabio A. (2017) TFEB-mTORC1 feedback loop in metabolism and cancer. **Cell Stress 1:** 7-10

Di Malta C., Ballabio A. (2018) Transcriptional regulation of mTORC1 in cancer. **Oncotarget 9:** 36734-36735

Di Malta C., Cinque L., Settembre C. (2019) Transcriptional Regulation of Autophagy: Mechanisms and Diseases. **Front Cell Dev Biol 7:** 114

Diao L., Chen Y.G. (2007) PTEN, a general negative regulator of cyclin D expression. **Cell Res 17:** 291-292

Doronzo G., Astanina E., Corà D., Chiabotto G., Comunanza V., Noghero A., Neri F., Puliafito A., Primo L., Spampanato C., Settembre C., Ballabio A.,

Camussi G., Oliviero S., Bussolino F. (2019) TFEB controls vascular development by regulating the proliferation of endothelial cells. **EMBO J 38:** e98250.

Doronzo G., Astanina E., Bussolino F. (2021) The Oncogene Transcription Factor EB Regulates Vascular Functions. **Front Physiol 12:** 640061

Emanuel R., Sergin I., Bhattacharya S., Turner J., Epelman S., Settembre C., Diwan A., Ballabio A., Razani B. (2014) Induction of lysosomal biogenesis in atherosclerotic macrophages can rescue lipid-induced lysosomal dysfunction and downstream sequelae. **Arterioscler Thromb Vasc Biol. 34:** 1942-1952

Erlich A.T., Brownlee D.M., Beyfuss K., Hood D.A. (2018) Exercise induces TFEB expression and activity in skeletal muscle in a PGC-1α-dependent manner. **Am J Physiol Cell Physiol 314(1):** C62-C72

Evans T.D., Zhang X., Jeong S.J., He A., Song E., Bhattacharya S., Holloway K.B., Lodhi I.J., Razani B. (2019) TFEB drives PGC-1α expression in adipocytes to protect against diet-induced metabolic dysfunction. **Sci Signal 12(606):** eaau2281

Fan Y., Lu H., Liang W., Garcia-Barrio M.T., Guo Y., Zhang J., Zhu T., Hao Y., Zhang J., Chen Y.E. (2018) Endothelial TFEB (Transcription Factor EB) positively regulates postischemic angiogenesis. **Circ Res 122:** 945-957

Fang L.M., Li B., Guan J.J., Xu H.D., Shen G.H., Gao Q.G., Qin Z.H. (2017) Transcription factor EB is involved in autophagy-mediated chemoresistance to doxorubicin in human cancer cells. **Acta Pharmacol Sin 38:** 1305-1316

Fantini J., Barrantes F.J. (2013) How cholesterol interacts with membrane proteins: an exploration of cholesterol-binding sites including CRAC, CARC, and tilted domains. **Front Physiol 4:** 31

Fantini J., Epand R.M., Barrantes F.J. (2019) Cholesterol-Recognition Motifs in Membrane Proteins. **Adv Exp Med Biol 1135:** 3-25

Ferron M., Settembre C., Shimazu J., Lacombe J., Kato S., Rawlings D.J., Ballabio A., Karsenty G. (2013) A RANKL-PKCβ-TFEB signaling cascade is necessary for lysosomal biogenesis in osteoclasts. **Genes Dev 27:** 955-969

Filipp F.V., Ratnikov B., De Ingeniis J., Smith J.W., Osterman A.L., Scott D.A. (2012) Glutamine-fueled mitochondrial metabolism is decoupled from glycolysis in melanoma. **Pigment Cell Melanoma Res 25(6):** 732-739

Fisher D.E., Carr C.S., Parent L.A., Sharp P.A. (1991) TFEB has DNA-binding and oligomerization properties of a unique helix-loop-helix/leucine-zipper family. **Genes Dev 5:** 2342-2352

Fischer G.M., Vashisht Gopal Y.N., McQuade J.L., Peng W., DeBerardinis R.J., Davies M.A. (2018) Metabolic strategies of melanoma cells: Mechanisms, interactions with the tumor microenvironment, and therapeutic implications. **Pigment Cell Melanoma Res. 31(1):** 11-30

Follenzi A., Ailles L.E., Bakovic S., Geuna M., Naldini L. (2000) Gene transfer by lentiviral vectors is limited by nuclear translocation and rescued by HIV-1 pol sequences. **Nat Genet 25(2):** 217-222

Gao S., Brown J., Wang H., Feng X. (2014) The role of glycogen synthase kinase 3-β in immunity and cell cycle: implications in esophageal cancer. **Arch Immunol Ther Exp (Warsz) 62(2):** 131-144

Garraway L.A., Widlund H.R., Rubin M.A., Getz G., Berger A.J., Ramaswamy S., Beroukhim R., Milner D.A., Granter S.R., Du J., Lee C., Wagner S.N., Li C., Golub T.R., Rimm D.L., Meyerson M.L., Fisher D.E., Sellers W.R. (2005) Integrative genomic analyses identify MITF as a lineage survival oncogene amplified in malignant melanoma. **Nature 436:** 117-122

Gaster M., Beck-Nielsen H. (2004) The reduced insulin-mediated glucose oxidation in skeletal muscle from type 2 diabetic subjects may be of genetic origin--evidence from cultured myotubes. **Biochim Biophys Acta 1690(1):** 85-91

Giatromanolaki A., Kalamida D., Sivridis E., Karagounis I.V., Gatter K.C., Harris A.L., Koukourakis M.I. (2015) Increased expression of transcription factor EB (TFEB) is associated with autophagy, migratory phenotype and poor prognosis in non-small cell lung cancer. **Lung Cancer 90:** 98-105

Giatromanolaki A., Sivridis E., Kalamida D., Koukourakis M.I. (2017) Transcription Factor EB Expression in Early Breast Cancer Relates to Lysosomal/Autophagosomal Markers and Prognosis. **Clin Breast Cancer 17:** e119-e125

Glick D., Barth S., Macleod K.F. (2010) Autophagy: cellular and molecular mechanisms. **J Pathol 221:** 3-12

Guo Y.J., Pan W.W., Liu S.B., Shen Z.F., Xu Y., Hu L.L. (2020) ERK/MAPK

signalling pathway and tumorigenesis. **Exp Ther Med 19:** 1997-2007

Haase S.B, Wittenberg C. (2014) Topology and control of the cell-cycle-regulated transcriptional circuitry. **Genetics 196:** 65-90

Harashima H., Dissmeyer N., Schnittger A. (2013) Cell cycle control across the eukaryotic kingdom. **Trends in Cell Biol 23:** 345-356

Haq R., Fisher D.E. (2011) Biology and clinical relevance of the micropthalmia family of transcription factors in human cancer. **J Clin Oncol 29:** 3474-3482

He R., Shi X., Zhou M., Zhao Y., Pan S., Zhao C., Guo X., Wang M., Li X., Qin R. (2018) Alantolactone induces apoptosis and improves chemosensitivity of pancreatic cancer cells by impairment of autophagy-lysosome pathway via targeting TFEB. **Toxicol Appl Pharmacol 356:** 159-171

He R., Wang M., Zhao C., Shen M., Yu Y., He L., Zhao Y., Chen H., Shi X., Zhou M., Pan S., Liu Y., Guo X., Li X., Qin R. (2019) TFEB-driven autophagy potentiates TGF-β induced migration in pancreatic cancer cells. **J Exp Clin Cancer Res 38:** 340

Hemesath T.J., Steingrímsson E., McGill G., Hansen M.J., Vaught J., Hodgkinson C.A., Arnheiter H., Copeland N.G., Jenkins N.A., Fisher D.E. (1994) Microphthalmia, a critical factor in melanocyte development, defines a discrete transcription factor family. **Genes Dev 8:** 2770-2780

Hodgkinson C.A., Moore K.J., Nakayama A., Steingrímsson E., Copeland

N.G., Jenkins N.A., Arnheiter H. (1993) Mutations at the mouse microphthalmia locus are associated with defects in a gene encoding a novel basic-helix-loop-helix-zipper protein. **Cell 74:** 395-404

Hsu C.L., Lee E.X., Gordon K.L., Paz E.A., Shen W.C., Ohnishi K., Meisenhelder J., Hunter T., La Spada A.R. (2018) MAP4K3 mediates amino acid-dependent regulation of autophagy via phosphorylation of TFEB. **Nat Commun 9:** 942

Hughes M.J., Lingrel J.B., Krakowsky J.M., Anderson K.P. (1993) A helix-loop-helix transcription factor-like gene is located at the mi locus. **J Biol Chem 268:** 20687-20690

Icard P., Fournel L., Wu Z., Alifano M., Lincet H. (2019) Interconnection between Metabolism and Cell Cycle in Cancer. **Trends Biochem Sci 44(6):** 490-501

Jenkins M.H., Steinberg S.M., Alexander M.P., Fisher J.L., Ernstoff M.S., Turk M.J., Mullins D.W., Brinckerhoff C.E. (2014) Multiple murine BRaf(V600E) melanoma cell lines with sensitivity to PLX4032. **Pigment Cell Melanoma Res 27:** 495-501

Joseph E.W., Pratilas C.A., Poulikakos P.I., Tadi M., Wang W., Taylor B.S., Halilovic E., Persaud Y., Xing F., Viale A., Tsai J., Chapman P.B., Bollag G., Solit D.B., Rosen N. (2010) The RAF inhibitor PLX4032 inhibits ERK signaling and tumor cell proliferation in a V600E BRAF-selective manner. **Proc Natl Acad Sci U S A 107(33):** 14903-14908

Kang Y., Li Y., Zhang T., Chi Y., Liu M. (2019) Effects of transcription factor

EB on oxidative stress and apoptosis induced by high glucose in podocytes. **Int J Mol Med 44(2):** 447-456

Kauffman E.C., Ricketts C.J., Rais-Bahrami S., Yang Y., Merino M.J., Bottaro D.P., Srinivasan R., Linehan W.M. (2014) Molecular genetics and cellular features of TFE3 and TFEB fusion kidney cancers. **Nat Rev Urol 11:** 465-475

Kidger A.M., Keyse S.M. (2016) The regulation of oncogenic Ras/ERK signalling by dual-specificity mitogen activated protein kinase phosphatases (MKPs). **Semin Cell Dev Biol 50:** 125-32

Kim E.K., Choi E.J. (2010) Pathological roles of MAPK signaling pathways in human diseases. **Biochim Biophys Acta 1802:** 396-405

Kim S., Song G., Lee T., Kim M., Kim J., Kwon H., Kim J., Jeong W., Lee U., Na C., Kang S., Kim W., Seong J.K., Jho E.H. (2021a) PARsylated transcription factor EB (TFEB) regulates the expression of a subset of Wnt target genes by forming a complex with β-catenin-TCF/LEF1. **Cell Death Differ:** Epub ahead of print

Kim J.H., Lee J., Cho Y.R., Lee S.Y., Sung G.J., Shin D.M., Choi K.C., Son J. (2021b) TFEB Supports Pancreatic Cancer Growth through the Transcriptional Regulation of Glutaminase. **Cancers (Basel) 13(3):** 483

Kimmelman A.C., White E. (2017) Autophagy and Tumor Metabolism. **Cell Metab 25(5):** 1037-1043

Klein K., Werner K., Teske C., Schenk M., Giese T., Weitz J., Welsch T.

(2016) Role of TFEB-driven autophagy regulation in pancreatic cancer treatment. **Int J Oncol 49:** 164-172

Kondoh K., Nishida E. (2007) Regulation of MAP kinases by MAP kinase phosphatases. **Biochim Biophys Acta 1773(8):** 1227-1237

Kuiper R.P., Schepens M., Thijssen J., van Asseldonk M., van den Berg E., Bridge J., Schuuring E., Schoenmakers E.F., van Kessel A.G. (2003) Upregulation of the transcription factor TFEB in t(6;11)(p21;q13)-positive renal cell carcinomas due to promoter substitution. **Hum Mol Genet 12:** 1661-1669

Kuiper R.P., Schepens M., Thijssen J., Schoenmakers E.F., van Kessel A.G. (2004) Regulation of the MiTF/TFE bHLH-LZ transcription factors through restricted spatial expression and alternative splicing of functional domains. **Nucleic Acids Res 32:** 2315-2322

Kundu S.T., Grzeskowiak C.L., Fradette J.J., Gibson L.A., Rodriguez L.B., Creighton C.J., Scott K.L., Gibbons D.L. (2018) TMEM106B drives lung cancer metastasis by inducing TFEB-dependent lysosome synthesis and secretion of cathepsins. **Nat Commun 9:** 2731

La Spada A.R. (2012) PPARGC1A/PGC-1α, TFEB and enhanced proteostasis in Huntington disease: defining regulatory linkages between energy production and protein-organelle quality control. **Autophagy 8(12):** 1845-1847

La Spina M., Contreras P.S., Rissone A., Meena N.K., Jeong E., Martina J.A. (2021) MiT/TFE Family of Transcription Factors: An Evolutionary

Perspective. **Front Cell Dev Biol 8:** 609683

Levy C., Khaled M., Fisher D.E. (2006) MITF: master regulator of melanocyte development and melanoma oncogene. **Trends Mol Med 12:** 406-414

Li Y., Xu M., Ding X., Yan C., Song Z., Chen L., Huang X., Wang X., Jian Y., Tang G., Tang C., Di Y., Mu S., Liu X., Liu K., Li T., Wang Y., Miao L., Guo W., Hao X., Yang C. (2016) Protein kinase C controls lysosome biogenesis independently of mTORC1. **Nat Cell Biol 18:** 1065-1077

Li S., Song Y., Quach C., Guo H., Jang G.B., Maazi H., Zhao S., Sands N.A., Liu Q., In G.K., Peng D., Yuan W., Machida K., Yu M., Akbari O., Hagiya A., Yang Y., Punj V., Tang L., Liang C. (2019) Transcriptional regulation of autophagy-lysosomal function in BRAF-driven melanoma progression and chemoresistance. **Nat Commun 10:** 1693

Liang J., Jia X., Wang K., Zhao N. (2018) High expression of TFEB is associated with aggressive clinical features in colorectal cancer. **Onco Targets Ther 11:** 8089-8098

Liu B., Wen X., Cheng Y. (2013) Survival or death: disequilibrating the oncogenic and tumor suppressive autophagy in cancer. **Cell Death Dis 4:** e892

Lu H., Fan Y., Qiao C., Liang W., Hu W., Zhu T., Zhang J., Chen Y.E. (2017) TFEB inhibits endothelial cell inflammation and reduces atherosclerosis. **Sci Signal 10**

Luo J. (2009) Glycogen synthase kinase 3beta (GSK3beta) in tumorigenesis and cancer chemotherapy. **Cancer Lett 273(2):** 194-200

Malumbres M. (2014) Cyclin-dependent kinases. **Genome Biology 15:** 122
Martina J.A., Chen Y., Gucek M., Puertollano R. (2012) MTORC1 functions as a transcriptional regulator of autophagy by preventing nuclear transport of TFEB. **Autophagy 8:** 903-914

Mansueto G., Armani A., Viscomi C., D'Orsi L., De Cegli R., Polishchuk E.V., Lamperti C., Di Meo I., Romanello V., Marchet S., Saha P.K., Zong H., Blaauw B., Solagna F., Tezze C., Grumati P., Bonaldo P., Pessin J.E., Zeviani M., Sandri M., Ballabio A. (2017) Transcription Factor EB Controls Metabolic Flexibility during Exercise. **Cell Metab 25(1):** 182-196

Marchand B., Arsenault D., Raymond-Fleury A., Boisvert F.M., Boucher M.J. (2015) Glycogen synthase kinase-3 (GSK3) inhibition induces prosurvival autophagic signals in human pancreatic cancer cells. **J Biol Chem 290:** 5592-5605

Martina J.A., Chen Y., Gucek M., Puertollano R. (2012) MTORC1 functions as a transcriptional regulator of autophagy by preventing nuclear transport of TFEB. **Autophagy 8:** 903-914

Martina J.A., Puertollano R. (2013) Rag GTPases mediate amino acid-dependent recruitment of TFEB and MITF to lysosomes. **J Cell Biol 200:** 475-491

Martina J.A., Diab H.I., Li H., Puertollano R. (2014a) Novel roles for the MiTF/TFE family of transcription factors in organelle biogenesis, nutrient

sensing, and energy homeostasis. **Cell Mol Life Sci 71:** 2483-2497

Martina J.A., Diab H.I., Lishu L., Jeong-A L., Patange S., Raben N., Puertollano R. (2014b) The nutrient-responsive transcription factor TFE3 promotes autophagy, lysosomal biogenesis, and clearance of cellular debris. **Sci Signal 7:** 309

Martina J.A., Diab H.I., Brady O.A., Puertollano R. (2016) TFEB and TFE3 are novel components of the integrated stress response. **EMBO J 35:** 479-495

Martina J.A., Puertollano R. (2017) TFEB and TFE3: The art of multi-tasking under stress conditions. **Transcription 8:** 48-54

Martina J.A., Puertollano R. (2018) Protein phosphatase 2A stimulates activation of TFEB and TFE3 transcription factors in response to oxidative stress. **J Biol Chem 293:** 12525-12534

Martini-Stoica H., Xu Y., Ballabio A., Zheng H. (2016) The Autophagy-Lysosomal Pathway in Neurodegeneration: A TFEB Perspective. **Trends Neurosci 39:** 221-234

Medina D.L., Fraldi A., Bouche V., Annunziata F., Mansueto G., Spampanato C., Puri C., Pignata A., Martina J.A., Sardiello M., Palmieri M., Polishchuk R., Puertollano R., Ballabio A. (2011) Transcriptional activation of lysosomal exocytosis promotes cellular clearance. **Dev Cell 21:** 421-430

McCubrey J.A., Steelman L.S., Chappell W.H., Abrams S.L., Wong E.W., Chang F., Lehmann B., Terrian D.M., Milella M., Tafuri A., Stivala F., Libra

M., Basecke J., Evangelisti C., Martelli A.M., Franklin R.A. (2007) Roles of the Raf/MEK/ERK pathway in cell growth, malignant transformation and drug resistance. **Biochim Biophys Acta 1773:** 1263-1284

Medina D.L., Di Paola S., Peluso I., Armani A., De Stefani D., Venditti R., Montefusco S., Scotto-Rosato A., Prezioso C., Forrester A., Settembre C., Wang W., Gao Q., Xu H., Sandri M., Rizzuto R., De Matteis M.A., Ballabio A. (2015) Lysosomal calcium signalling regulates autophagy through calcineurin and TFEB. **Nat Cell Biol 17:** 288-299

Meeth K., Wang J.X., Micevic G., Damsky W., Bosenberg M.W. (2016) The YUMM lines: a series of congenic mouse melanoma cell lines with defined genetic alterations. **Pigment Cell Melanoma Res 29(5):** 590-597

Mendoza M.C., Er E.E., Blenis J. (2011) The Ras-ERK and PI3K-mTOR pathways: cross-talk and compensation. **Trends Biochem Sci 36:** 320-328

Markey M.P., Angus S.P., Strobeck M.W., Williams S.L., Gunawardena R.W., Aronow B.J., Knudsen E.S. (2002) Unbiased analysis of RB-mediated transcriptional repression identifies novel targets and distinctions from E2F action. **Cancer Res 62(22):** 6587-6597

Möller K., Sigurbjornsdottir S., Arnthorsson A.O., Pogenberg V., Dilshat R., Fock V., Brynjolfsdottir S.H., Bindesboll C., Bessadottir M., Ogmundsdottir H.M., Simonsen A., Larue L., Wilmanns M., Thorsson V., Steingrimsson E., Ogmundsdottir M.H. (2019) MITF has a central role in regulating starvation-induced autophagy in melanoma. **Sci Rep 9:** 1055

Muhle-Goll C., Gibson T., Schuck P., Schubert D., Nalis D., Nilges M.,

Pastore A. (1994) The dimerization stability of the HLH-LZ transcription protein family is modulated by the leucine zippers: a CD and NMR study of TFEB and c-Myc. **Biochemistry 33:** 11296-11306

Müller-Höcker J., Babaryka G., Schmid I., Jung A. (2008) Overexpression of cyclin D1, D3, and p21 in an infantile renal carcinoma with Xp11.2 TFE3-gene fusion. **Pathol Res Pract 204:** 589-597

Nabar N.R., Kehrl J.H. (2017) The Transcription Factor EB Links Cellular Stress to the Immune Response**. Yale J Biol Med 90:** 301-315

Nakatogawa H., Suzuki K., Kamada Y., Ohsumi Y. (2009) Dynamics and diversity in autophagy mechanisms: lessons from yeast. **Nat Rev Mol Cell Biol 10:** 458-467

Napolitano G., Ballabio A. (2016) TFEB at a glance. **J Cell Sci 129:** 2475-2481

Napolitano G., Esposito A., Choi H., Matarese M., Benedetti V., Di Malta C., Monfregola J., Medina D.L., Lippincott-Schwartz J., Ballabio A. (2018) mTOR-dependent phosphorylation controls TFEB nuclear export. **Nat Commun 9:** 3312

Němejcová K., Dundr P., Jakša R., Bártů M., Stružinská I., Hojný J., Hájková N., Kodet O. (2020) Comprehensive Analysis of PTEN in Primary Cutaneous Melanoma. **Folia Biol (Praha) 66:** 7-16

Ostrowski S.M., Fisher D.E. (2021) Biology of Melanoma. **Hematol Oncol Clin North Am 35:** 29-56

Owens D.M., Keyse S.M. (2007) Differential regulation of MAP kinase signalling by dual-specificity protein phosphatases. **Oncogene 26(22):** 3203-3213

Palmieri M., Impey S., Kang H., di Ronza A., Pelz C., Sardiello M., Ballabio A. (2011) Characterization of the CLEAR network reveals an integrated control of cellular clearance pathways. **Hum Mol Genet 20:** 3852-3866

Palmieri M., Pal R., Nelvagal H.R., Lotfi P., Stinnett G.R., Seymour M.L., Chaudhury A., Bajaj L., Bondar V.V., Bremner L., Saleem U., Tse D.Y., Sanagasetti D., Wu S.M., Neilson J.R., Pereira F.A., Pautler R.G., Rodney G.G., Cooper J.D., Sardiello M. (2017) mTORC1-independent TFEB activation via Akt inhibition promotes cellular clearance in neurodegenerative storage diseases. **Nat Commun 8:** 14338

Pan H.Y., Alamri A.H., Valapala M. (2019) Nutrient deprivation and lysosomal stress induce activation of TFEB in retinal pigment epithelial cells. **Cell Mol Biol Lett 24:** 33

Paoluzzi L., Maki R.G. (2019) Diagnosis, Prognosis, and Treatment of Alveolar Soft-Part Sarcoma: A Review. **JAMA Oncol 5:** 254-260

Parenti G., Andria G., Ballabio A. (2015) Lysosomal storage diseases: from pathophysiology to therapy. **Annu Rev Med 66:** 471-486

Pastore N., Brady O.A., Diab H.I., Martina J.A., Sun L., Huynh T., Lim J.A., Zare H., Raben N., Ballabio A., Puertollano R. (2016) TFEB and TFE3 cooperate in the regulation of the innate immune response in activated

macrophages. **Autophagy 12:** 1240-1258

Pastore N., Vainshtein A., Klisch T.J., Armani A., Huynh T., Herz N.J., Polishchuk E.V., Sandri M., Ballabio A. (2017) TFE3 regulates whole-body energy metabolism in cooperation with TFEB. **EMBO Mol Med 9(5):** 605-621

Perera R.M., Stoykova S., Nicolay B.N., Ross K.N., Fitamant J., Boukhali M., Lengrand J., Deshpande V., Selig M.K., Ferrone C.R., Settleman J., Stephanopoulos G., Dyson N.J., Zoncu R., Ramaswamy S., Haas W., Bardeesy N. (2015) Transcriptional control of autophagy-lysosome function drives pancreatic cancer metabolism. **Nature 524:** 361-365

Perera R.M., Di Malta C., Ballabio A. (2019) MiT/TFE Family of Transcription Factors, Lysosomes, and Cancer. **Annu Rev Cancer Biol 3:** 203-222

Ploper D., De Robertis E.M. (2015) The MITF family of transcription factors: Role in endolysosomal biogenesis, Wnt signaling, and oncogenesis. **Pharmacol Res 99:** 36-43

Ploper D., Taelman V.F., Robert L., Perez B.S., Titz B., Chen H.W., Graeber T.G., von Euw E., Ribas A., De Robertis E.M. (2015b) MITF drives endolysosomal biogenesis and potentiates Wnt signaling in melanoma cells. **Proc Natl Acad Sci USA 112:** E420-429

Pogenberg V., Ogmundsdóttir M.H., Bergsteinsdóttir K., Schepsky A., Phung B., Deineko V., Milewski M., Steingrímsson E., Wilmanns M. (2012) Restricted leucine zipper dimerization and specificity of DNA recognition of the melanocyte master regulator MITF. **Genes Dev 26:** 2647-2658

Puertollano R., Ferguson S.M., Brugarolas J., Ballabio A. (2018) The complex relationship between TFEB transcription factor phosphorylation and subcellular localization. EMBO J 37: e98804

Raben N., Puertollano R. (2016) TFEB and TFE3: Linking Lysosomes to Cellular Adaptation to Stress. **Annu Rev Cell Dev Biol 32:** 255-278

Radu A., Neubauer V., Akagi T., Hanafusa H., Georgescu M.M. (2003) PTEN induces cell cycle arrest by decreasing the level and nuclear localization of cyclin D1. **Mol Cell Biol 23:** 6139-6149

Raimondi S., Suppa M., Gandini S. (2020) Melanoma Epidemiology and Sun Exposure. **Acta Derm Venereol 100:** adv00136

Rastrelli M., Tropea S., Rossi C.R., Alaibac M. (2014) Melanoma: epidemiology, risk factors, pathogenesis, diagnosis and classification. **In Vivo 28:** 1005-1011

Ratnikov B.I., Scott D.A., Osterman A.L., Smith J.W., Ronai Z.A. (2017) Metabolic rewiring in melanoma. **Oncogene 36(2):** 147-157

Riganti C., Aldieri E., Bergandi L., Fenoglio I., Costamagna C., Fubini B., Bosia A., Ghigo D. (2002) Crocidolite asbestos inhibits pentose phosphate oxidative pathway and glucose 6-phosphate dehydrogenase activity in human lung epithelial cells. **Free Radic Biol Med 32(9):** 938-949

Riganti C., Gazzano E., Polimeni M., Costamagna C., Bosia A., and Ghigo D. (2004) Diphenyleneiodonium inhibits the cell redox metabolism and

induces oxidative stress. **J Biol Chem *279*:** 47726-47731

Roczniak-Ferguson A,. Petit C.S., Froehlich F., Qian S., Ky J., Angarola B., Walther T.C., Ferguson S.M. (2012) The transcription factor TFEB links mTORC1 signaling to transcriptional control of lysosome homeostasis. **Sci Signal 5:** ra42

Roskoski R. Jr. (2012) ERK1/2 MAP kinases: structure, function, and regulation. **Pharmacol Res 66:** 105-143

Roskoski R. Jr. (2019) Targeting ERK1/2 protein-serine/threonine kinases in human cancers. **Pharmacol Res 142:** 151-168

Roux P.P., Blenis J. (2004) ERK and p38 MAPK-activated protein kinases: a family of protein kinases with diverse biological functions. **Microbiol Mol Biol Rev 68:** 320-344

Ruocco M.R., Avagliano A., Granato G., Vigliar E., Masone S., Montagnani S., Arcucci A. (2019) Metabolic flexibility in melanoma: A potential therapeutic target. **Semin Cancer Biol. 59:** 187-207

Sakamaki J.I., Long J.S., New M., Van Acker T., Tooze S.A., Ryan K.M. (2018) Emerging roles of transcriptional programs in autophagy regulation. **Transcription 9:** 131-136

Sakamoto H., Yamashita K., Okamoto K., Kadowaki T., Sakai E., Umeda M., Tsukuba T. (2018) Transcription factor EB influences invasion and migration in oral squamous cell carcinomas. **Oral Dis 24:** 741-748

Salma N., Song J.S., Arany Z., Fisher D.E. (2015) Transcription Factor Tfe3 Directly Regulates Pgc-1alpha in Muscle. **J Cell Physiol 230(10):** 2330-2336

Salma N., Song J.S., Kawakami A., Devi S.P., Khaled M., Cacicedo J.M., Fisher D.E. (2017) Tfe3 and Tfeb Transcriptionally Regulate Peroxisome Proliferator-Activated Receptor γ2 Expression in Adipocytes and Mediate Adiponectin and Glucose Levels in Mice. **Mol Cell Biol 37(15):** e00608-16

Santana-Codina N., Mancias J.D., Kimmelman A.C. (2017) The Role of Autophagy in Cancer. **Annu Rev Cancer Biol 1:** 19-39

Sardiello M., Palmieri M., di Ronza A., Medina D.L., Valenza M., Gennarino V.A., Di Malta C., Donaudy F., Embrione V., Polishchuk R.S., Banfi S., Parenti G., Cattaneo E., Ballabio A. (2009) A gene network regulating lysosomal biogenesis and function. Science 325: 473-477

Sardiello M., Ballabio A. (2009b) Lysosomal enhancement: a CLEAR answer to cellular degradative needs. **Cell Cycle 8:** 4021-4022

Sato S., Roberts K., Gambino G., Cook A., Kouzarides T., Goding C.R. (1997) CBP/p300 as a co-factor for the Microphthalmia transcription factor. **Oncogene 14:** 3083-3092

Savoia P., Fava P., Casoni F., Cremona O. (2019) Targeting the ERK Signaling Pathway in Melanoma. **Int J Mol Sci 20:** 1483

Scalise M., Pochini L., Cosco J., Aloe E., Mazza T., Console L., Esposito A., Indiveri C. (2019) Interaction of Cholesterol With the Human SLC1A5

(ASCT2): Insights Into Structure/Function Relationships. **Front Mol Biosci 6:** 110

Schilling J.D., Machkovech H.M., He L., Diwan A., Schaffer J.E. (2013) TLR4 activation under lipotoxic conditions leads to synergistic macrophage cell death through a TRIF-dependent pathway. **J Immunol 190(3):** 1285-1296

Seo J.W., Choi J., Lee S.Y., Sung S., Yoo H.J., Kang M.J., Cheong H., Son J. (2016) Autophagy is required for PDAC glutamine metabolism. **Sci Rep 6:** 37594

Seternes O.M., Kidger A.M., Keyse S.M. (2019) Dual-specificity MAP kinase phosphatases in health and disease. **Biochim Biophys Acta Mol Cell Res 1866(1):** 124-143

Settembre C., Di Malta C., Polito V.A., Garcia Arencibia M., Vetrini F., Erdin S., Erdin S.U., Huynh T., Medina D., Colella P., Sardiello M., Rubinsztein D.C., Ballabio A. (2011) TFEB links autophagy to lysosomal biogenesis. **Science 332:** 1429-1433

Settembre C., Zoncu R., Medina D.L., Vetrini F., Erdin S., Erdin S., Huynh T., Ferron M., Karsenty G., Vellard M.C., Facchinetti V., Sabatini D.M., Ballabio A. (2012) A lysosome-to-nucleus signalling mechanism senses and regulates the lysosome via mTOR and TFEB. **EMBO J 31:** 1095-1108

Settembre C., Fraldi A., Medina D.L., Ballabio A. (2013a) Signals from the lysosome: a control centre for cellular clearance and energy metabolism. **Nat Rev Mol Cell Biol 14:** 283-296

Settembre C., De Cegli R., Mansueto G., Saha P.K., Vetrini F., Visvikis O., Huynh T., Carissimo A., Palmer D., Klisch T.J., Wollenberg A.C., Di Bernardo D., Chan L., Irazoqui J.E., Ballabio A. (2013b) TFEB controls cellular lipid metabolism through a starvation-induced autoregulatory loop. **Nat Cell Biol 15:** 647-658

Settembre C., Medina D.L. (2015) TFEB and the CLEAR network. **Methods Cell Biol 126:** 45-62

Sha Y., Rao L., Settembre C., Ballabio A., Eissa N.T. (2017) STUB1 regulates TFEB-induced autophagy-lysosome pathway. **EMBO J 36:** 2544-2552

Sharma B. (2011) Kinetic Characterisation of Phosphofructokinase Purified from Setaria cervi: A Bovine Filarial Parasite. **Enzyme Res 2011:** 939472

Shen J., Zhang Y., Yu H., Shen B., Liang Y., Jin R., Liu X., Shi L., Cai X. (2016) Role of DUSP1/MKP1 in tumorigenesis, tumor progression and therapy. **Cancer Med 5(8):** 2061-2068

Sherr C.J., Beach D., Shapiro G.I. (2016) Targeting CDK4 and CDK6: from discovery to therapy. **Cancer Discov 6:** 353-367

Slade L., Pulinilkunnil T. (2017) The MiTF/TFE Family of Transcription Factors: Master Regulators of Organelle Signaling, Metabolism, and Stress Adaptation. **Mol Cancer Res 15:** 1637-1643

Song W., Zhang C.L., Gou L., He L., Gong Y.Y., Qu D., Zhao L., Jin N., Chan

T.F., Wang L., Tian X.Y., Luo J.Y., Huang Y. (2019) Endothelial TFEB (Transcription Factor EB) Restrains IKK (IκB Kinase)-p65 Pathway to Attenuate Vascular Inflammation in Diabetic db/db Mice. **Arterioscler Thromb Vasc Biol 39:** 719-730

Steingrímsson E., Tessarollo L., Reid S.W., Jenkins N.A., Copeland N.G. (1998) The bHLH-Zip transcription factor TFEB is essential for placental vascularization. **Development 125:** 4607-4616

Steingrímsson E., Copeland N.G., Jenkins N.A. (2004) Melanocytes and the microphthalmia transcription factor network. **Annu Rev Genet 38:** 365-411

Sun Y., Liu W.Z., Liu T., Feng X., Yang N., Zhou H.F. (2015) Signaling pathway of MAPK/ERK in cell proliferation, differentiation, migration, senescence and apoptosis. **J Recept Signal Transduct Res 35:** 600-604

Sun J., Lu H., Liang W., Zhao G., Ren L., Hu D., Chang Z., Liu Y., Garcia-Barrio M.T., Zhang J., Chen Y.E., Fan Y. (2021) Endothelial TFEB (Transcription Factor EB) Improves Glucose Tolerance via Upregulation of IRS (Insulin Receptor Substrate) 1 and IRS2. **Arterioscler Thromb Vasc Biol 41(2):** 783-795

Tachibana M., Perez-Jurado L.A., Nakayama A., Hodgkinson C.A., Li X., Schneider M., Miki T., Fex J., Francke U., Arnheiter H. (1994) Cloning of MITF, the human homolog of the mouse microphthalmia gene and assignment to chromosome 3p14.1-p12.3. **Hum Mol Genet 3:** 553-557

Taelman V.F., Dobrowolski R., Plouhinec J.L., Fuentealba L.C., Vorwald P.P., Gumper I., Sabatini D.D., De Robertis E.M. (2010) Wnt signaling

requires sequestration of glycogen synthase kinase 3 inside multivesicular endosomes. **Cell 143:** 1136-1148

Takahashi-Yanaga F., Sasaguri T. (2008) GSK-3beta regulates cyclin D1 expression: a new target for chemotherapy. **Cell Signal 20(4):** 581-589

Takeda K., Yasumoto K., Kawaguchi N., Udono T., Watanabe K., Saito H., Takahashi K., Noda M., Shibahara S. (2002) Mitf-D, a newly identified isoform, expressed in the retinal pigment epithelium and monocyte-lineage cells affected by Mitf mutations. **Biochim Biophys Acta 1574:** 15-23

Tassone B., Saoncella S., Neri F., Ala U., Brusa D., Magnuson M.A., Provero P., Oliviero S., Riganti C., Calautti E. (2017) Rictor/mTORC2 deficiency enhances keratinocyte stress tolerance via mitohormesis. **Cell Death Differ 24(4):** 731-746

Thacker S.A., Bonnette P.C., Duronio R.J. (2003) The contribution of E2F-regulated transcription to Drosophila PCNA gene function. **Curr Biol 13(1):** 53-58

Tong Y., Song F. (2015) Intracellular calcium signaling regulates autophagy via calcineurin-mediated TFEB dephosphorylation. **Autophagy 11:** 1192-1195

Trivedi P.C., Bartlett J.J., Mercer A., Slade L., Surette M., Ballabio A., Flibotte S., Hussein B., Rodrigues B., Kienesberger P.C., Pulinilkunnil T. (2020) Loss of function of transcription factor EB remodels lipid metabolism and cell death pathways in the cardiomyocyte. **Biochim Biophys Acta Mol Basis Dis 1866(10):** 165832

Vachtenheim J., Ondrušová L. (2015) Microphthalmia-associated transcription factor expression levels in melanoma cells contribute to cell invasion and proliferation. **Exp Dermatol 24:** 481-484

Vander Heiden M.G., Lunt S.Y., Dayton T.L., Fiske B.P., Israelsen W.J., Mattaini K.R., Vokes N.I., Stephanopoulos G., Cantley L.C., Metallo C.M., Locasale J.W. (2011) Metabolic pathway alterations that support cell proliferation. **Cold Spring Harb Symp Quant Biol 76:** 325-334

Vander Heiden M.G., DeBerardinis R.J. (2017) Understanding the Intersections between Metabolism and Cancer Biology. **Cell 168(4):** 657-669

Vazquez A., Kamphorst J.J., Markert E.K., Schug Z.T., Tardito S., Gottlieb E. (2016) Cancer metabolism at a glance. **J Cell Sci 129(18):** 3367-3373

Vega-Rubin-de-Celis S., Peña-Llopis S., Konda M., Brugarolas J. (2017) Multistep regulation of TFEB by MTORC1. **Autophagy 13:** 464-472

Wellbrock C., Arozarena I. (2015) Microphthalmia-associated transcription factor in melanoma development and MAP-kinase pathway targeted therapy. **Pigment Cell Melanoma Res 28:** 390-406

Wellbrock C., Arozarena I. (2016) The Complexity of the ERK/MAP-Kinase Pathway and the Treatment of Melanoma Skin Cancer. **Front Cell Dev Biol 4:** 33

Wenzel E.S., Singh A.T.K. (2018) Cell-cycle checkpoints and aneuploidy on the path to cancer. **In Vivo 32:** 1-5

White E. (2012) Deconvoluting the context-dependent role for autophagy in cancer. **Nat Rev Cancer 12:** 401-410

Wibom R., Hagenfeldt L., von Döbeln U. (2002) Measurement of ATP production and respiratory chain enzyme activities in mitochondria isolated from small muscle biopsy samples. **Anal Biochem 311(2):** 139-151

Widlund H.R., Fisher D.E. (2003) Microphthalamia-associated transcription factor: a critical regulator of pigment cell development and survival. **Oncogene 22:** 3035-3041

Williamson S.R., Grignon D.J., Cheng L., Favazza L., Gondim D.D., Carskadon S., Gupta N.S., Chitale D.A., Kalyana-Sundaram S., Palanisamy N. (2017) Renal Cell Carcinoma With Chromosome 6p Amplification Including the TFEB Gene: A Novel Mechanism of Tumor Pathogenesis? **Am J Surg Pathol 41:** 287-298

Wyvekens N., Rechsteiner M., Fritz C., Wagner U., Tchinda J., Wenzel C., Kuithan F., Horn L.C., Moch H. (2019) Histological and molecular characterization of TFEB-rearranged renal cell carcinomas. **Virchows Arch 474:** 625-631

Yamamoto H., Komekado H., Kikuchi A. (2006) Caveolin is necessary for Wnt-3a-dependent internalization of LRP6 and accumulation of beta-catenin. **Dev Cell 11:** 213-223

Yang S., Wang X., Contino G., Liesa M., Sahin E., Ying H., Bause A., Li Y., Stommel J.M., Dell'antonio G., Mautner J., Tonon G., Haigis M., Shirihai O.S., Doglioni C., Bardeesy N., Kimmelman A.C. (2011) Pancreatic cancers

require autophagy for tumor growth. **Genes Dev 25:** 717-729

Yang S.T., Kreutzberger A.J.B., Lee J., Kiessling V., Tamm L.K. (2016) The role of cholesterol in membrane fusion. **Chem Phys Lipids 199:** 136-143

Yasumoto K., Takeda K., Saito H., Watanabe K., Takahashi K., Shibahara S. (2002) Microphthalmia-associated transcription factor interacts with LEF-1, a mediator of Wnt signaling. **EMBO J 21:** 2703-2714

Yu S., Wang Z., Ding L., Yang L. (2020) The regulation of TFEB in lipid homeostasis of non-alcoholic fatty liver disease: Molecular mechanism and promising therapeutic targets. **Life Sci 246:** 117418

Zhan T., Rindtorff N., Boutros M. (2017) Wnt signaling in cancer. **Oncogene 36(11):** 1461-1473

Zhan H.Q., Li S.T., Shu Y., Liu M.M., Qin R., Li Y.L., Gan L. (2018) Alpha gene upregulates TFEB expression in renal cell carcinoma with t(6;11) translocation, which promotes cell canceration. **Int J Oncol 52:** 933-944

Zhang Z., Wang H., Ding Q., Xing Y., Xu D., Xu Z., Zhou T., Qian B., Ji C., Pan X., Zhong A., Ying Z., Zhou C., Shi M. (2017) The tumor suppressor p53 regulates autophagosomal and lysosomal biogenesis in lung cancer cells by targeting transcription factor EB. **Biomed Pharmacother 89:** 1055-1060

Zhao G.Q., Zhao Q., Zhou X., Mattei M.G., De Crombrugghe B. (1993) TFEC, a basic helix-loop-helix protein, forms heterodimers with TFE3 and inhibits TFE3-dependent transcription activation. **Mol Cell Biol 13:** 4505-

4512

Zhao B., Dierichs L., Gu J.N., Trajkovic-Arsic M., Axel Hilger R., Savvatakis K., Vega-Rubin-de-Celis S., Liffers S.T., Peña-Llopis S., Behrens D., Hahn S., Siveke J.T., Lueong S.S. (2020) TFEB-mediated lysosomal biogenesis and lysosomal drug sequestration confer resistance to MEK inhibition in pancreatic cancer. **Cell Death Discov 6:** 12

Zhitomirsky B., Assaraf Y.G. (2015) Lysosomal sequestration of hydrophobic weak base chemotherapeutics triggers lysosomal biogenesis and lysosome-dependent cancer multidrug resistance. **Oncotarget 6:** 1143-1156